BEHAVIOUR OF SHEAR WALL MODELS

WITH

CIRCULAR WALL OPENINGS

BEHAVIOUR OF SHEAR WALL MODELS
WITH
CIRCULAR WALL OPENINGS

by

AEJAZ AHMED QURESHI, B.SC., B.E.(CIVIL)

A Thesis

Submitted to the Faculty of Graduate Studies

in Partial Fulfilment of the Requirements

for the Degree

Master of Engineering

McMaster University

February, 1968

MASTER OF ENGINEERING (1968)
(Civil Engineering)

McMASTER UNIVERSITY
Hamilton, Ontario.

TITLE: Behaviour of Shear Wall Models with Circular Wall Openings

AUTHOR: Aejaz Ahmed Qureshi, B.Sc.,B.E.(Civil) Karachi University

SUPERVISOR: Dr. A. C. Heidebrecht

NUMBER OF PAGES: x, 120

SCOPE AND CONTENTS:

This thesis describes the development of a technique to build small scale shear wall building models containing circular wall-openings and without floors, using a suitable concrete mortar. Tests were conducted to study the behaviour of such models under lateral static loads. The behaviour of these models is compared with those containing no wall openings. The test and analytical results as predicted by Vlasov's theory are compared to investigate the effect of such openings in shear wall models. Analysis of the problem is also attempted using Rosman's shear connection approach.

ACKNOWLEDGEMENTS

I am sincerely grateful to DR. A. C. HEIDEBRECHT. This work would not have been possible without his assistance and advice.

I would also like to express my appreciation to Dr. W. K. Tso and Dr. H. Robinson for their constructive suggestions.

This investigation was made possible through the financial assistance of the CANADA EMERGENCY MEASURES ORGANIZATION, to whom I extend my sincere thanks.

TABLE OF CONTENTS

TABLE OF CONTENTS (cont'd)

LIST OF FIGURES

LIST OF FIGURES (cont'd)

LIST OF TABLES

NOTATION

A	Cross-sectional area of the model
A_1, A_2	Cross-sectional areas of side and middle piers respectively
a_x, a_y	Coordinates of the shear centre
b	Clear span of the connecting beams
c_1, c_2	Distance of side and middle piers from the centre of the openings, respectively
E	Modulus of elasticity
e	Eccentricity with respect to shear centre
G	Modulus of elasticity in shear
H	Distance between the cross-sections of the piers
h	Distance between the centre lines of the connecting beams
hp	Height of a connecting beam
I_1, I_2	Moments of inertia of side and middle piers, respectively
I_d	Torsional rigidity
I_p	Reduced moment of inertia of a connecting beam
I_{po}	Moment of inertia of a connecting beam
I_x, I_y	Moments of inertia of the section with respect to x and y axes , respectively
I_ω	Sectorial moment of inertia
ℓ	Distance from the top of the model to the end of the rows of openings as shown in Fig. 23 & 24
ℓ_m	Length of the model
M_1, M_2	Bending moment at an arbitrary cross-section for side and middle piers, respectively

$M_{xpl} M_{ypl}$	Bending moment about the principal axes for side piers
n	Distance of the centroid of the pier from the point of intersection of the back wall and principal axes, x_p (see Fig. 24)
O	Centroid of the model section
Q	Lateral load
S	Shear centre
T',T	Shear force and integral shear force in the continuous connection at an arbitrary cross-section of the model, respectively
u	Longitudinal displacement in Z-direction
v	Transverse displacement directed along the tangent of the profile line of the cross-section
W	Transverse normal displacement
Z	Distance measured from the bottom of the model
z	Distance measured from the top of the model
α_x	Distance of the shear centre from the back wall of the model
δ	Wall thickness
ε	Longitudinal strain
ω	Principal sectorial area
ξ,η	Displacements of shear centre in the x and y directions, respectively
$\theta(Z)$	Rotation of the section about shear centre
$\delta T, \delta Q$	Mutual displacements of the cut ends of the continuous connection in the base system at any arbitrary cross-section, due to T and Q, respectively
δ_{HT}, δ_{HQ}	Values of the displacements δ_T, δ_Q at the bottom of the model

CHAPTER I

INTRODUCTION

1. DESCRIPTION OF SHEAR WALL STRUCTURES

A shear wall is a structural system providing stability against wind, earth tremors or blasts, deriving its stiffness from inherent structural form. Such a system may be constructed in steel or concrete and may be either solid or perforated. The system can consist of a plane wall, part of a curved wall, a closed hoop, or a rectangular box with a system of concentric or eccentric cores.

In recent years shear walls have been widely used in commercial and residential buildings to provide adequate lateral stiffness. The rapid increase of shear wall construction is mainly due to the speed and economy with which they can be constructed and their flexibility in structural and architectural planning. [1.2]

In building layouts, shear walls may be provided in many types of structures. They may consist of shear walls aligned parallel to each other, interconnected by floor slabs at each storey level. They can also be provided in box-core type structures consisting of shear walls of channel or other cross-sectional shape with interconnected slabs. In framed structures, shear wall assemblies act in conjunction with the frame to give it adequate lateral stiffness.

The wide acceptance of shear wall structures as a rational and economical form of multi-storey construction and rapid growth in height of such structures has produced a situation in which a greater knowledge of their structural behaviour is necessary for further development. Although, in recent years, a growing research effort has been directed to the problems in this field, the subject is still in its infancy. At present, approximate design methods can be used to predict the complex interactions between the walls, floor slabs, service cores and frames which comprise a shear wall structure. But wider use of these structures demands more precise information about their behaviour and more sophisticated techniques to predict their behaviour. Therefore, the general purpose of research on shear wall structures is to provide this information in order to assist in the development of more realistic design criteria.

2. THE NATURE OF THE SHEAR WALL RESEARCH PROGRAMME AT McMASTER UNIVERSITY

An extensive programme of investigation of the behaviour of shear wall buildings is being conducted in the Department of Civil Engineering at McMaster University under the sponsorship of the Canada Emergency Measures Organization. The programme essentially consists of building small scale shear wall models and subjecting these models to both static and dynamic lateral loads. The first phase of this programme was the investigation of the static behaviour of models containing only shear walls but with no wall openings or floors. This study was conducted by Afsar [3] and was completed early in 1967. The present study represents the second phase of the project and embodies the investigation of the static behaviour of shear wall building models with wall openings but also without floors. A concurrent study is the investigation of the static behaviour of shear wall models with floors but without wall openings. The next stages are the static behaviour of models with both floors and wall openings and also the dynamic behaviour of all types of models which have been studied statically.

3. AIMS AND OBJECTIVES OF THE PRESENT STUDY

The major aim of the present study is the investigation of the overall effect of the openings on the behaviour of the shear wall models. The experimental programme essentially consisted of casting shear wall building models with two bands of circular openings but without floors and testing them under static lateral loading. Since the concern is with the overall behaviour of the model, it was found suitable to have circular openings in the model so as to avoid any local effects due to stress concentration around the corners of rectangular or square openings.

The present investigation being a part of a major experimental programme, it was found suitable to use the same model shape and dimensions as were used in the first phase of this programme [3]. This standardization of the dimensions of the models was also necessary to correlate and compare the results of different phases of the programme and to find the effect of different factors introduced at the different stages. For the same reasons it was also decided to retain concrete mortar as the modelling material.

4. METHODS OF ANALYSIS OF SHEAR WALLS

A complete review of previous research in the field of shear wall structures has been done by Coull and Smith [4]. A comprehensive account of techniques used for the analysis of shear wall structures has also been given by Afsar [3]. The flow diagram in Fig.1 shows the relationship between the most common methods of Elastic Analysis of laterally loaded shear walls. In this study, discussion shall be restricted to those dealing specifically with the analysis of shear walls with rows of openings.

In the so-called Frame analogies, the shear walls with rows of openings are idealized as an interconnection of columns and beams. The equivalent frame method [5], and the wide column frame analogy [6-9] are basic frame analogy methods. Several authors have used the latter analogy with various techniques for obtaining the solution. Some authors have used the method of influence coefficients [6] while another group [7-9] arrived at an elegant solution by treating the row of beams as a continuous medium in pure shear connecting the adjacent wall sections. The method of influence coefficients and the other one termed as the shear connection method are both essentially compatibility methods [10]. In both these approaches axial deformation of the beams has been neglected.

In the method of panel elements, the wall is idealized as a system of elements, the properties of which in aggregation are similar to that of the real continuous structure. The division of these elements is arbitrary and the accuracy of the solution depends largely on the degree of refinement of the element mesh. The McCormick-Hrenikof framework analogy [11-13], Grinter's grid analogy [14] and more recent development of the finite element method [15] are the various idealizations used in this type of approach [3].

Of all these methods for the analysis of shear walls with openings, two recent developments of major interest are the finite element method [15] and shear connection method as developed by Rosman [9]. Rosman has derived solutions for a wall with two symmetric bands of openings with various conditions of support at the lower end. Two loading cases, a uniform wind pressure and a point load at the top of the building were considered. Rosman's method, like other frame analogy methods, enables an overall picture of the stresses and deformations to be obtained. Rosman's method is also simple enough so that only hand calculations are required. The finite-element method on the other hand requires elaborate computer programming. The finite-element technique is potentially useful for the study of the effect of stress concentrations.

A very recent development in the analysis of shear walls is the application of the well-known Vlasov's thin-walled beam theory [3,16]. The salient features of this approach are that it predicts the overall behaviour of the shear wall structures for different boundary conditions due to different types of foundations without resorting to any elaborate computer programming. The theory is more sophisticated than any frame analogy used so far since it takes into account the interaction of walls in different planes and the effects of floor slabs. It also recognizes the distinctive feature of thin-walled beams, namely that they undergo longitudinal extensions as a result of torsion. Afsar [3] compared the experimental results from tests conducted on a model of an eight-storey building without floors with theoretical calculations based on this theory. He reported close qualitative agreement between the two and concluded that the theory should predict the behaviour of tall shear wall buildings with floors.

5. EXPERIMENTAL INVESTIGATIONS OF SHEAR WALL BUILDINGS WITH OPENINGS

The first major experimental investigation of the behaviour of shear walls with openings appears to have been conducted by Benjamin and William [17 — 19]. Large numbers of tests were made on large scale models of single storey shear walls and shear wall assemblies connected by diaphragms. Based on their investigations, a convenient engineering analysis of a wall containing openings has been suggested [20]. Methods of strength of materials were applied to predict the behaviour of shear walls containing openings. Another major conclusion from their long-term research programme was the absence of scale-effect in the behaviour of shear walls. This opened up the way for future small-scale model studies in the field of shear walls.

Japanese investigators also seem to have made various experimental studies in the field of shear walls containing openings [21], but these are not generally available as English translations. Futami and Fujimoto [21] carried out photoelastic investigations on two-storey walls containing a single opening in each storey, in order to determine the shear forces carried by the wall columns.

The behaviour of uniform walls with regular sets of similar openings has attracted many investigators.

Chitty and Wan [22] used models cut from celluloid sheets consisting of numerous cross-girders. They subjected these models to lateral loads and compared the deflections and moments at different stories with those predicted by the continuous medium theory developed by Chitty [23]. Barnard and Schwaighoffer [24] used ¼-inch thick epoxy sheets to build a model of coupled shear walls on 1/64 scale to find the accuracy of Rosman's theory [9]. McLeod [15] used 1/16-inch thick aluminum sheets to build a model of shear walls with rectangular openings. He used a 5/8-inch thick mild steel plate bolted to a rigid floor to clamp the model at the base. Loading was applied through a pulley system and deflections were measured by means of an Amsler Mirror Extensometer.

It can, therefore, be seen that to date every investigator has used different techniques of model building and testing. All these investigations were essentially for the plane-stress problem. The author is unable to find any literature about the testing of three-dimensional shear wall building models. Frischmann and Prabhu [2] have cited two examples of model testing, but no detail of experimental procedure or results has been given. Recently, Stiller [25] used four-storey models containing openings, but his studies were mainly confined to investigation of concentration of stresses around the openings by photoelastic techniques. There is, therefore, an obvious need for experimental work on three-dimensional models of shear walls with wall openings. This type of experimental programme forms a major part of the present study.

CHAPTER II

CONSTRUCTION OF MODELS

1. DESCRIPTION OF THE MODELS

In this programme of experimental investigation of shear wall models, it was decided to build models having identical dimensions but introducing different features such as floors and wall-openings at different stages. This would enable a detailed study of the effects introduced by these different features. The basic shape is that used in the first phase of this programme, as described previously and as shown in Fig. 2. For the present study, it was decided to include wall-openings as the next stage of the total programme of investigation. In this case, the models contain two rows of circular openings placed symmetrically in the back wall of the model as shown in Fig. 2, 3(a). The dimensions of the model were the same as those built in the previous study [3].

The choice of a circular shape for the openings was based on two reasons. The first reason is to eliminate any possible stress-concentrations which would occur at the sharp corners if rectangular or square openings were used. This is to prevent cracking around such corners which cannot be easily reinforced in this type of model construction.

This leads to the second reason for the provision of circular openings, namely the facility and ease with which these openings can be introduced in the models without resorting to any reinforcement around these openings. The actual construction of these models, as described later in this chapter, showed that it was feasible to build models without any cracks around these openings. Also during the testing of these models no cracks were developed around these openings. This proved the judicious choice of the circular shape for the openings.

Arrangement of the openings for the two models is shown in Fig. 2, 3(a). It can be seen that model I contained seven openings per row with no openings at the bottom storey of the model. The second model contained eight openings per row corresponding to one for each storey of the eight-storey model. This enabled a comparison of the behaviour of shear-wall building models with and without openings in the basement. This also made it possible to determine the overall effect on the behaviour of the model introduced by these openings in the bottom storey of the model.

2. CRITICAL STUDY OF THE PREVIOUS TECHNIQUE OF MODEL BUILDING AND ITS IMPROVEMENT

In the previous stage of this programme, difficulties in obtaining completely sound models were reported. Shrinkage cracks were found in all six models poured in the initial programme. Afsar appeared to have solved the major problems of designing appropriate formwork for the model and of pouring, placing the model with formwork in position and stripping the formwork from the model proper. He recommended the use of a new mix with lower water/cement ratio to avoid shrinkage cracks. He also mentioned the possibility that the bending of the aluminium plate fixed to the formwork during hoisting of the model induced sufficiently large stresses which could cause cracking.

In view of all these factors it was decided to modify the original technique so as to ensure the following objectives.

(a) Low shrinkage - The concrete mortar should be redesigned to produce lower shrinkage.

(b) Avoiding of undue stresses during hoisting - The use of aluminium plate fixed to the formwork should be avoided if possible.

(c) Avoiding undue stresses of the model while in place before loading - Model should not be permitted to stand for a long period, with its top and bottom fixed, before testing.

The modelling technique and setting up of the model was accordingly changed to accomplish the above objectives. The use of the base plate was altogether discarded. A new technique of fixing the bottom of the model was used which allowed the model to stand in its place with its top and bottom free until immediately before the actual testing of the models. A detailed description of the revised modelling and erection techniques is given in the subsequent sections of this and the next chapter, under proper headings.

3. DESIGN OF CONCRETE MIX

An extensive programme of mix design was undertaken by the author in the early stages of the project. The mix was supposed to meet the specific requirements of low shrinkage and good workability. The following were the contents of the mix used in the previous phase of the programme:

Ultracal 30	2%
High early-strength cement	38%
Ottawa sand	25%
Dolomite limestone chips (1/8")	35%
Water (percent by weight of ultrcal 30 and high early-strength cement)	53%

To improve workability it was decided to use ordinary portland cement instead of high early-strength cement. Also the use of ultracal 30 was altogether eliminated since it causes shrinkage due to extremely fast setting of mix.

A number of small batches of trial mixes were hand-mixed in the laboratory. These trial mixes were poured into plastic coated plywood moulds to obtain 1/2" thick 18" x 12" slabs. These slabs were examined for surface voids and uniformity of the final product. Twelve such tests were made before arriving at the final mix. The object of low shrinkage was achieved by keeping low water to cement ratio in the mix, while low workability was overcome by vibrating the mix in formwork both internally and externally.

The following mix is recommended for the remaining tests in the programme:

Normal portland cement	= 28.6%
Ottawa sand	= 35.7%
Dolomite limestone chips (1/8")	= 35.7%
Water (percents by weight of cement used)	= 47.5%

4. PROPERTIES OF THE MATERIAL

The following table describes the ultimate strength of 2 inch test cubes made from the redesigned mix, at different ages.

Age	Compressive Strength psi
24 hrs.	2,100
72 hrs.	3,725
7 days	4,500
14 days	5,825
28 days	6,875

Table 1. The ultimate strength of 2-inch test cubes at different ages.

An extensive programme of investigation of material properties was conducted by one of the senior undergraduate students in the summer of 1967. The modulus of elasticity of the mix was determined from both dynamic and static tests.

Sufficient control specimens were made for each model so that the rate of gain in strength could be ascertained as well as the strength on the day of the test. The models and control specimens consisting of beams, cubes and cylinders were poured and cured under approximately the same conditions. The models and specimens were kept wet in the forms for at least four days after pouring.

Beams of dimensions 4" x 3" x 16" were used to find the elastic properties of the mix by dynamic tests. Cubes (2" size) and cylinders (6" diameter) were used for static tests. The modulus of elasticity of the concrete ranged from 4.00×10^6 psi to 5.00×10^6 psi.

5. DESCRIPTION OF FORMWORK, POURING AND ERECTION

The original formwork enabled the casting of the model and base together in a single pour [3]. In the present study, it was decided to discard the base altogether and retain the formwork without base plate for casting the model proper. Since the function of the base plate was only to fix the bottom of the model, another technique of fixing the model with the help of two-inch angles was used for this purpose. Details of this technique are described in Chapter III.

Wooden circular disks of 5-inch diameter and ½ inch thick were used to introduce the desired number of openings in the back wall of the models. Fig.3(b) shows the formwork with these disks in place, ready for pouring of model I. A ¾-inch bevel was provided around the edges of these disks to facilitate their final removal from the model proper.

All the panels of the formwork were carefully wrapped with polyethelene sheets to avoid sticking between the form-work and concrete surfaces. This technique was used successfully by Afsar [3]. The edges of the circular disks used for introducing openings in the model were also wrapped with polyethelene.

The method of pouring and erection was essentially the same as used by Afsar except that an extensive use of the vibrators was employed during pouring to improve the worka-bility of the concrete. For compaction of the concrete, tapping and rod vibrator were used externally against the formwork. A pencil vibrator was also inserted between the panels constitu-ting the side walls of the model to achieve better results.

The model was cured for four days before being erected on its final test position.

6. A CRITICAL REVIEW OF THE PRESENT MODELLING TECHNIQUE

The present modelling technique seems to have solved the major problem of getting completely sound models

without any cracks. This technique is continuing to be used to prepare models for the concurrent studies and it has so far given quite satisfactory results as far as soundness of the models is concerned. Still the technique is not perfect as far as control of the dimensions of the model and alignment of its side walls is concerned.
The most critical dimension of the model is its thickness which is supposed to be 0.500 in. for all the walls constituting the model. But the results obtained for the two models prepared for the present study were not at all satisfactory. Table 2 shows the thickness of the different walls of the model No. 1 at different levels. It can be seen that the model did not contain walls of uniform thickness and the average thickness of these walls was also different. This discrepancy was more pronounced for model No.2 .

This lack of control over the dimensions of the model points towards the necessity of improvement in the design and construction of the formwork. The factors contributing towards the bad control over the dimensions of the model and suggestions for minimizing these effects are as follows:

(a) Warping of the different components of the formwork - The present formwork consists of both wooden pieces and of pieces made from laminated plywood. Laminated plywood has given quite good results as far as warping is concerned. But the wooden pieces and especially

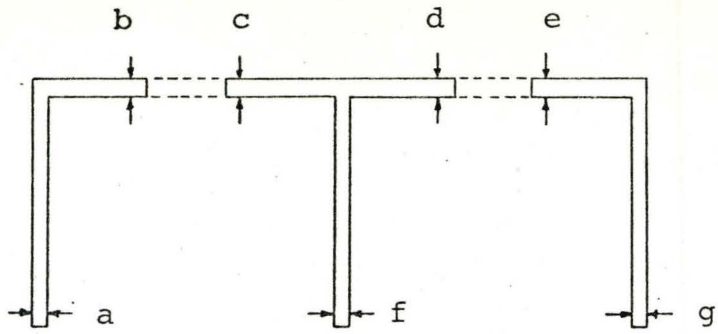

Thickness in sections / level	a inch	b inch	c inch	d inch	e inch	f inch	g inch
z=18	.577	.587	.529	.543	.509	.564	.475
z=30	.688	.563	.556	.603	.516	.558	.534
z=42	.623	.520	.490	.533	.550	.538	.509
z=54	.628	.522	.523	.607	.530	.520	.520
z=66	.552	.522	.529	.568	.570	.577	.487
z=78	.603	.511	.522	.745	.572	.557	.607
z=90	.524	.532	.530	.643	.530	.507	.610

Table 2. VARIATION IN THICKNESS of various sections of the model I at different levels.

2" x 2" pieces used to reinforce the plywood panels showed considerable warping. Since these pieces are attached to the panels constituting the walls of the model,this results in non-uniformity of the thickness of the walls. Better results can be achieved if these 2" x 2" pieces reinforcing the panels would be constructed from laminated plywood. Moreover laminations of these pieces should be carried out such that any possible warping of these pieces takes place in a plane parallel to that of the panel itself thereby assuring the planeness of the panel.

(b) Sliding of the different panels constituting the different walls of the models during pouring - The panels are bolted to a wooden platform. Since the platform is made of wood and the holes made for the passage of the bolts are usually bigger than the bolts themselves, there is every possibility that these bolts move within these holes causing the sliding of the panels. This sliding results in the enlargement of the space between these panels and hence enlargement of the thickness of the walls. Rigorous external and internal vibrations of these panels are obviously the major factors causing this sliding action. Since the vibrations are necessary for compaction of the mix, the only remedy that can be suggested is that all the holes made for securing the panels to the platform be reinforced by metal. Metallic reinforcement will ensure permanent holes for the bolts, thereby eliminating the repetitive drilling of these holes which has so far been practised very frequently.

These improvements have been suggested with a view that these can be carried out on the existing formworks, thereby saving the enormous cost involved in making new formwork .

CHAPTER III

LOADING AND TESTING OF MODELS

1. DESIGN AND DESCRIPTION OF LOADING CAP

The loading cap which was used to transmit the horizontal force to the model consisted of a 44" x 4-1/2" x 1/4" aluminium plate (Fig. 4, 5). Aluminium angles of 2-inch size were bolted to the underside of this plate. These angles were in turn fixed to the back wall of the model using a gel type concrete adhesive (available under the commercial name of Colma Dur and manufactured by Sika Chemical Company, New Jersey, U.S.A.). Another plate of dimensions 44" x 11-1/2" x 1/4" was connected to the three 'legs' of the model in order to maintain its regular 'E' shape during the loading process. Two inch angles with slotted holes were bolted to the underside of this plate so that the walls of the model were enclosed by the angles.

This arrangement of the top plate was quite different than the one used in the initial study of the programme [3]. The advantages provided by this arrangement were that it provided a well-defined line of action of the horizontal force in addition to maintaining the regular 'E' shape of the model.

2. DESCRIPTION OF THE LOADING SYSTEM

The hydraulic jack used in the previous study [3] was replaced by a screw type jack. This device was incorporated with a system of gears to give precise control of the load during both loading and unloading cycles as the previous loading device did not permit control during unloading.

The remainder of the arrangement for the loading system is almost the same as used in the first phase of the programme. Fig. 6 illustrates the loading system with its various connecting elements. The same load cell used in the initial study was used in the present tests.

3. INSTRUMENTATION AND SETTING UP OF THE MODEL FOR TESTING

As mentioned earlier, a new procedure of setting up of the model was used in this study so as to avoid cracking of the model before actual testing. The model was allowed to stand in its place with its top and bottom free, while strain gauges and dial gauges were attached to it. A steel frame with its bottom fixed to the aluminium base plate was used to support the dial gauges at different levels. Fig. 7 shows the positions of dial gauges used in model I while Fig. 8 shows the dial gauges used in model II. Fig. 9 shows the positions of strain gauges used in model I and model II.

After the completion of instrumentation, the base of the model was fixed using 2" angles which were bonded to the model surface using the same special adhesive as used for attachment of the loading cap (Colma Dur Gel). These angles were in turn bolted to the aluminium base plate. This completed the fixing of the base of the model. Fig. 10 shows the arrangement of the angles used to fix the bottom of the models. Testing of the models was started after allowing 24 hours for the adhesive to set.

4. SOME COMMENTS ON INSTRUMENTATION

In the first model of the present study, the arrangement and positions of strain gauges were kept essentially the same as in the previous study [3]. In case of dial gauges two more gauges were introduced on each side wall and middle wall to give more information about the variation of deflections along the height of the model. A total number of 30 strain gauges and 39 dial gauges were used in the first model.

In the second model, 3 more dial gauges were introduced on each outer face of the side and middle walls to record deflections of these walls normal to the loading. Moreover 6 more strain gauges were added to the back wall of the model to find the variations of the strains in a cross-section located between two openings.

These modifications increased the total number of strain gauges and dial gauges for model II to 36 and 48 respectively.

These large numbers of gauges were necessary to obtain information about the strains and deflections at the various sections of the model. However, the testing of the two models in the present study has showed that there is not much variation in the values of strains at the top level of the model (i.e. at z = 89"). It is very difficult to record precisely these small variations in the strain gauges used at that level. The order of error introduced due to inherent properties of the electrical circuit used to measure the strain variations in these gauges has rendered these readings unreliable. Therefore, the author considers it unnecessary to use 10 strain gauges at the top level. The author recommends that no strain gauges be used at this level, these gauges can be introduced at some lower level of the model where more precise and reliable information can be expected.

The author would also recommend the introduction of more gauges at the back wall of the model. This would facilitate the determination of the exact pattern of variation of strains in the regions separated by bands of openings.

CHAPTER IV

OBSERVATIONS AND EXPERIMENTAL RESULTS

1. CRACKING PATTERN AT FAILURE

Fig. 11 and 12 show the photographs of crack patterns for the two models. The failure in the both models was accompanied by a lound sound, the crack appeared to start at the corner farthest from the loading point and then progressed rapidly in both directions into the side and back walls. The crack pattern at the back of the wall is almost straight for model I while for model II the cracks entered into the lower openings; this can be attributed to development of stress concentrations around these openings.

2. LOAD - STRAIN RESULTS

Fig. 20, 21 show the typical experimental strain values for different loads for location No. 6 of the two models. The strain patterns predicted by the two theories used for analysis which are described in Chapter V, have also been plotted on the same diagram for purposes of comparison. It can be seen that there is close agreement between theoretical and experimental values. The theoretical values are usually smaller than the experimental ones and strain values predicted by

Vlasov's theory are smaller than those predicted by Rosman's theory for the same transverse load.

Fig. 16 — 19 show the typical strain distribution pattern over the cross-section as predicted by Vlasov's theory. Fig. 25 - 28 show the strain pattern as predicted by Rosman's theory. For purposes of comparison, the experimental values have also been plotted on these diagrams. It can be seen that there is closer agreement between experimental strain values and those predicted by the two theories for model I. For model II, the values predicted by the two theories are smaller than the experimental ones at all locations escept for location No. 2 and 10. This shows that the presence of opening at the lowest storey of the model drastically changes the strain distribution pattern. Generally, Rosman's theory seems to depict larger values than Vlasov's theory except for location No. 8 and 9 where Vlasov's theory predicts larger values for strains than Rosman's theory.

3. LOAD - DEFLECTION RESULTS

Fig. 13 shows typical patterns of deflections along the height for various loads. For both the models, the deflection variation pattern is of the same type and the deflection of all the walls is approximately the same.

Fig. 14 shows rotation of the whole section for model II at an exaggerated scale. It can be observed that rotation of the whole section is of the same type as predicted by Vlasov's theory. However, the rotation of the corner farther from the point of load application is larger than that nearer to it. The deflections of the side and middle walls are approximately the same, and deflections of the middle line of the back wall are very small as compared to those of the corners at lower levels, but they become quite significant at higher levels. The deflections of the middle line take place in the same direction as those of the corner farther from the loading point.

CHAPTER V

ANALYSIS OF RESULTS

1. METHOD OF ANALYSIS BASED ON VLASOV'S THIN-WALLED BEAM THEORY

In the initial phase of this programme, the Vlasov's theory of thin-walled beams was adopted for the analysis of shear wall models without any floors or openings [3,16]. In the present study, two rows of openings have been introduced at the back wall of the model. Vlasov's theory does not take into account the presence of any such openings in the analysis of thin-walled beam. Since one of the main aims and objectives of this study is to correlate the results of the present stage of the programme with those of the previous one, it is useful to compare the behaviour of the present models with that predicted by Vlasov's theory. In this context it is important to note that it is not possible to compare directly the experimental results of the two phases due to changes in modelling and testing techniques which have changed the material properties and the line of action of loads. Since Vlasov's theory was found to be in good qualitative agreement with experimental results in the initial study, it shall be used to predict the behaviour of the present models without any openings. The comparison of these theoretical values with experimental ones will give an estimate of the effect of introducing the wall-openings. It will also check the validity of gross deflection calculation based on Vlasov's theory for thin-walled beam with openings, and probable errors introduced by using such a theory.

2. BRIEF DESCRIPTION OF VLASOV'S THEORY FOR THIN-WALLED BEAMS

Vlasov's theory of thin-walled beams is described in detail in his book entitled "Thin-Walled Elastic Beams" [16]. A comprehensive account of this thoery has also been given by Afsar [3].

The theory is based on two geometrical hypotheses. The first is that a thin-walled beam can be considered as a shell of rigid (undeformable) section. This means that the stresses (normal or tangential) on the cross-section of the beam do not change when the external transverse load on the beam element is replaced by another load statically equivalent to the first one. According to the second assumption, the shearing deformations of the middle surface can be assumed to vanish. This means that the coordinate lines which are initially orthogonal, remain orthogonal after deformation and a small change in the angle between these lines is neglected.

Making use of these two hypotheses, Vlasov derived the following expressions for transverse deflections:

$$V(Z,y) = \xi(Z) - (y-a_y)\ \theta(Z) \quad - (1)$$

$$W(Z,x) = \eta(Z) + (x-a_x)\ \theta(Z) \quad - (2)$$

where V and W are the displacements of a point with coordinates x and y along coordinate axes ox and oy respectively and a_x and a_y are the coordinates of the shear centre (see Fig. 15).

Equations (1) and (2) mean that transverse displacement of the cross-section of the beam in its own plane can be regarded as consisting of rigid body displacement and its rotation about the shear centre of the section which acts as an instantaneous centre of rotation for the section. This has been illustrated in Fig. 15.

The second assumption leads to the conclusion that the longitudinal displacements u(Z,s) in the section Z = const. of a thin-walled beam of open cross-section are made up of displacements linear in the cartesian coordinates of the point on the profile line and displacements proportional to the sectorial area.* This is true provided that there are no bending deformations of the cross-section and the middle surface is free of shear.

---

* Refer to Appendix B for defination.

Mathematically, it can be written as

$$u(Z,s) = \zeta(Z) - \xi'(Z)\ x(s) - \eta'(Z)\ y(s) - \theta'(Z)\ \omega(s) \qquad - (3)$$

where $\zeta(Z)$ is an arbitrary function describing the longitudinal displacement of the point which serves as the origin of the coordinates s, and $\omega(s)$ is the sectorial area of the point under consideration with coordinates $x(s)$ and $y(s)$.

Equation (3) on differentiation yields the expression for the longitudinal strain 'ε',

$$\varepsilon = \frac{du}{dZ} = \zeta'(Z) - \xi''(Z)\ x(s) - \eta''(Z)\ y(s) - \theta''(Z)\ \omega(s) \qquad - (4)$$

Equations (1) and (4) allow the determination of the deflections and longitudinal strains at any point of the middle surface of a thin-walled beam when the four functions ζ, ξ, η and θ are known.

These functions can be evaluated from the following linearly uncoupled differential equations derived from equilibrium considerations.

$$E\ A\ \zeta'' = 0 \qquad (5)$$

$$E\ I_y\ \xi^{IV} = q_x \qquad (6)$$

$$E\ I_x\ \eta^{IV} = q_y \qquad (7)$$

$$E\ I_\omega\ \theta^{IV} - G\ I_d\ \theta'' = m \qquad (8)$$

These equations are simplified forms of Vlasov's differential equations of equilibrium for a beam in principal coordinates for the use when the lateral edges of the beam are free from shear forces and the external load is composed only of transverse specific forces $q_x(Z)$ and $q_y(Z)$ and a moment $m(Z)$.

Boundary Conditions:

The boundary conditions for the present case are similar to that of a cantilever beam, fixed at the bottom and free at the top. The transverse load has an eccentricity 'e' equal to the distance of the shear centre from the back wall of the model. This causes combined flexural and torsional stresses in the model.

There are no applied loads in the x and Z directions, hence functions ζ and ξ are both zero. The compressive stresses due to self weight of the model have been neglected. The solution of basic equations (7) and (8) for these boundary conditions has been given in reference [3]. The resulting equations are,

$$\eta(Z) = \frac{Q}{6E\ I_x}\ (3\ \ell_m Z^2 - Z^3) \tag{9}$$

$$\eta''(Z) = \frac{Q}{E\ I_x}\ (\ell_m - Z) \tag{10}$$

$$\theta(Z) = \frac{Q.e}{G.\ I_d}\ [Z - \frac{\ell_m}{K}\ (\tanh K(1-\cosh \frac{K}{\ell_m} Z) + \sinh \frac{K}{\ell_m} Z)] \tag{11}$$

$$\theta''(Z) = \frac{Q.e}{G.\ I_d} \cdot \frac{K}{\ell_m}\ [\tanh K \cosh \frac{K}{\ell_m} Z - \sinh \frac{K}{\ell_m} Z] \tag{12}$$

where,

$$\frac{K}{\ell_m} = \sqrt{\frac{G\ I_d}{E\ I_\omega}}\quad , \quad \text{and } \ell_m = \text{length of the model.}$$

The values of transverse deflections $V(Z,y)$ and $W(Z,x)$ and longitudinal strains $\varepsilon(Z,s)$ are computed from the following relationships.

$$V(Z,y) = -y\ \theta(Z) \tag{13}$$

$$W(Z,x) = \eta(Z) + (x - a_x)\ \theta(Z) \tag{14}$$

$$\varepsilon(Z,x) = -\eta''(Z)\ y(s) - \theta''(Z)\ \omega(s) \tag{15}$$

3. COMPARISON OF TYPICAL RESULTS

(a) Comparison on the basis of recorded strains:

Fig. 16 - 19 show the comparison of the strains across some typical sections of the two models for loads 250 and 500 lbs. It is interesting to note that for both the models, strains with the exception of location No. 5 very well agree qualitatively with those predicted by Vlasov. However, the experimental values at section Z = 17" for model I indicate large deviation from theoretical values for location Nos. 8 and 9. These values are approximately 150% of those predicted by theory. These differences decrease at higher section (Z = 53") of the model and differences reduce to 50 - 100%.

The differences between theoretical and experimental values are very large for model II. With the exception of location Nos. 2 and 6, the experimental values are 50 to 500% greater than the theoretical ones. The large differences are prominent for location Nos. 1, 8 and 9. This shows that the extension of the openings to the lowest storey of the model drastically changes the strain distribution pattern.

However, one trend is very obvious in strain values for both the models, and that is the strain variations for location Nos. 8 and 9 are symmetrical about the datum line and if they are joined by a straight line it locates the point of intersection of middle wall and the back wall as point of zero strain.

Fig. 20 and 21 show the load-strain curve for both the models for location No. 6 at the lowest level where strains were recorded. The experimental strain values are greater than the theoretical ones but the agreement is much closer for model I than model II. Maximum difference for model I is 20% against 50% for model II.

(b) Comparison of the deflections:

The tables 3 and 4 given on the following page show the comparison between the deflections given by theory and those recorded experimentally by dial gauges. There is no relationship between the theoretical and experimental values. The experimental deflections are far larger than the theoretical ones.

Height 'Z'	Deflections for Model I			Deflections for Model II		
	Theoretical 10^{-3} x inch	Experimental 10^{-3} x inch	$\frac{\text{Experimental}}{\text{Theoretical}}$	Theoretical 10^{-3} x inch	Experimental 10^{-3} x inch	$\frac{\text{Experimental}}{\text{Theoretical}}$
17"	0.3	12.3	41	.3	7.0	23
29"	1.0	25.4	25	0.9	13.5	15
41"	1.8	33.4	19	1.6	21.0	13
53"	2.9	49.0	17	2.6	29.0	11
65"	4.2	60.0	14	3.7	36.0	10
77"	5.5	73.0	13	4.9	44.0	9
89"	7.0	83.0	12	6.2	52.0	8

TABLE 3 Comparison of Deflections at Location (1) for load = 250 lb.

Height 'Z'	Deflections for Model I			Deflections for Model II		
	Theoretical 10^{-3} x inch	Experimental 10^{-3} x inch	$\frac{\text{Experimental}}{\text{Theoretical}}$	Theoretical 10^{-3} x inch	Experimental 10^{-3} x inch	$\frac{\text{Experimental}}{\text{Theoretical}}$
17"	0.2	8.5	43	0.2	6.8	34
53"	1.4	31.0	22	1.3	16.0	12
89"	3.4	52.0	15	3.0	28.0	9

TABLE 4 Comparison of Deflections at Location (2) for load = 250 lb.

For model I the deflections determined experimentally are 12 to 41 times those predicted by the theory for location No. 1. The ratio falls rapidly as the height increases from Z = 17" to Z = 89". A similar trend is observed for location No. 2 of model I, and it is also present in the behaviour of model II at both the locations.

Fig. 14 shows the rotation of model II at Z = 53" based on recorded deflections for loads 250 and 500 lbs. It can be observed that the deflections of corner nearer to the loading point are about 60% of the deflections of the corner farther from the loading point. The same trend is also present in the behaviour of model I but the percentage difference is only 30%.

4. DISCUSSION OF THE CONDITIONS AFFECTING RESULTS

(a) Effect of the openings:

The major factor accounting for the discrepancies between the theoretical and experimental behaviour of the two models is the presence of openings in the experimental models. Since these openings have been provided in two rows placed symmetrically at the back wall of the model, they divide the model into three distinct solid regions. These solid regions consist of two 'L' shaped piers and one 'T' shaped pier in the middle; these three can be imagined to be connected by two perforated regions. These regions which are pierced with openings will offer little resistance to normal forces or moments. Therefore, rotation of the piers about these regions containing openings can take place without much resistance being offered from this region. The observation that this effect is more pronounced for model II than model I, is in accord with this statement.

Table 5 shows the differential rotation of the side piers for model I at different levels for various loads which have been computed from experimental results. It also shows the rotation of each side pier about the perforated region which have been computed with the assumption that both the piers deflect equally, and the middle pier assumes an intermediate position between the two.

It must be carefully noted that the principal axes of the side piers are inclined to the line of action of loading (Fig. 24) such that the deflection of the two side piers will take place parallel to the line of action of loading as well as in a direction perpendicular to it. This results in the increased rotation of these piers about the perforated region. It should also be observed that the second model contained one more opening per row than the first one. This additional opening will have the effect of increasing the rotation of these piers as the resistance of the perforated region will be lesser in this case than for the model I. This means that the effect would be more

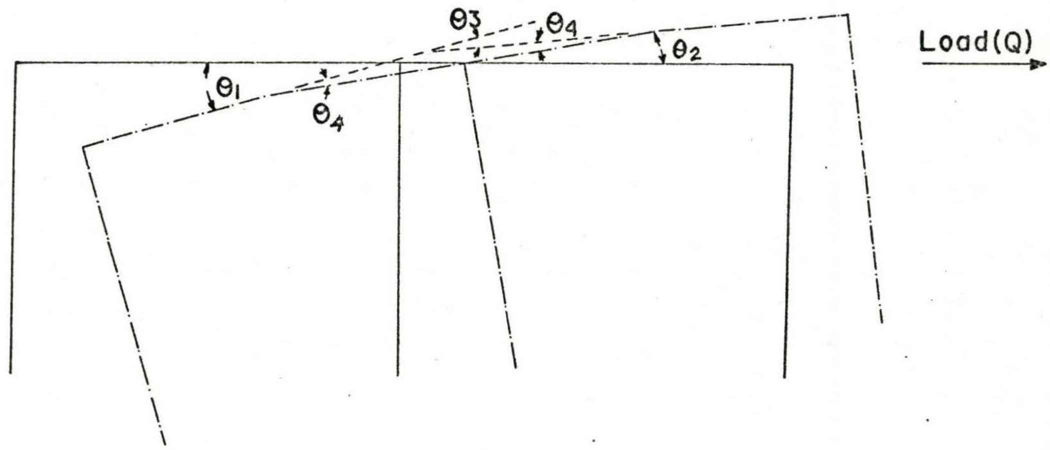

Assumed Deflected Cross-Section

Load Q	Height Z	Angle θ_1 $10^{-4}\times$ rad	Angle θ_2 10^{-4} rad	Angle $\theta_3=\theta_1-\theta_2$ $10^{-4}\times$ rad	Angle $\theta_4=\theta_3/2$
250 lbs.	17" 53" 89"	6.05 16.00 32.50	4.40 10.00 19.00	1.65 6.00 13.50	0.83 3.00 6.75
500 lbs.	17" 53" 89"	14.05 38.00 74.50	9.15 21.50 39.00	4.90 16.50 35.50	2.45 8.25 17.75

TABLE 5

ROTATION OF THE PIERS ABOUT PIERCED REGION FOR MODEL I pronounced for model II than model I.

This also leads to the conclusion that the basic assumption in Vlasov's theory that the cross-section of the beam can be treated as rigid for transverse loads is not valid for models with bands of wall-openings.

The model does not contain a completely rigid section as envisaged in Vlasov's theory, however, it will be more realistic to treat the section as consisting of three solid rigid sections connected by a diaphragm as explained earlier. Therefore, the behaviour of the model will be similar to a composite body made of three piers connected by two similar diaphragms. This composite approach has been adopted by Rosman [9] and analysis of the present models according to this approach shall be given in the following sections of this chapter.

Another major effect introduced by the openings is observed in the behaviour of the strains over the cross-section of the model. In Vlasov's theory these strains are supposed to vary linearly over the cross-section of the thin-walled beam. Fig. 16 - 19 show the variation of the strains over the cross-section of the two models and they clearly indicate that actual strain variation on the back wall of the model is not linear. Hence the Vlasov's theory will give erroneous results if employed to predict the behaviour of thin-walled beam containing openings.

(b) Effect of other factors:

(i) Non-uniform thickness of the different walls of the models

As mentioned earlier, the two experimental models had walls of thickness varying from height to height. Table 2 shows the thickness of the various points on the cross-section of the model I for different levels. This variation is at random without following any observable pattern. Also, this variation of thickness was more pronounced for model II. The theoretical models representing the two experimental ones as shown in Fig. 22, were assumed to have walls of uniform thickness throughout the whole height which was computed as the average over the whole height from Table 1. The side walls were supposed to have equal average values.

It is very difficult to evaluate the effects of this thickness variation on the overall behaviour of the model as this variation is at random without following any observable pattern. However, if the model contains walls of different thicknesses then the shear centre will not lie at the line of symmetry of the section. Any shift of the shear centre from line of symmetry will result in unequal deflections of the two corners of the model. The deflection pattern at the back wall of the models indicates that the shear centre at higher levels has shifted towards the corner nearer to the loading point. This shift in the shear centre is the major cause of unequal deflections of the two corners of the models.

The shifting of the shear centre from the line of symmetry will also disturb the symmetrical pattern of distribution of the strains across the cross-section of the theoretical model without any wall-openings. However, it can be very well expected that since the average dimensions of the actual models have been taken in the representative models for analysis, there should not be any major effect of the thickness variation on the maximum stresses.

(ii) Effect of the top plate:

The top plate consists of loading plate and an auxiliary plate which serves the purpose of retaining the geometrical shape of the cross-section of the model. It may be argued that the presence of such a plate at the top of the model would restrict the warping of the section at that level and this may change the assumed boundary conditions. However, Afsar [3] has investigated the effect of such a plate and has reported no apparent change in the boundary conditions.

5. ROSMAN'S THEORY AS METHOD OF ANALYSIS

As stated in chapter I, Rosman [9] has presented a mathematical model of the behaviour of shear walls having one or two rows of openings, and subjected to lateral loads. It was decided to attempt an analysis of the models based on this approach in addition to the analysis discussed previously.

The basic concept in this approach consists in the replacement of the connecting beams by a continuous lamina connection (Fig. 23). The integral shear forces in the continuous connections of individual piers are chosen as the statically redundant functions. Deformations due to bending moment, the contribution of normal forces in the piers and shear forces in the connecting beams are taken into account.

The following assumptions have been made in this approach (Refer to Fig. 23 and 24):

(i) The upper end beam has one-half the cross-section of an interior connecting beam.

(ii) Walls containing two bands of openings are assumed to be symmetric.

(iii) The points of contraflexure of the connecting beams are assumed to be at midspan.

(iv) The connecting beams have rectangular cross-sections and they are considered absolutely rigid in their longitudinal direction.

With the last two assumptions, the piers will deflect equally. The laminas are considered cut at their mid-points, and shear forces T' are considered to be acting at the points of contraflexure (see Fig. 23). On considering the deformations of the cut laminas, compatibility conditions may be set up to give zero resultant relative deformation at the cut, and this leads to the establishment of the following second order differential equation governing the variation of integral shear force T (Detailed derivations given in Appendix C).

$$\frac{d^2T}{dz2} - \alpha^2 T = -\gamma z^2 \tag{16}$$

where $$T = \int_0^x T'dz$$

is the integral of the shear force in the continuous connection, from the top of the wall to the position z, with

$$\alpha^2 = \frac{12\ I_p}{hb^3} \left(\frac{2H^2}{2I_1+I_2} + 1/A_1\right)$$

$$\gamma = \frac{Q.\ell}{2I_1+I_2} \cdot \frac{12\ I_p}{hb^3}$$

and I_p is the reduced moment of inertia of the connecting beam which has been introduced to take the influence of the shear forces in these beams

$$I_p = \frac{I_{po}}{1+2.4\left(\frac{hp}{b}\right)^2}$$

The differential equation (16) when solved for the proper boundary conditions applicable to the present case, yields

$$T = c \text{ Sinh } \quad z + \frac{\gamma}{\alpha^2} \quad z \tag{17}$$

where
$$c = - \frac{\gamma}{\alpha^3 \text{ Cosh } \alpha\ell} \tag{18}$$

Rosman's theory is applicable to shear walls having rectangular openings while the present study is concerned with circular openings. Stiller [25] conducted an investigation into the stresses associated with openings of various shapes in a shear wall. He concluded that there is very little difference in the overall stresses associated with openings of various shapes if the areas of the openings are equal. Only in the case of very wide openings in narrow diaphragms is the difference likely to become considerable. This leads to the conclusion that rectangular openings can be substituted for the circular openings such that the areas of the two sets of openings are equal. Rectangular openings of breadth = 5.000" and depth = 3.938" satisfy this condition, hence they have been selected in the theoretical model for Rosman's theory as shown in Fig. 24. Th e span of the beam 'b' has been kept at 5 inches which is essentially the same as in the experimental models. This also keeps the dimensions of the different piers identical with those used in the experimental model.

6. COMPARISON OF TYPICAL RESULTS

(a) Comparison on the basis of recorded strains.

Fig. 25-28 show the comparison of theoretical strains with those recorded experimentally for the two models. It can be seen that there is good agreement between the two values for model I. For model II there is qualitative agreement except for the gauge location No. 5 where the signs of the strains do not agree for height Z = 53". Generally the reocrded strains are greater than the theoretical ones for locations (8) and (9) in the middle pier of both the models.

Load strain curves given in Fig. 20 and 21 for location No. 6 show that the strain values as predicted by Rosman's theory for a given load are greater than those predicted by Vlasov's theory. A comparison of these theoretical values with experimental ones shows that Rosman's theory gives a better estimate of the strains.

(b) Comparison of Deflections

Fig. 29-32 show the comparison of deflections recorded experimentally with those computed theoretically. It can be seen that for model No. 1 the deflections recorded experimentally for location 5 are larger than those predicted by the theory. The ratio of experimental to theoretical deflections is 4.4 at Z = 17", which falls off gradually to 1.47 at Z = 89". For location No. 5, the deflections predicted by the theory become larger than those recorded in the laboratory at about Z = 80" while for lower levels they are smaller than the experimental ones. The ratio of experimental to theoretical deflections at this location is 3.5 at Z = 17", 1.3 at Z = 53" and only 0.91 at Z = 89". This shows that there is good agreement of theoretical and experimental values at the top of the model.

For model No. 2, the experimental deflections and those predicted by Rosman's theory are generally of the same order. The experimental value is 3.04 times the theoretical value at Z = 17" and is 0.90 times the theoretical value at Z = 89". At location 6, the theoretical values are generally larger than those recorded experimentally. At Z = 53", the experimental deflection is approximately the same as that predicted by the theory, while at Z = 89", it is only 0.70 times the theoretical one.

7. DISCUSSION ON FACTORS AFFECTING THE RESULTS FOR ROSMAN'S THEORY

(a) In Rosman's theory, the connecting beams have been assumed to be rigid in their own planes. In the derivation of compatibility equation the axial shortening of the connecting beam has been neglected. Fig. 33 shows the forces acting on the connecting beams transferred to the piers. If 'My' denotes the moment caused by these axial forces, then the moments acting on each side pier will be

$$M_{r1} = M_1 - My \qquad \text{(a)}$$

and that in the middle pier

$$M_{r2} = M_2 + 2My \qquad \text{(b)}$$

Hence it can be seen that these axial forces will modify the moments acting on the three piers according to equations (a) and (b). In the present case these forces will also cause moments about the longitudinal axes of the piers which will cause torsion of these piers.

This means that these axial forces will have significant effect on the behaviour of the model, and neglecting these forces is the major cause of the discrepancy between the theoretical and experimental results.

(b) In Rosman's theory, all the piers are assumed to have approximately the same rigidities so that the points of contraflexure in the connecting beams can be assumed at midspan. In the present study the side piers have moments of inertia equal to 34.4 m^4 while central pier has a moment of inertia equal to 151.3 in^4. This means that rigidity of the middle pier is 4.3 times the rigidities of the adjacent piers. This can cause an appreciable amount of shift in the point of contraflexure. However, Schwaighofer [26] has reported that no observable shift in the points of contraflexure of the connecting beams as long as the ratio of rigidities of the adjacent walls is equal or less than 8. His conclusion is based on the results of photoelastic tests conducted on two interconnected walls. If the same results are taken as applicable to the present case, there would not be any significant effect on the state of stress in the model.

(c) It has been mentioned before that Rosman has adopted wide column analogy in his theory. This means that the span of the connecting beams has been assumed the same as the clear span of the opening. This assumption is questionable since the connecting beam which is supposed to cantilever from the adjacent pier will have some extension in the pier. This extended cantilever would retain its constant moment of inertia and cross-sectional values for some distance into the pier, when the remaining pier would be effectively a rigid arm. Michael [27] has suggested that account can be taken of the joint flexibility by extending the beam length into the pier by an amount equal to half the beam depth.

Calculations were made for strains and deflections for model II in which the span of the connecting beams was increased by an amount equal to half the beam depth as suggested by Michael [27]. A slight increase in strains for locations (5) and (6) was noticed at level Z = 5", while for location (7), there was a slight decrease in strain. For a load Q = 250 lb., and level Z = 5", the increment in strains for locations (5) and (6) was 0.08 and 0.15 μ-inch/inch respectively, while for location (7) the decrease in strains was 0.35 μ-inch/inch. At higher levels no significant change in strains was noticed.

The effect of this modification on deflections of the model was even less significant. For a load Q = 500 lb., the deflection at level Z = 89" increased from 0.102081 inch to 0.102116 inch which means an increment of 3.5×10^{-5} inch. This increment becomes smaller at the lower levels of the model, reducing to 1.3×10^{-5} inch at Z = 53".

CHAPTER VI

CONCLUSIONS AND RECOMMENDATIONS

1. CONCLUSIONS BASED ON EXPERIMENTAL RESULTS

(a) The introduction of rows of openings in shear wall models changes the pattern of strain distribution across the cross-section and results in a significant increase in the deflections of the model.

(b) Even though the diameter of the wall openings in the models was smaller than the space between openings, the present study shows that the introduction of such openings in rows in shear wall models drastically changes the behaviour of the models and the effect of these rows of openings cannot be ignored.

(c) There is a marked difference between the behaviour of a model having openings in second and higher floors and that having openings in the bottom floor as well. The extension of the rows of openings to the bottom floor markedly changes the distribution of strains across the cross-section.

2. CONCLUSIONS BASED ON METHODS OF ANALYSIS

(a) On the basis of the comparisons of the experimental results with those predicted by the two theories used for analysis, it is concluded that Rosman's theory gives better correlation between the predicted and experimental curves.

(b) Vlasov's theory gives good qualitative account of the overall behaviour of the models. But quantitatively the results predicted by this theory and especially those for the deflections are in gross error. This leads to the conclusion that Vlasov's theory cannot be used to give a quantitative estimate of the behaviour of these particular models.

(c) Rosman's theory can be used to predict the behaviour of the shear wall models having rows of circular wall openings if the areas of the set of rectangular openings used in the theoretical models are set equal to those of the circular openings used in the experimental models.

(d) In spite of the experimental scatter, Rosman's theory predicts strain distributions across the section which are in fair agreement with the experimental results. The deflection near the top of the models as predicted by this theory is fairly close to the experimental value. Therefore, Rosman's theory can be used to predict the maximum deflection of the shear wall models having rows of wall openings.

3. A COMPREHENSIVE REVIEW OF THE EXPERIMENTAL PROCEDURES AND RECOMMENDATIONS

The modelling technique evolved during the past and present experimental studies seems to have solved the

the major problem of getting completely sound models without any cracks. Some of the suggestions given in section (2.6) were carried out on the formworks used in the concurrent study. It has yielded better results in terms of the control of the dimensions of the model and alignment of component walls. However, the finished models obtained in the present study did not appear to have homogeneous surface throughout. The segregation of the concrete mix due to extensive vibrations was the major cause of this defect in the models, and the effect was more pronounced near the free edges of the prong walls of the model. The author would, therefore, suggest the avoidance of excessive vibrations being given to the formwork during the casting of the models. Hopefully, a good judgement in this direction can yield models with homogeneous surface throughout.

As far as curing, drying and placing of the models is concerned, it is recommended that they should be kept essentially the same as practised in the present and initial studies of this programme. Care should be taken that model be kept wet while in formwork. Drying of the models should be allowed only when the formwork has been stripped off, otherwise shrinkage stresses set up in the model may cause its cracking.

The technique of fixing the base and loading cap have proved to be quite reliable in the present and concurrent experimentations. The loading system has given very good control of the load during both loading and unloading cycles. Therefore, it will be advisable to retain these techniques in the future experimentations.

As stated before in section (3.4), the author would like to make some recommendations as far as instrumentation of the models is concerned. The author recommends that no strain gauges be used at the top level of the model (i.e. at Z = 89"). The author would also recommend that more strain gauges be introduced at the back wall of the model so that exact pattern of variation of strains in the regions separated by openings may be determined.

The deflection gauges in the present study were mounted at seven different levels on the prong walls of the model. The experimental results of the present and the past studies have shown that the deflections of all the three prong walls of the model are the same. Therefore, the author would recommend that only three main levels (i.e. Z = 17", 53" and 89") be retained for mounting the deflection gauges. For obtaining further information about the deflection variation along the height of the model, extra deflection gauges can be mounted at intermediate levels on any one of the three prong walls.

Hopefully, these recommendations about instrumentation may save some of the time spent on mounting these large numbers of deflection and strain gauges.

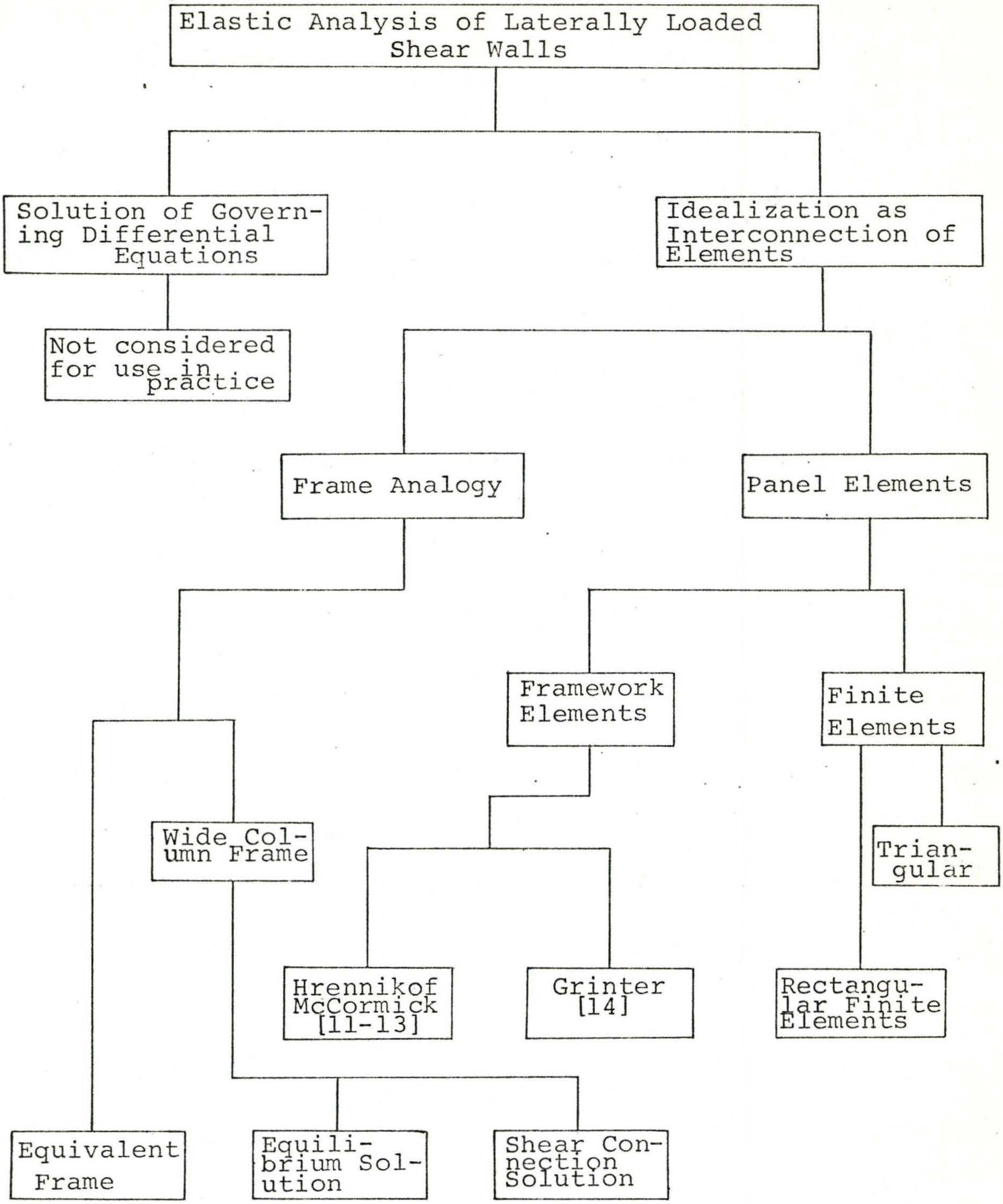

Fig. 1 - Flow Diagram Showing Possible Methods of Analysis of Shear Walls

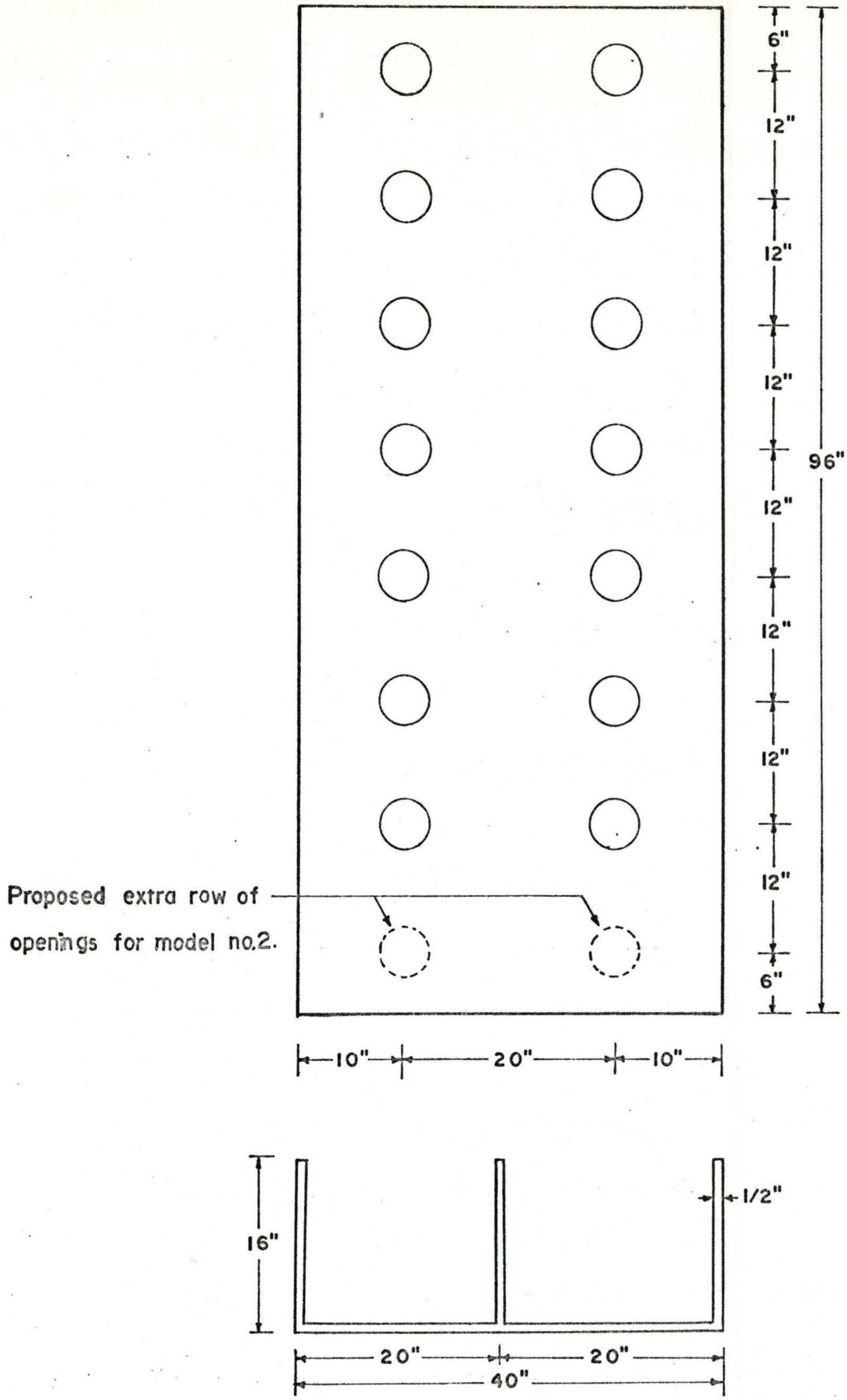

FIG. 2 — A DIMENSIONAL SKETCH OF THE PROPOSED MODELS.

Fig. 3a

Photograph Showing the Formwork with Disks in Place, Ready for Pouring of Model I

Fig. 3b Photograph of Model I Showing the Position of the Openings

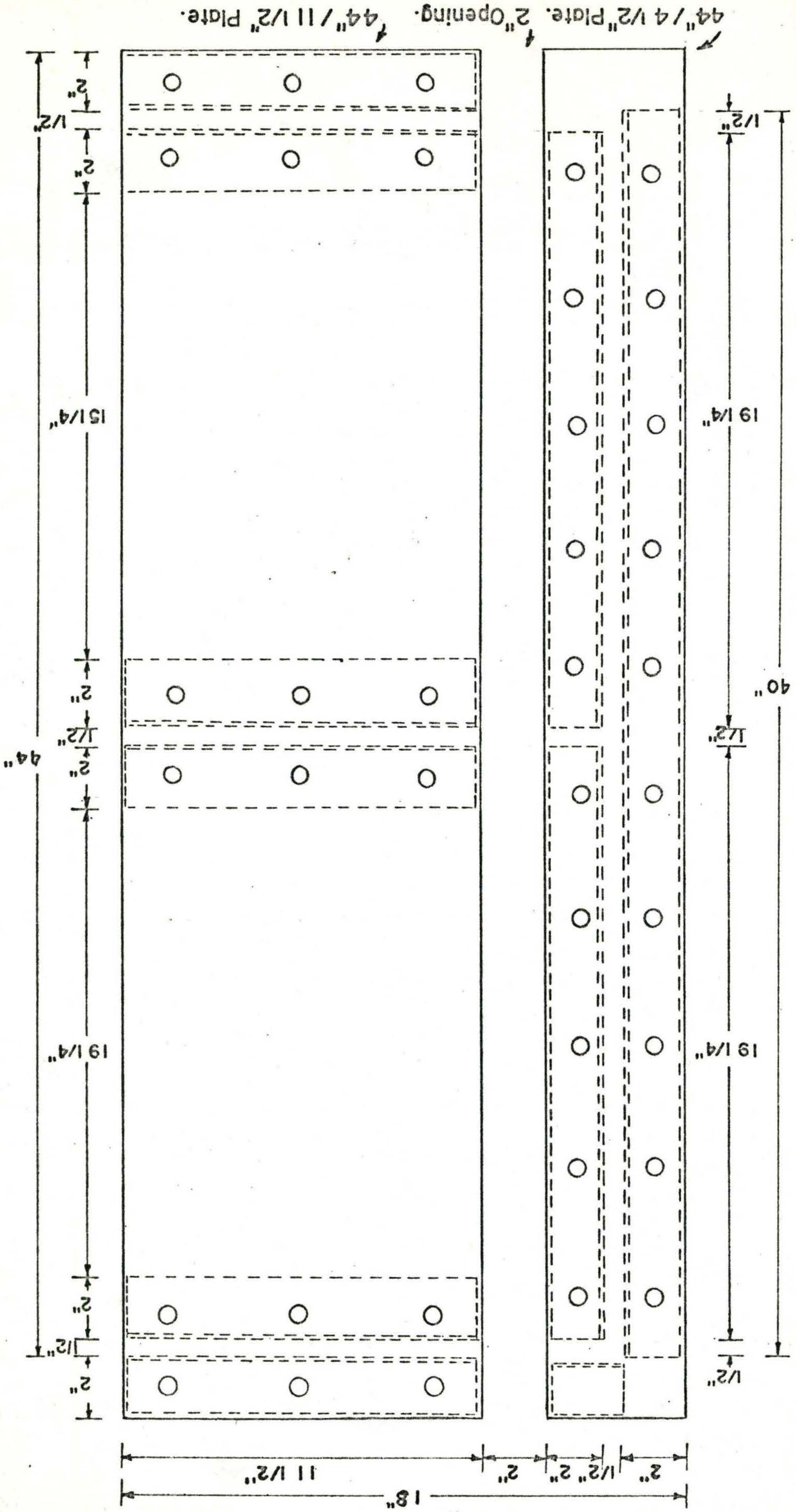

FIG. 4—LOADING CAP WITH TOP PLATE.

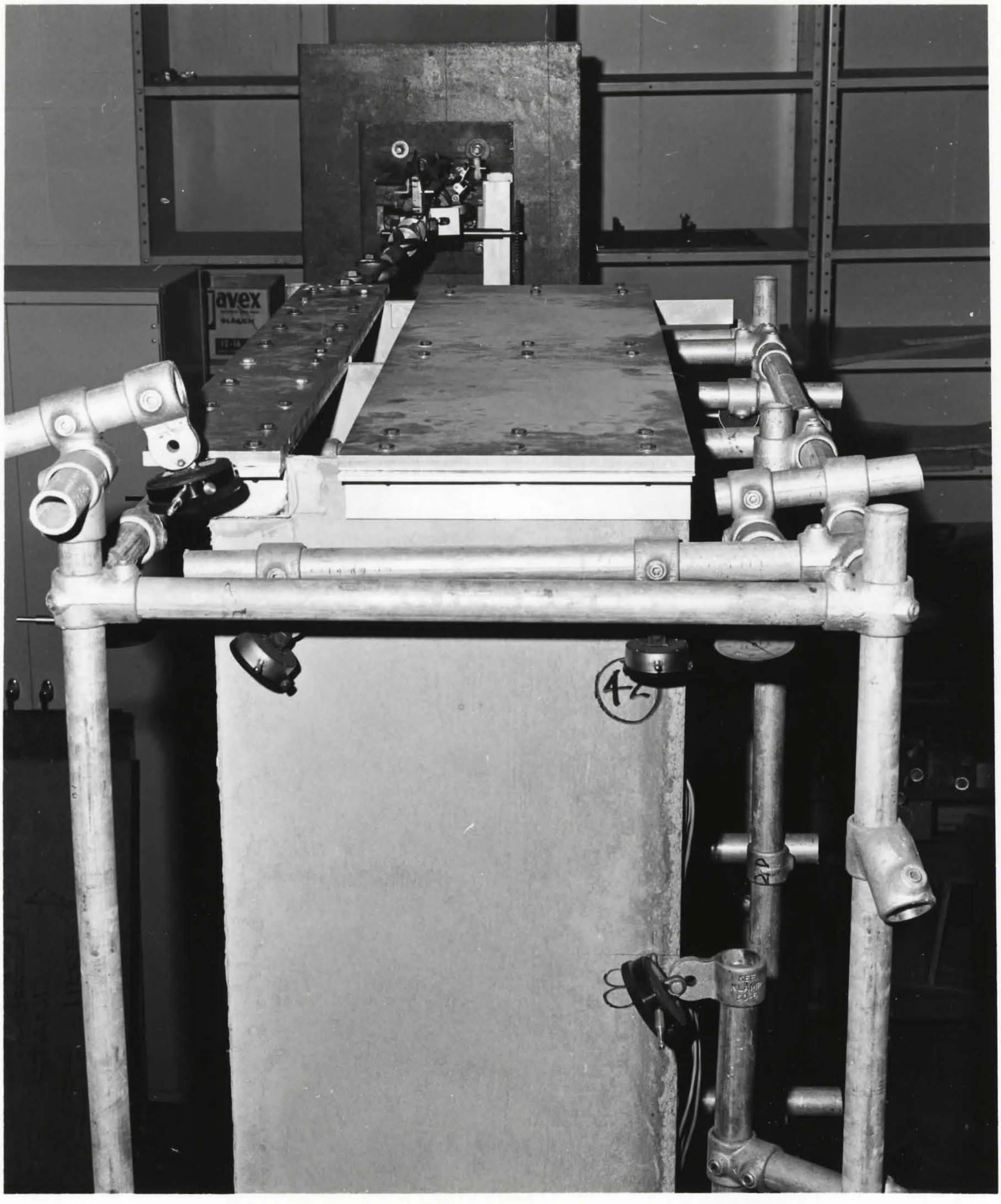

Fig. 5

Photograph Showing the Top Plate and Loading Cap in Position

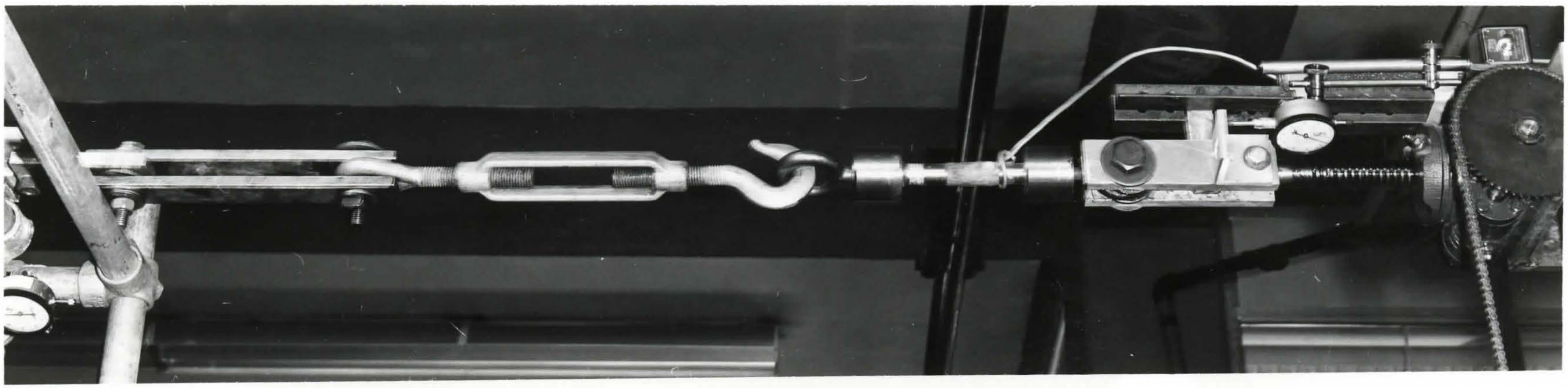

Fig. 6

Photograph Showing a Partial View of the Loading Device and Various Elements Connecting that Loading Device and Loading Cap

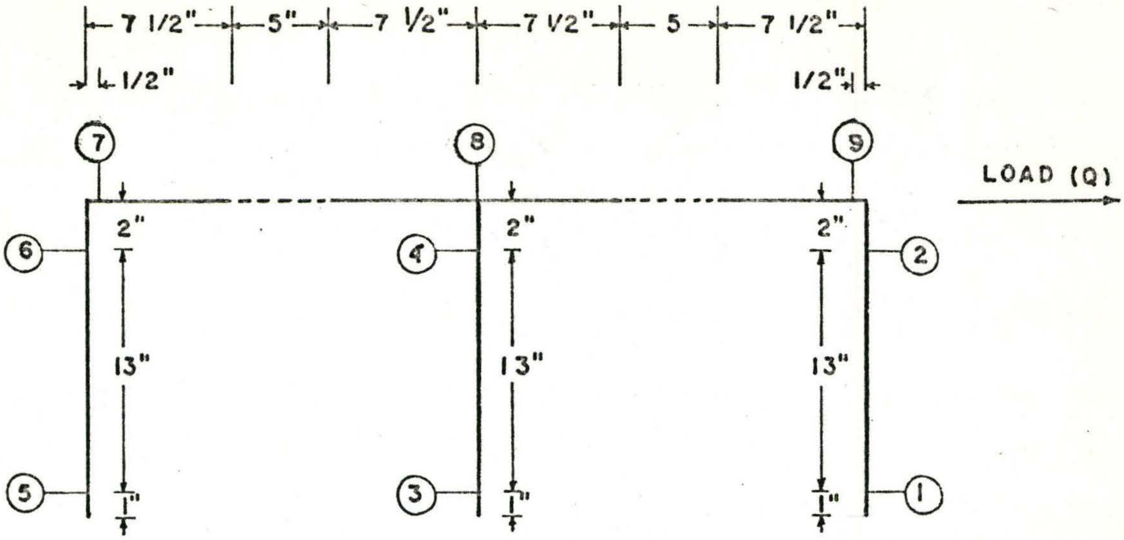

Z = 17", 53" & 89".

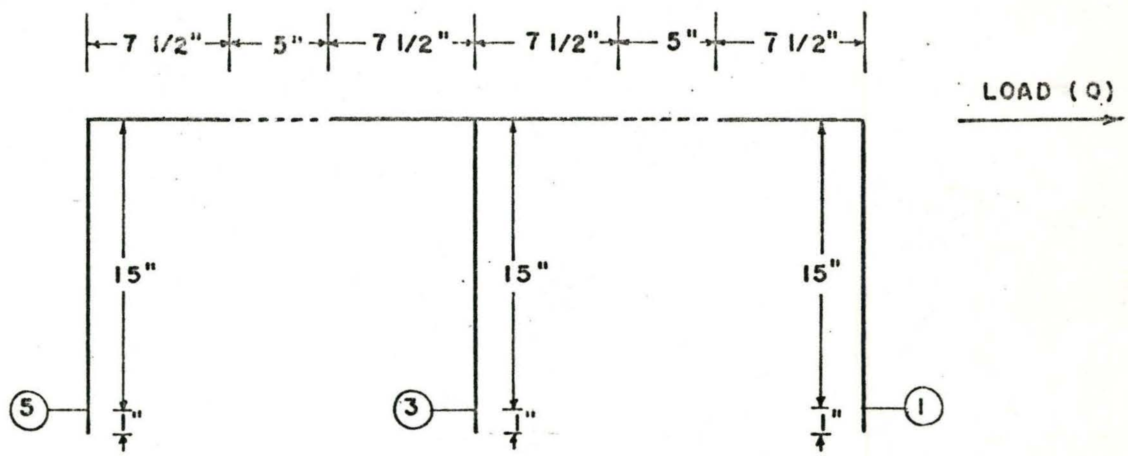

Z = 29", 41", 65" & 77".

FIG.7 _ LOCATION OF DIAL GAUGES.

MODEL NO.1.

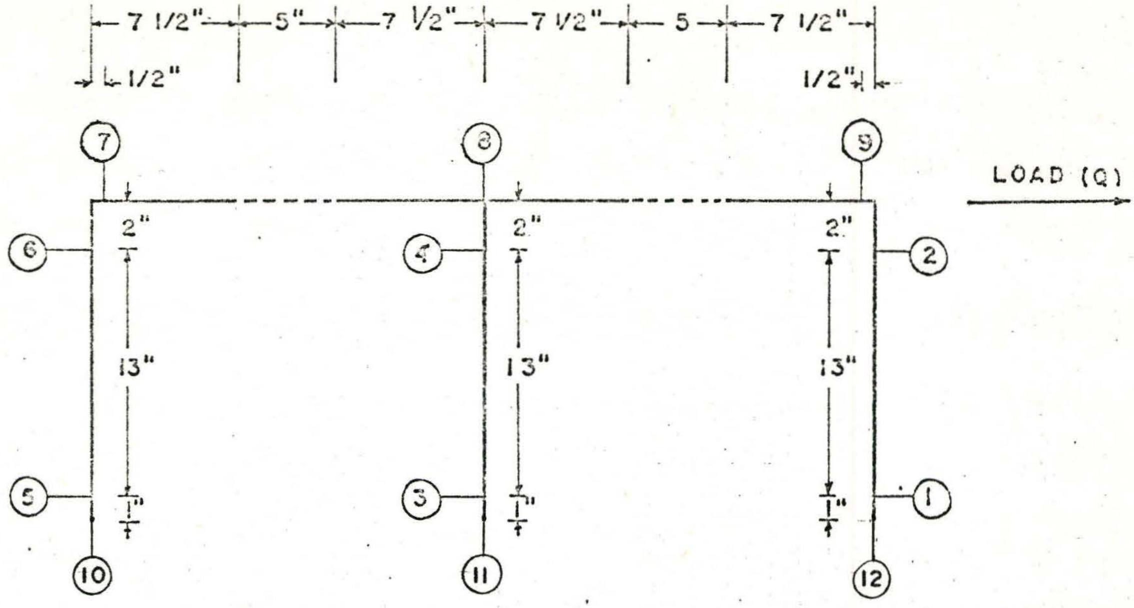

Z = 17", 53" & 89".

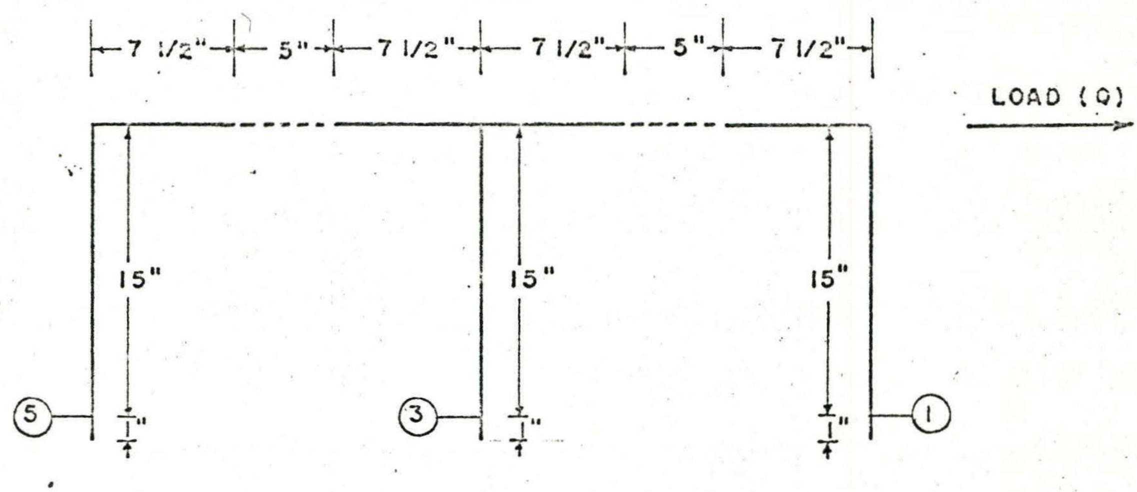

Z = 29", 41", 65" & 77".

FIG. 8 — LOCATION OF DIAL GAUGES.

MODEL NO.2.

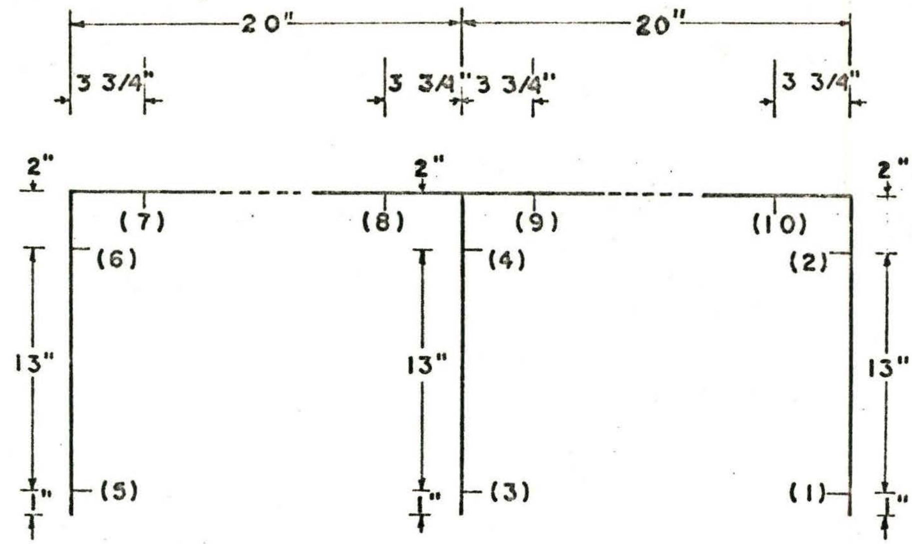

(A) Z = 17", 53" & 89".

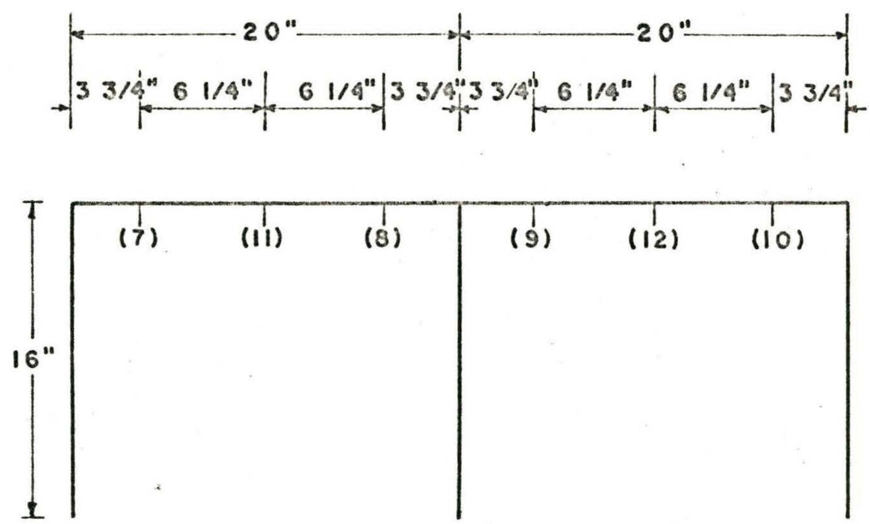

Z = 11".

(B) EXTRA STRAIN GAUGES FOR MODEL NO. 2.

FIG. 9 _ LOCATION OF STRAIN GAUGES.

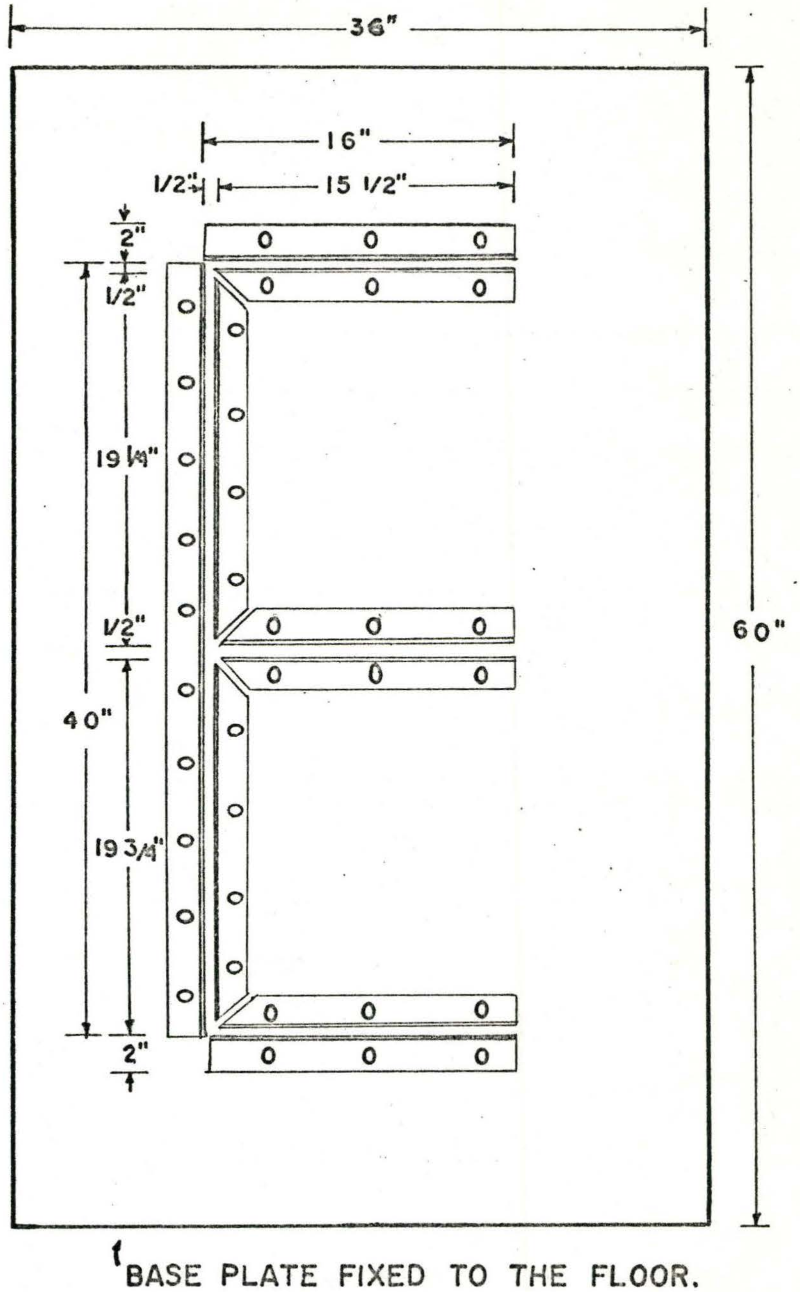

All angles used are of size 2"X2"X1/4."

FIG. 10_ARRANGEMENT OF THE ANGLES USED TO FIX THE BOTTOM OF THE MODELS.

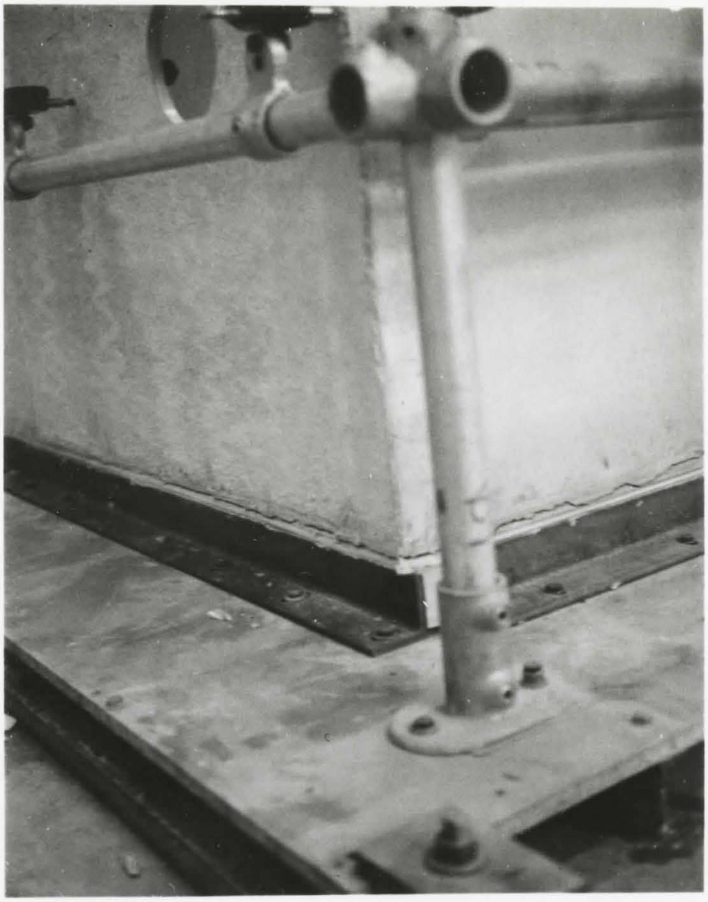

Photographs Showing the Crack Patterns for Model I

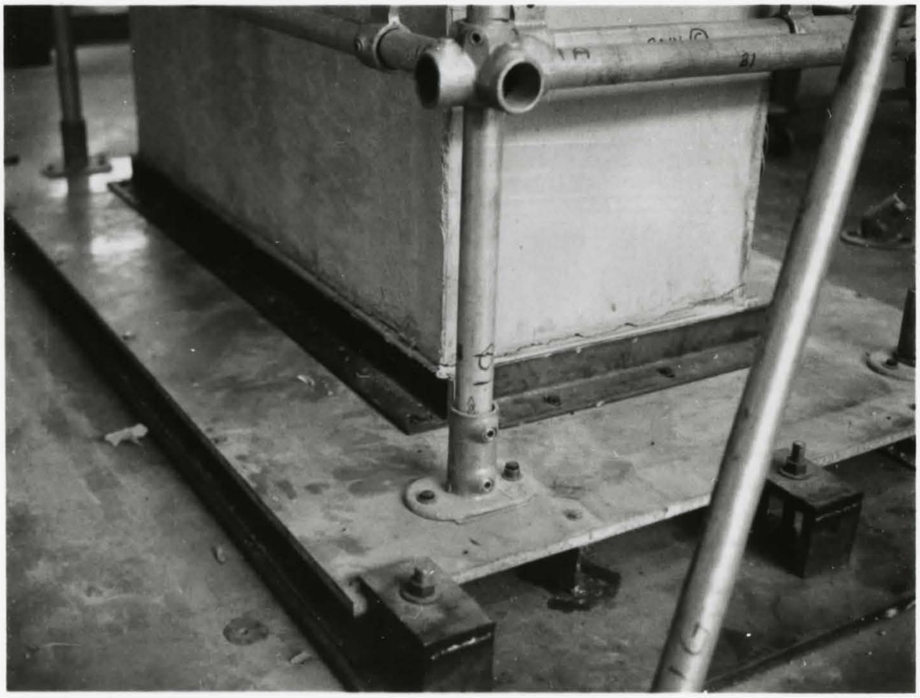

Fig. 11

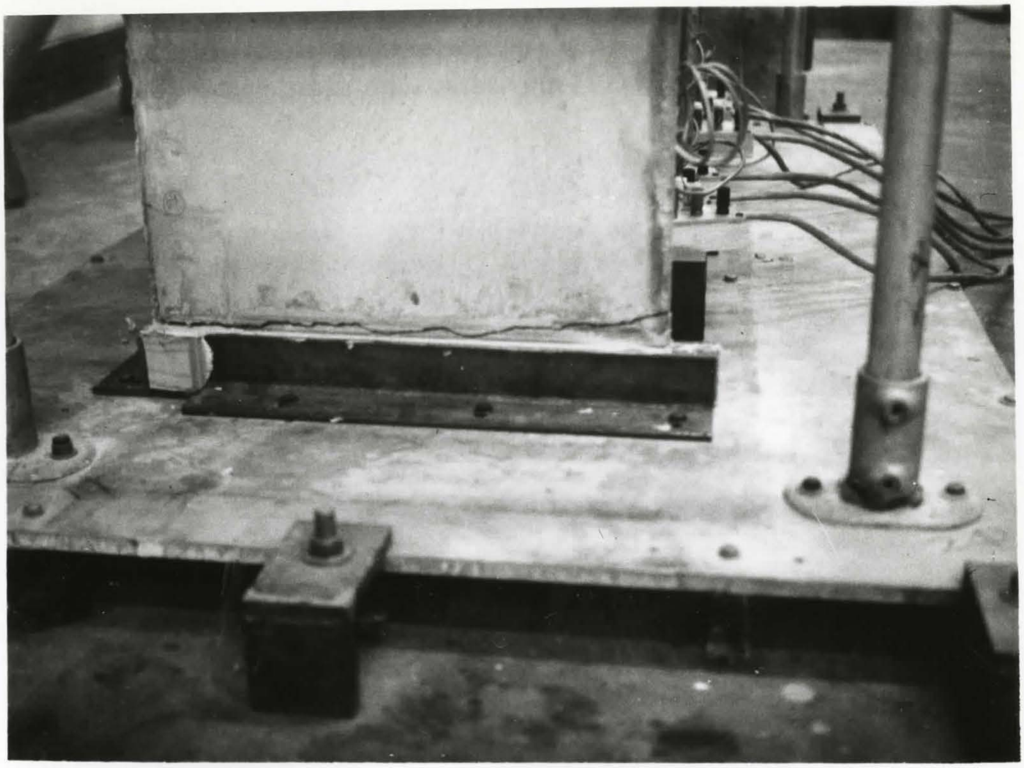

Photographs Showing the Crack Patterns for Model I

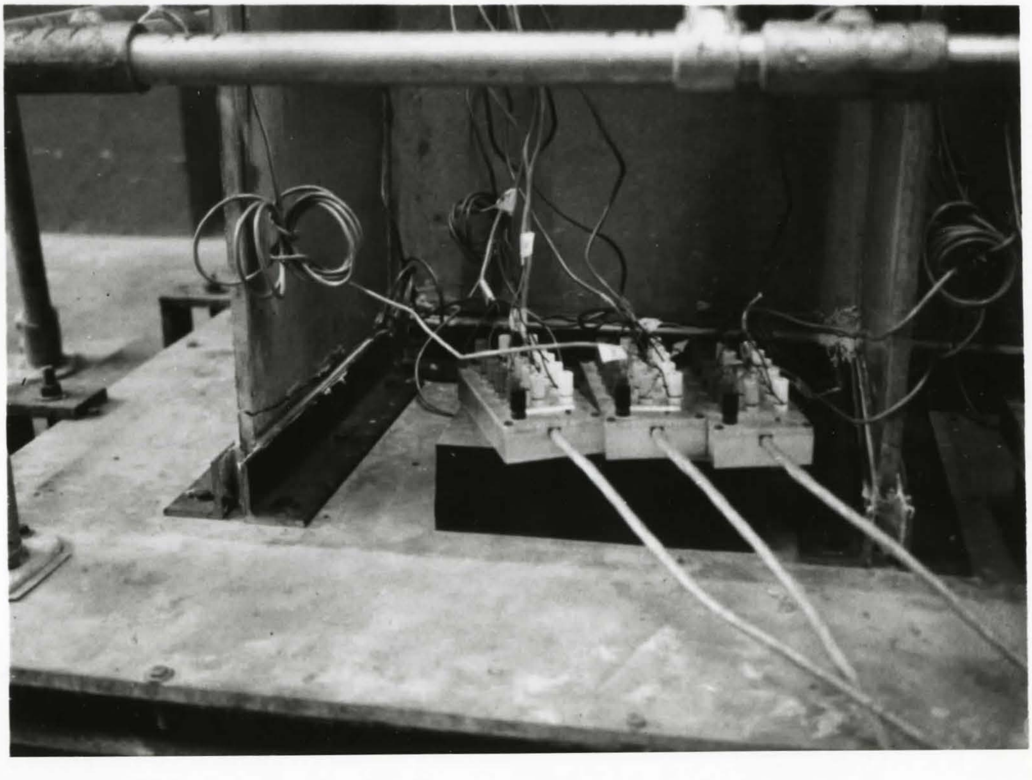

Fig. 11a

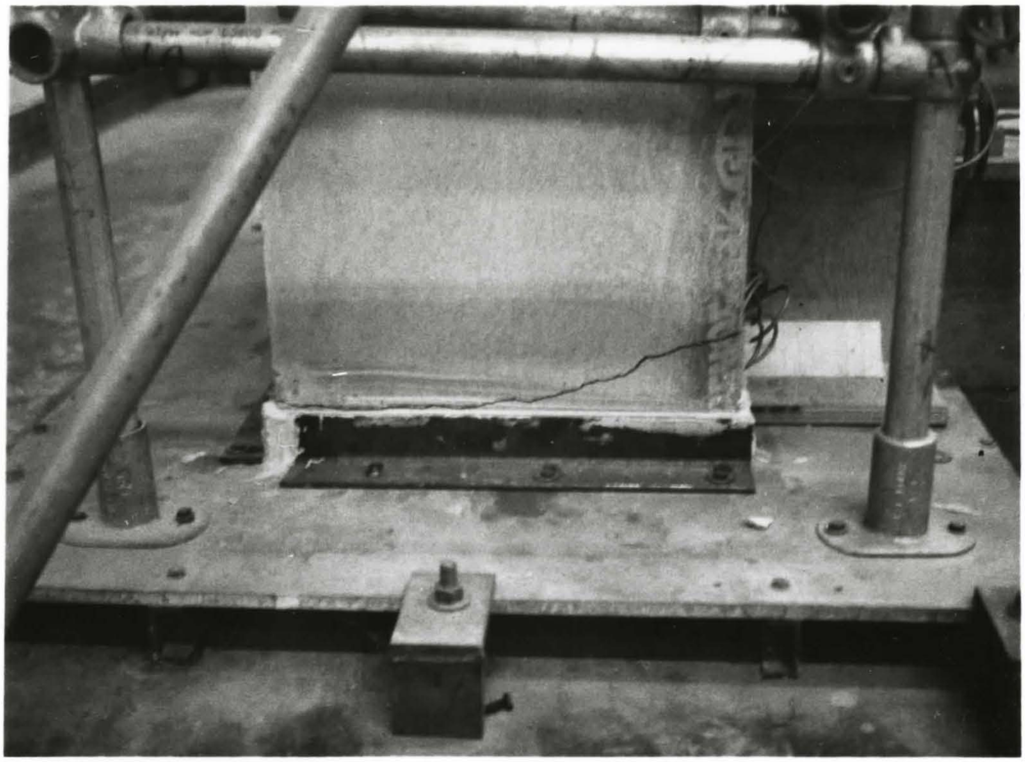

Photographs Showing the Crack Patterns for Model II

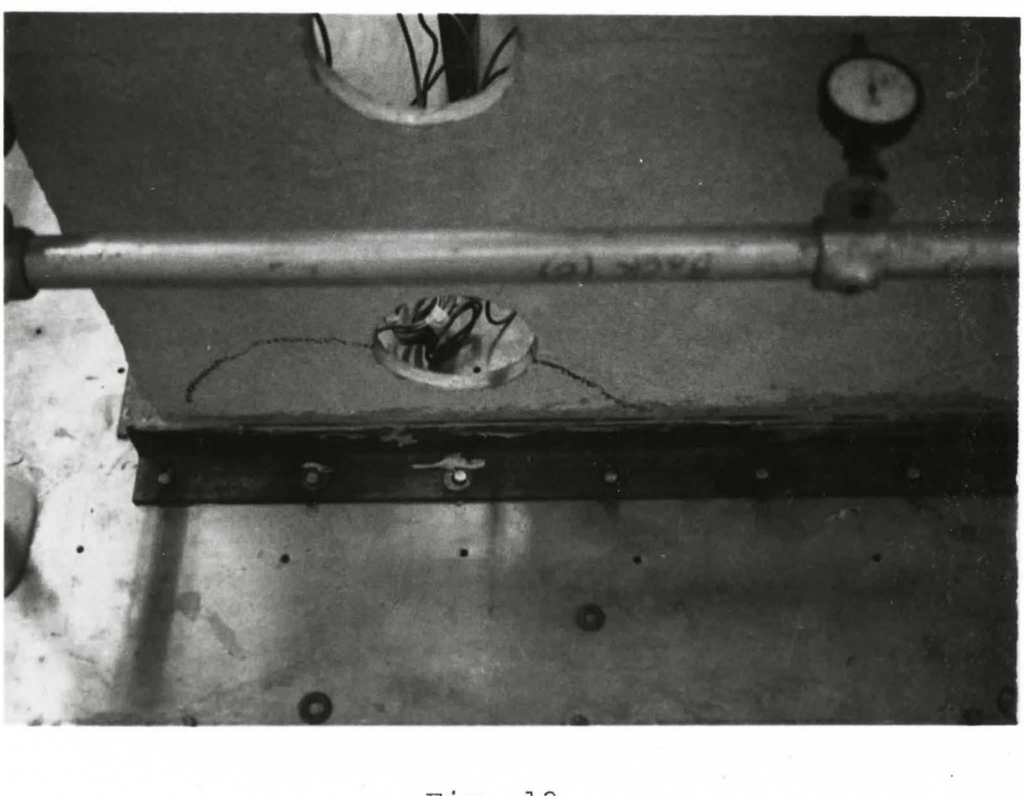

Fig. 12

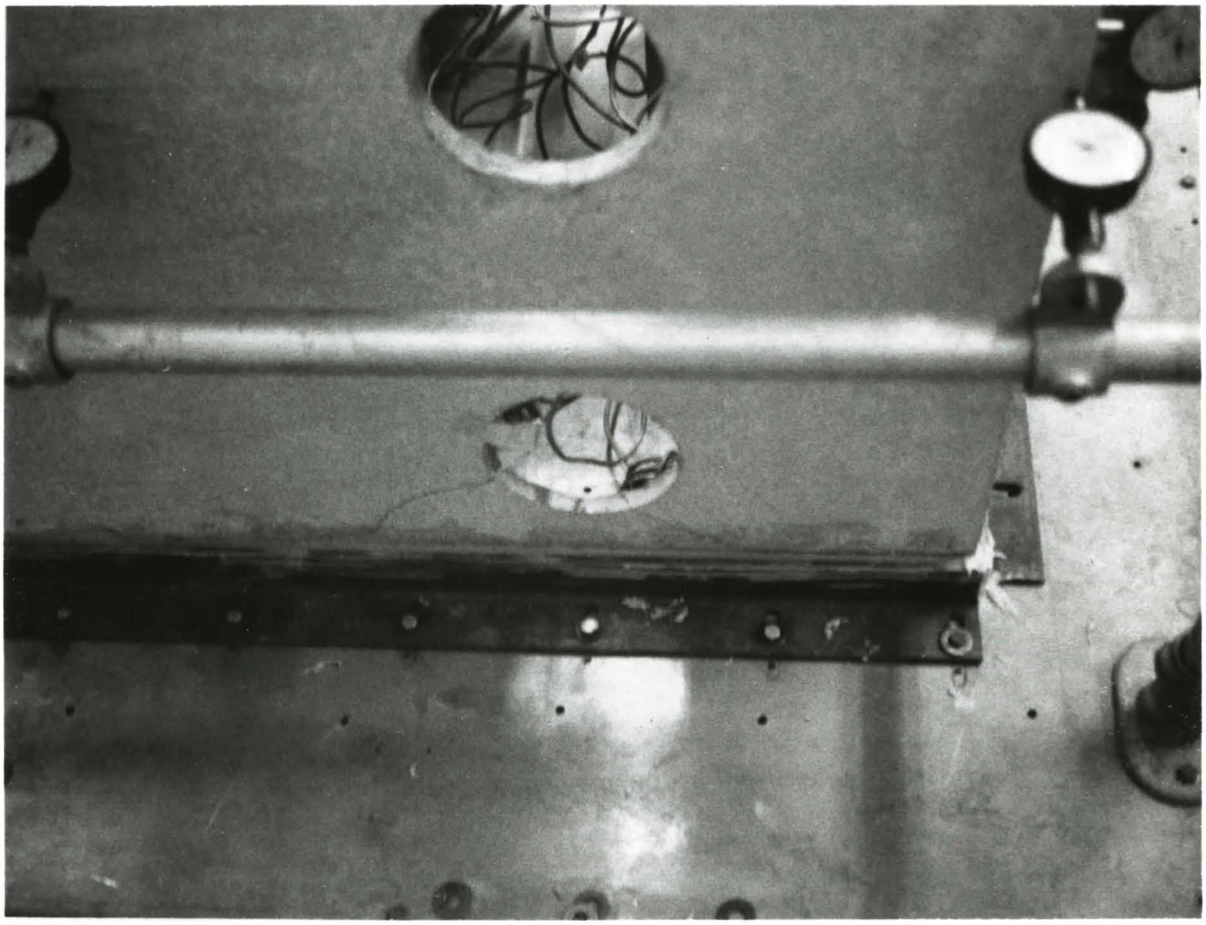

Fig. 12a

Photograph Showing the Crack Patterns for Model II

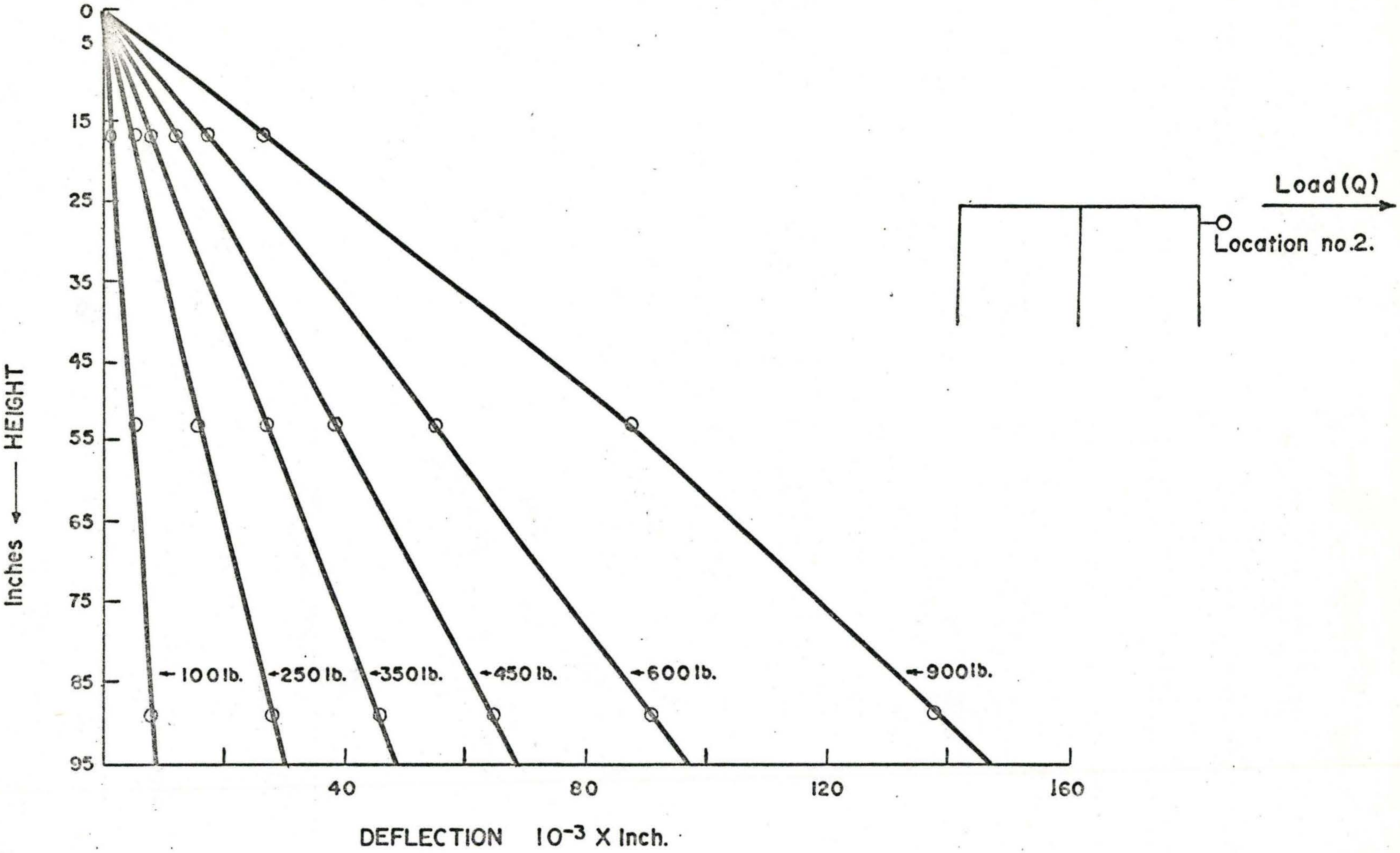

FIG. 13 _ TYPICAL DEFLECTION PATTERNS ALONG THE HEIGHT (MODEL NO. 2).

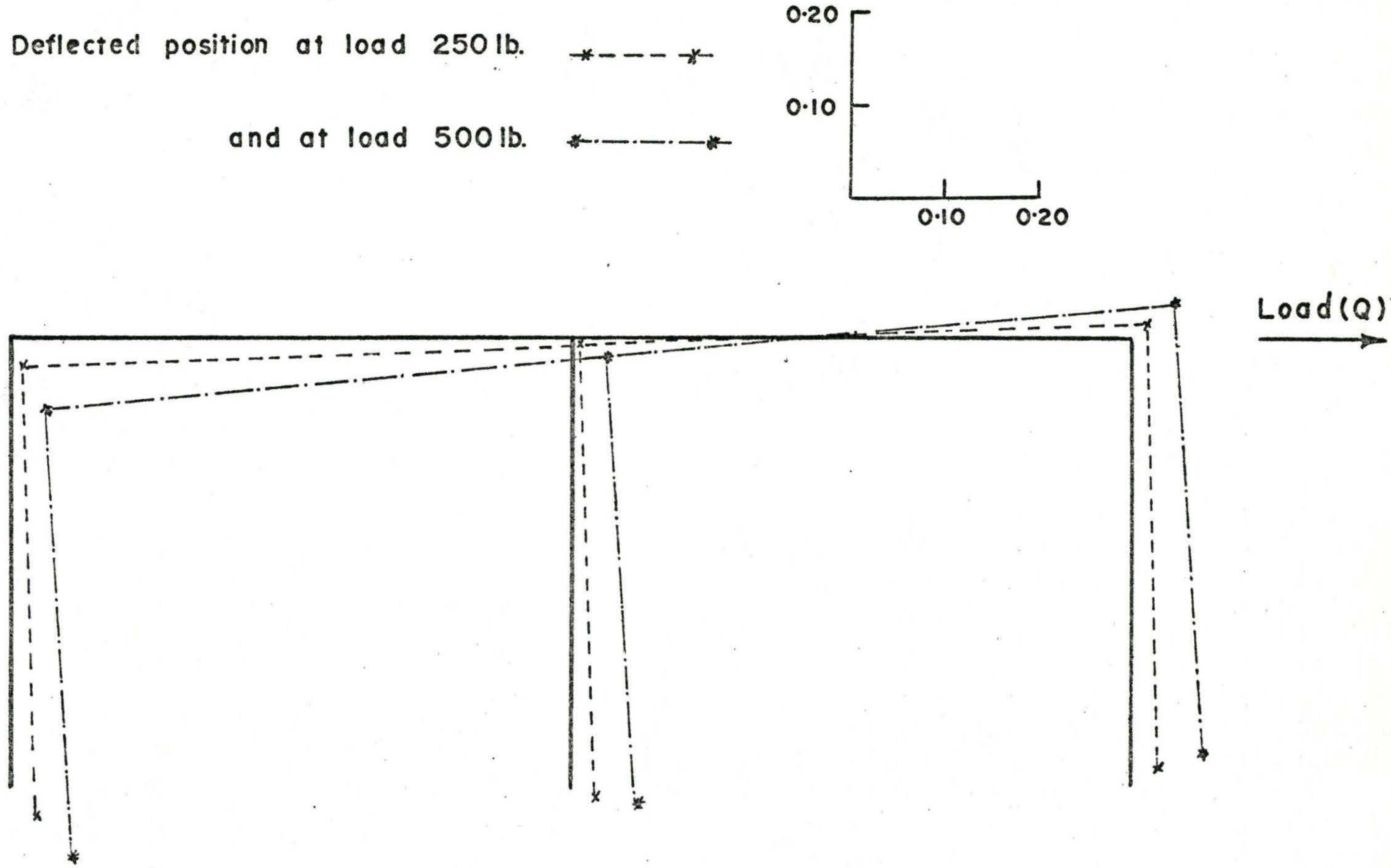

Z = 53"   MODEL NO. 2.

FIG. 14_ROTATION OF THE MODEL AT DIFFERENT LOADS.

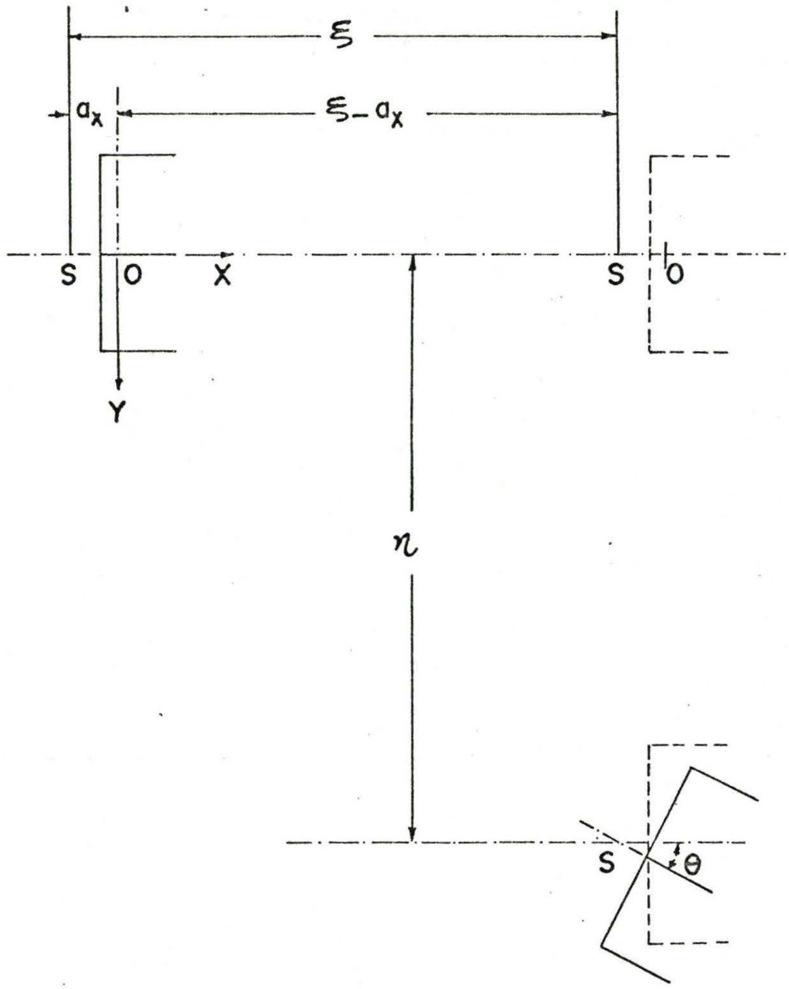

O — Centroid of the section.

S — Shear centre.

FIG.15 — DISPLACEMENT OF THE SECTION UNDER FLEXURAL — TORSIONAL LOADING.

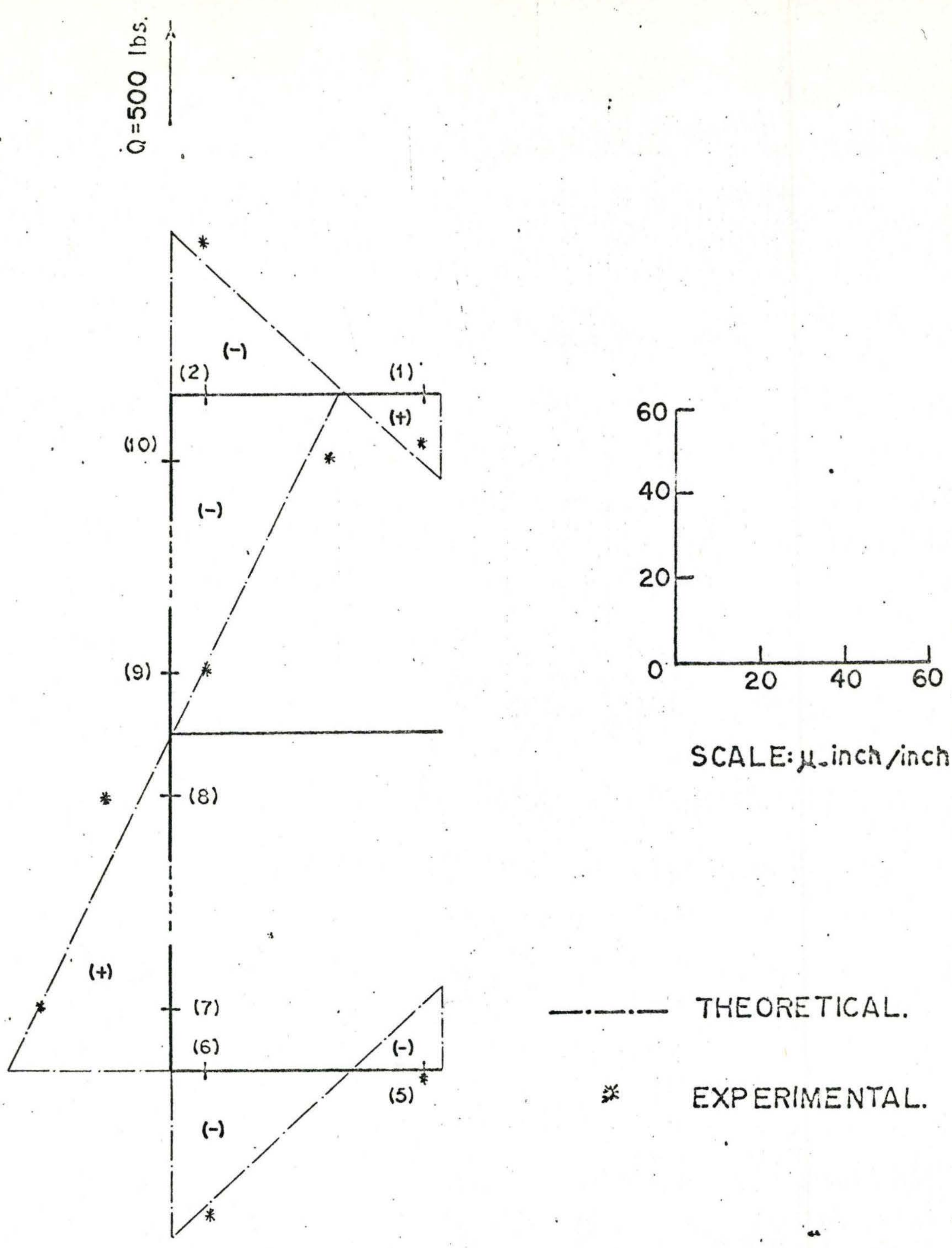

Points 1 to 10 refer to locations shown in FIG.9.

Z = 17"   MODEL NO.1.

FIG.16 _ COMPARISON OF STRAIN DISTRIBUTION.
(VLASOV'S THEORY)

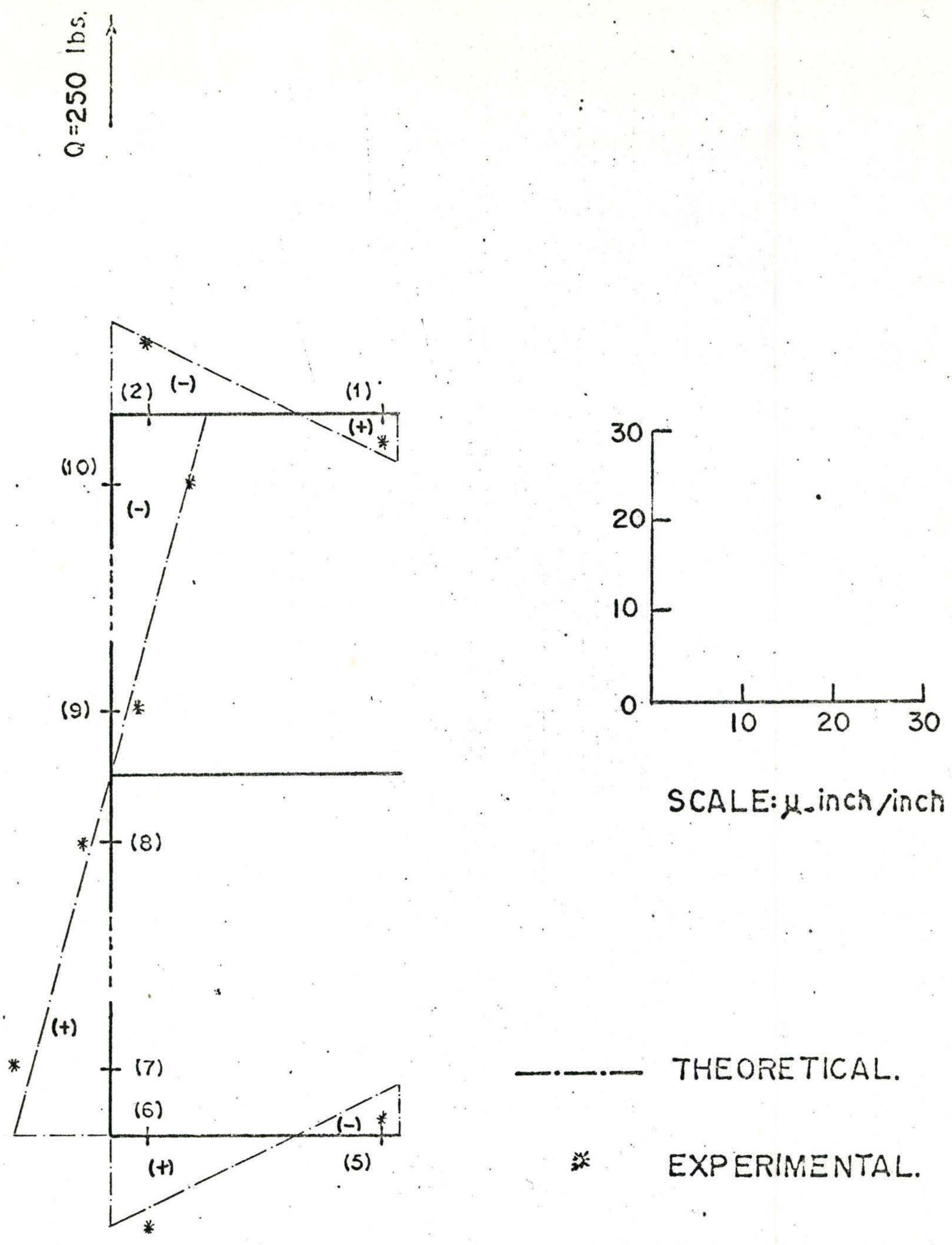

Points 1 to 10 refer to locorions shown in FIG.9.

Z = 53". MODEL NO.1.

FIG.17 _COMPARISON OF STRAIN DISTRIBUTION.
(VLASOV'S THEORY)

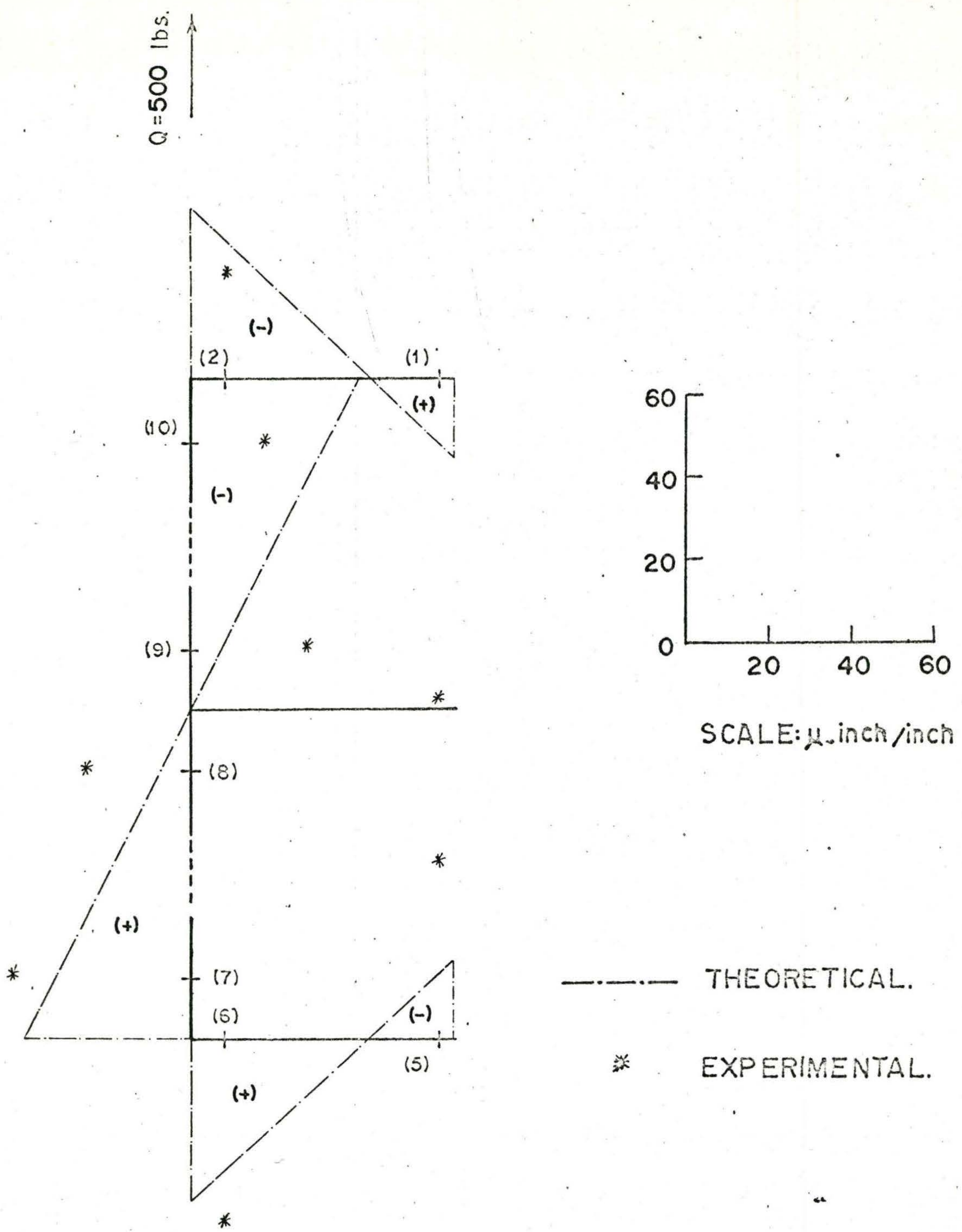

Points 1 to 10 refer to locations shown in FIG.9.

Z = 5". MODEL NO.2.

FIG.18 _ COMPARISON OF STRAIN DISTRIBUTION.
(VLASOV'S THEORY)

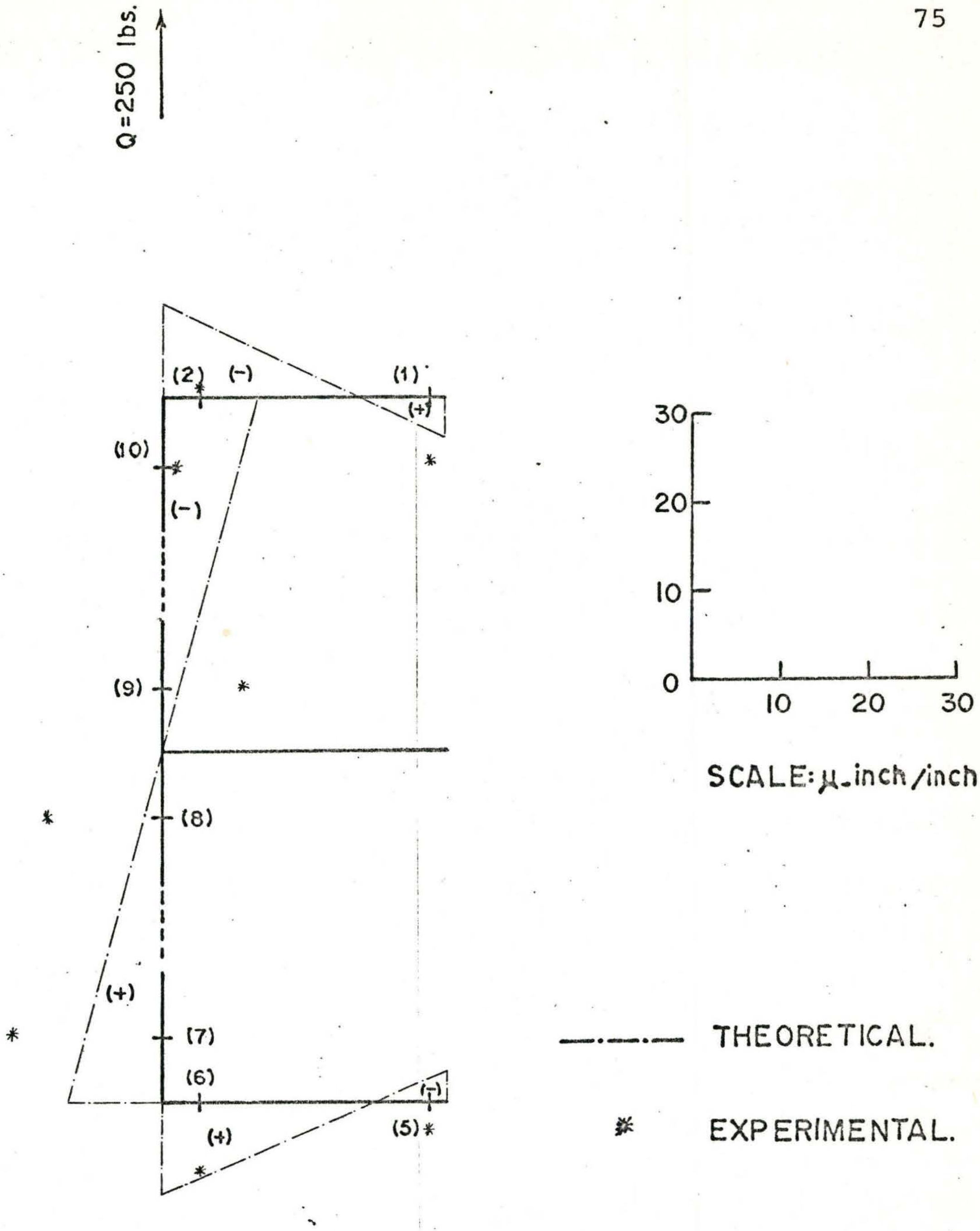

Points 1 to 10 refer to locations shown in FIG.9.

Z = 53"   MODEL NO.2.

FIG.19 _ COMPARISON OF STRAIN DISTRIBUTION.
(VLASOV'S THEORY.)

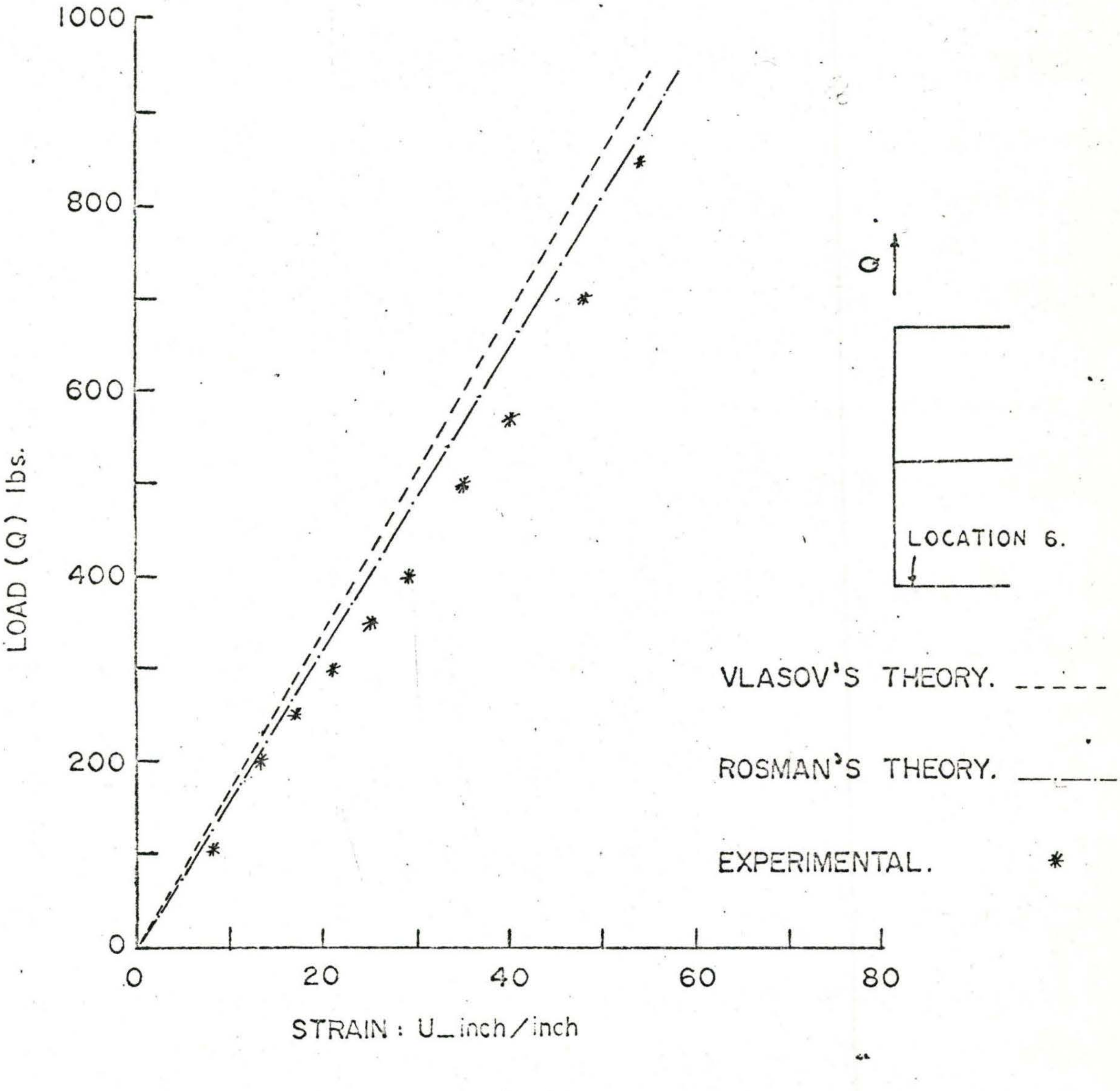

Z = 17."

FIG.20 _COMPARISON OF LOAD_STRAIN CURVES.

MODEL NO.1.

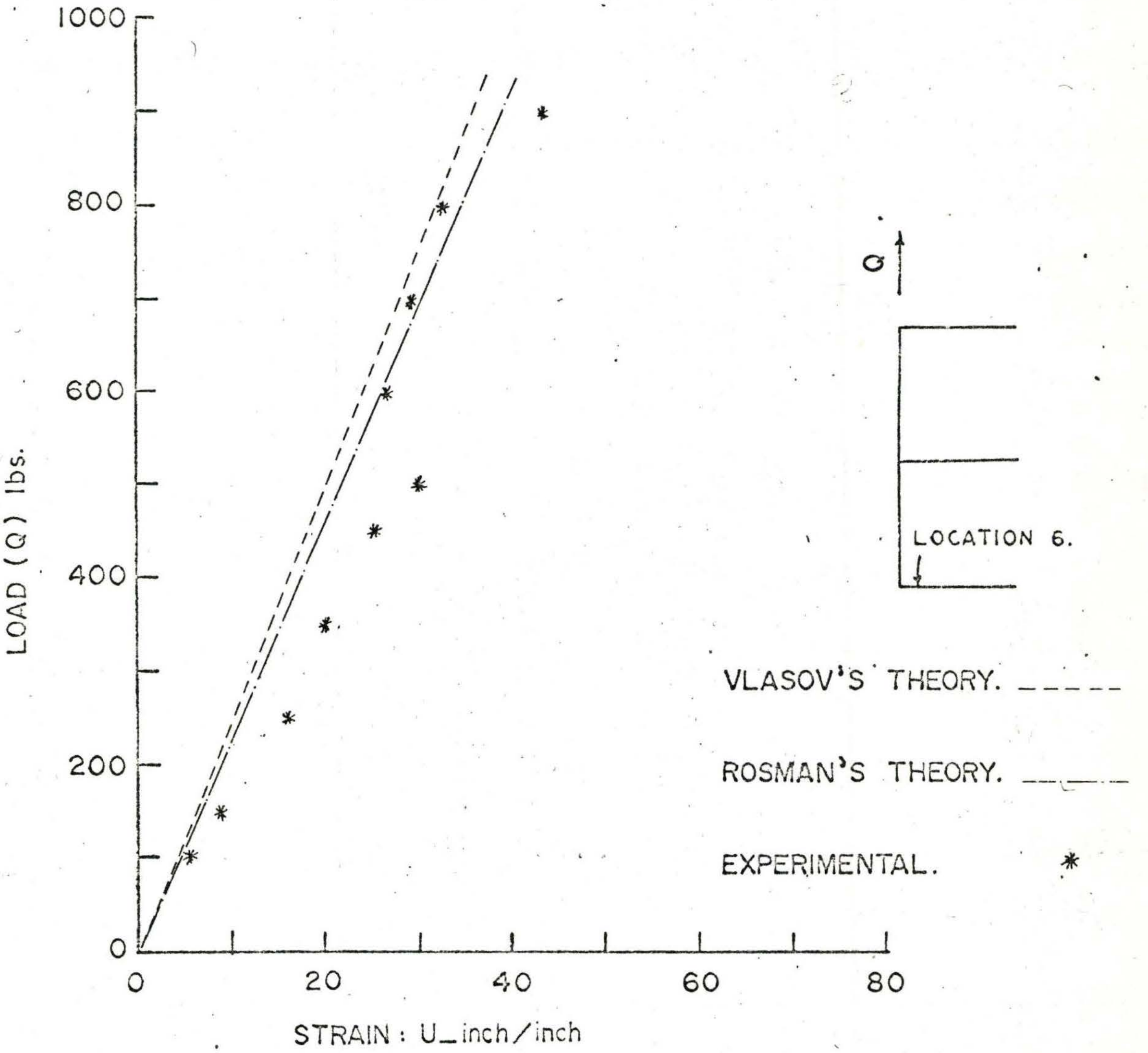

Z =5."

FIG.21 _COMPARISON OF LOAD_STRAIN CURVES.

MODEL NO.2.

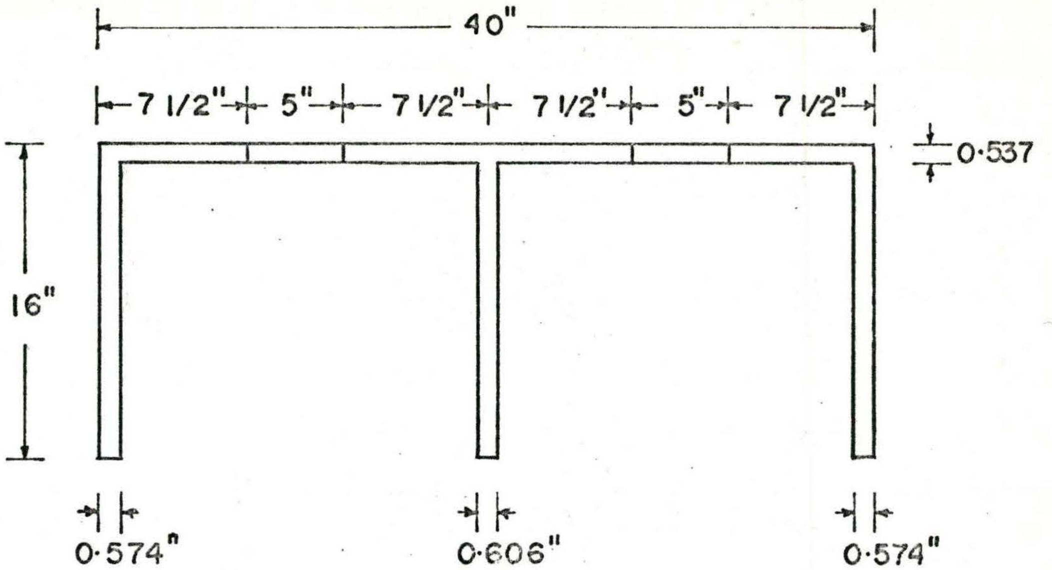

(a) MODEL NO.1.

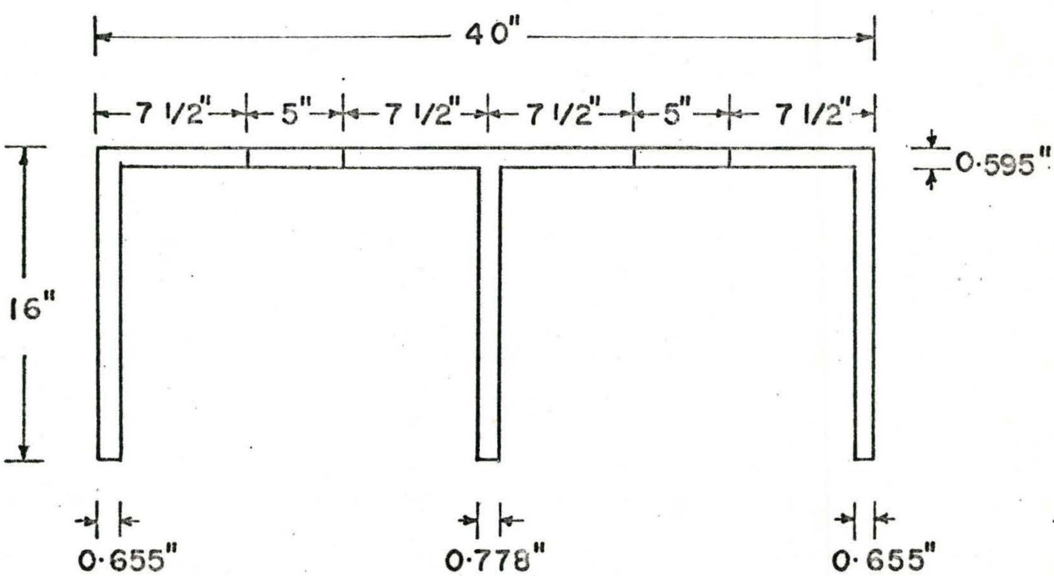

(b) MODEL NO.2.

FIG.22_AVERAGE DIMENSIONS OF THE EXPERIMENTAL MODELS.

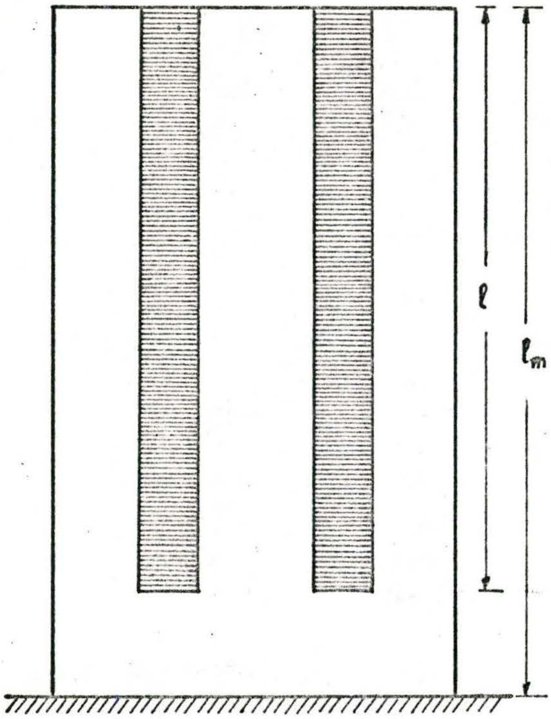

(a) Substitute system.

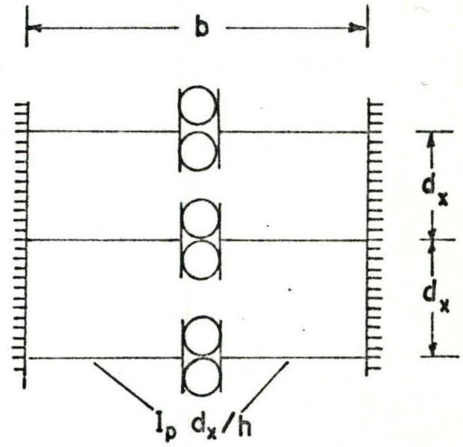

(b) Detail of the base system.

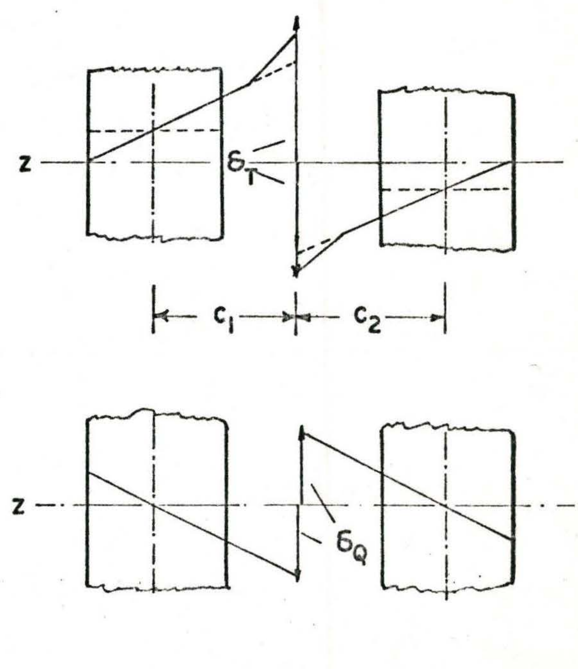

(c) Displacement diagrams for an arbitrary cross section of the base system due to T and Q respectively.

FIG. 23 — EXPLANATION OF ROSMAN'S THEORY.

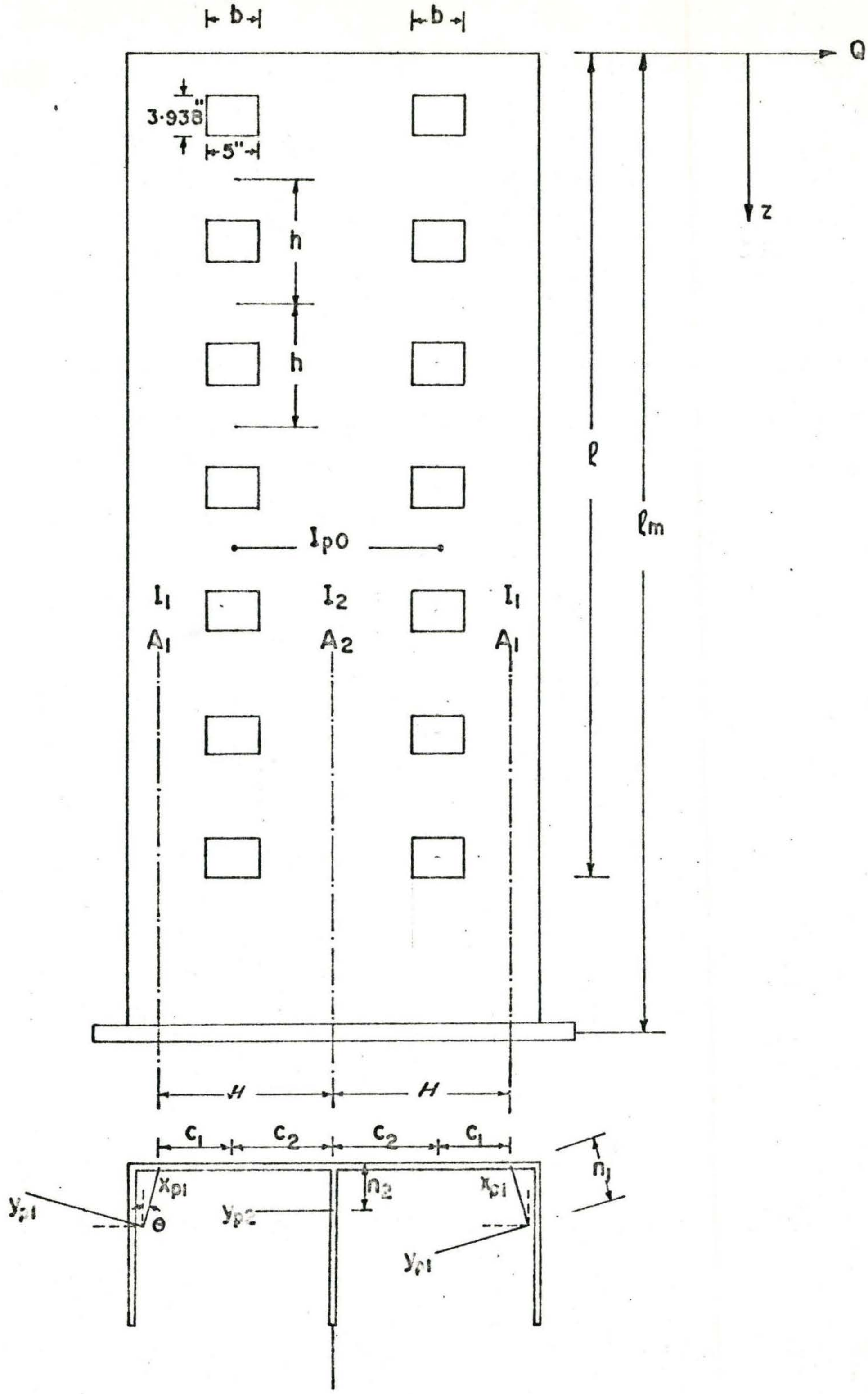

FIG.24_VARIOUS CONSTANTS USED IN ROSMAN'S THEORY.

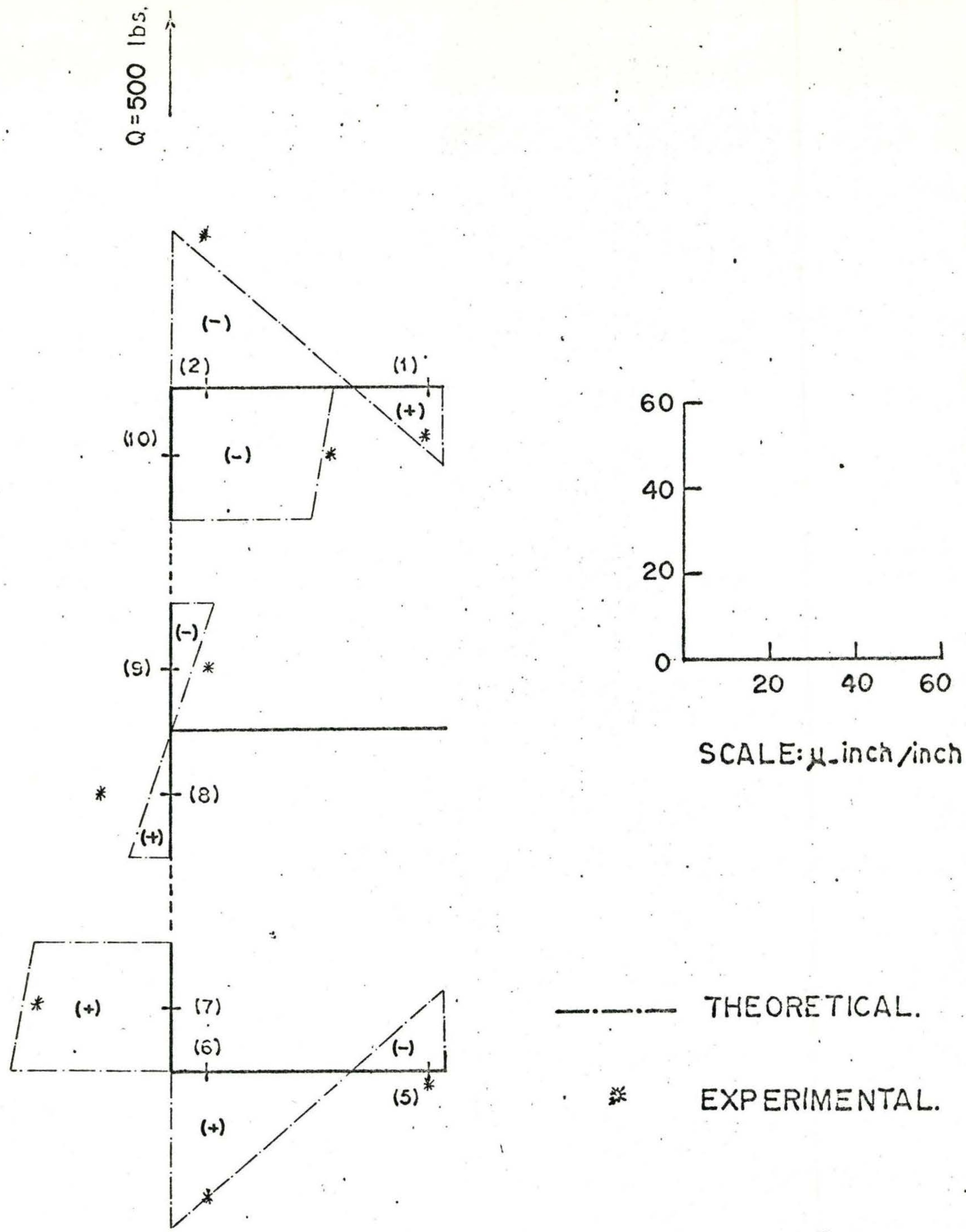

Points 1 to 10 refer to locations shown in FIG.9.

Z = 17"   MODEL NO.1.

FIG.25 _ COMPARISON OF STRAIN DISTRIBUTION.

(ROSMAN'S THEORY)

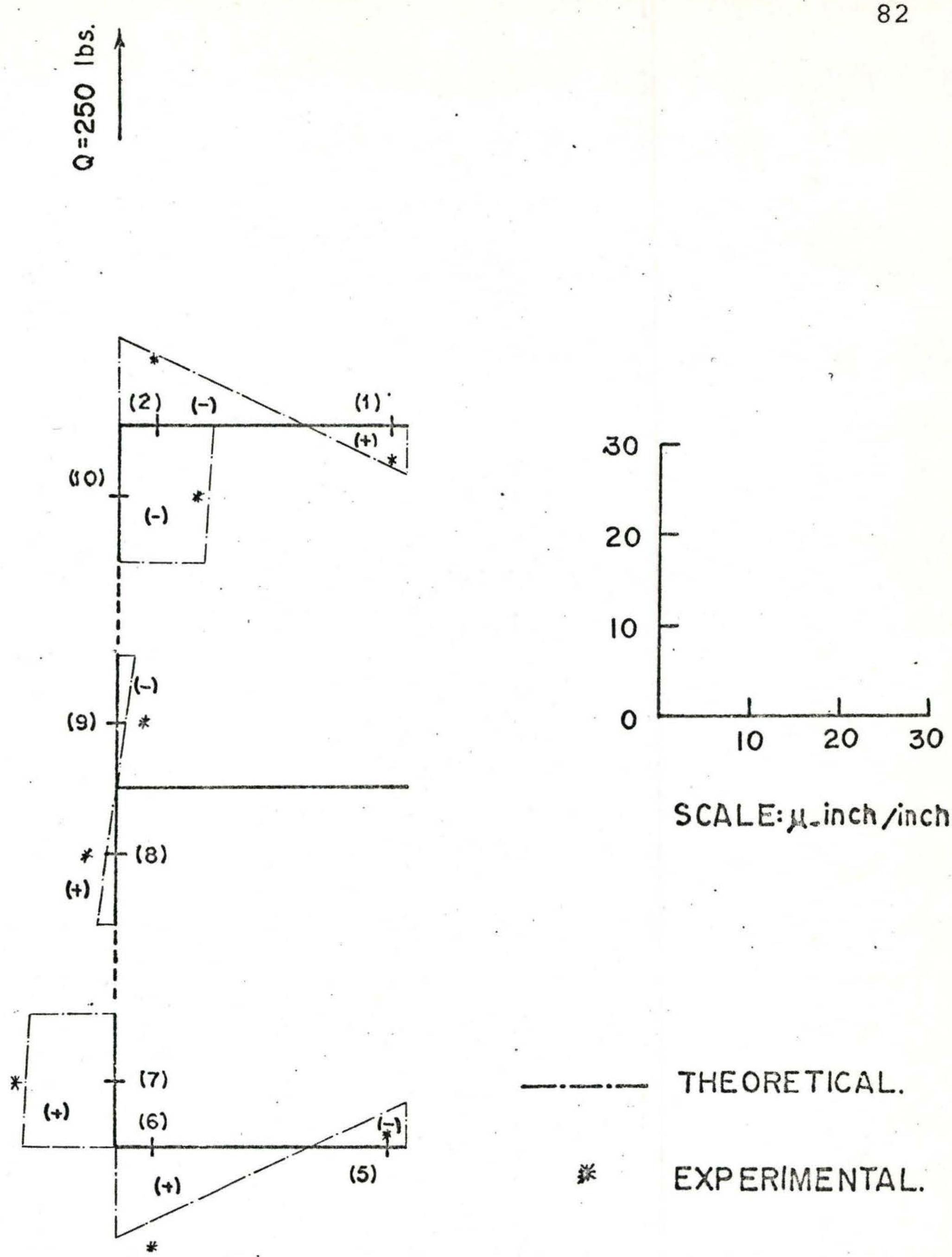

Points 1 to 10 refer to locations shown in FIG.9.

Z = 53"   MODEL NO.1.

FIG.26 _ COMPARISON OF STRAIN DISTRIBUTION.

(ROSMAN'S THEORY.)

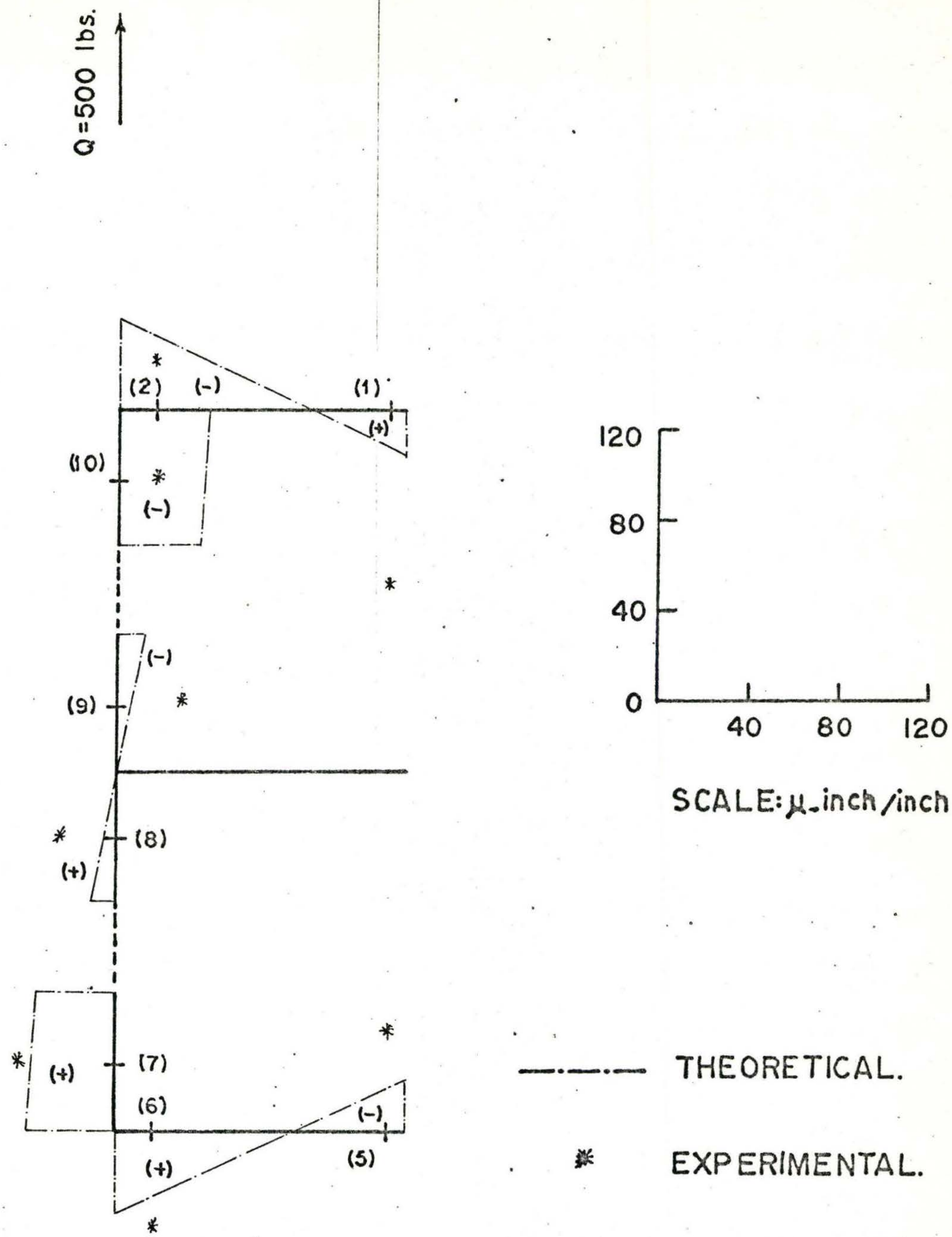

Points 1 to 10 refer to locarions shown in FIG.9.

Z = 5". MODEL NO.2.

FIG.27 _COMPARISON OF STRAIN DISTRIBUTION.

(ROSMAN'S THEORY)

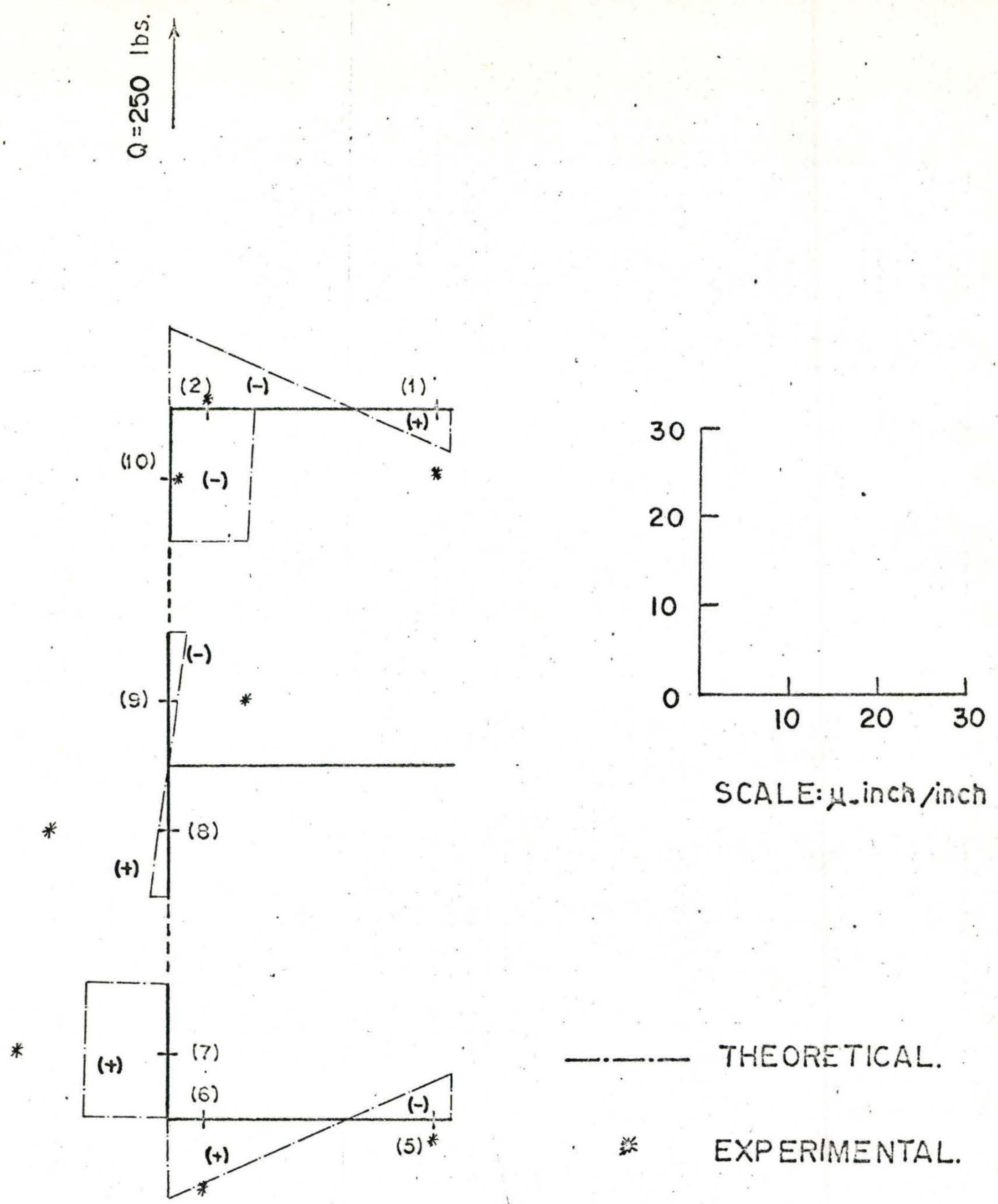

Points 1 to 10 refer to locations shown in FIG.9.

Z = 53"   MODEL NO.2.

FIG.28 _ COMPARISON OF STRAIN DISTRIBUTION.

(ROSMAN'S THEORY)

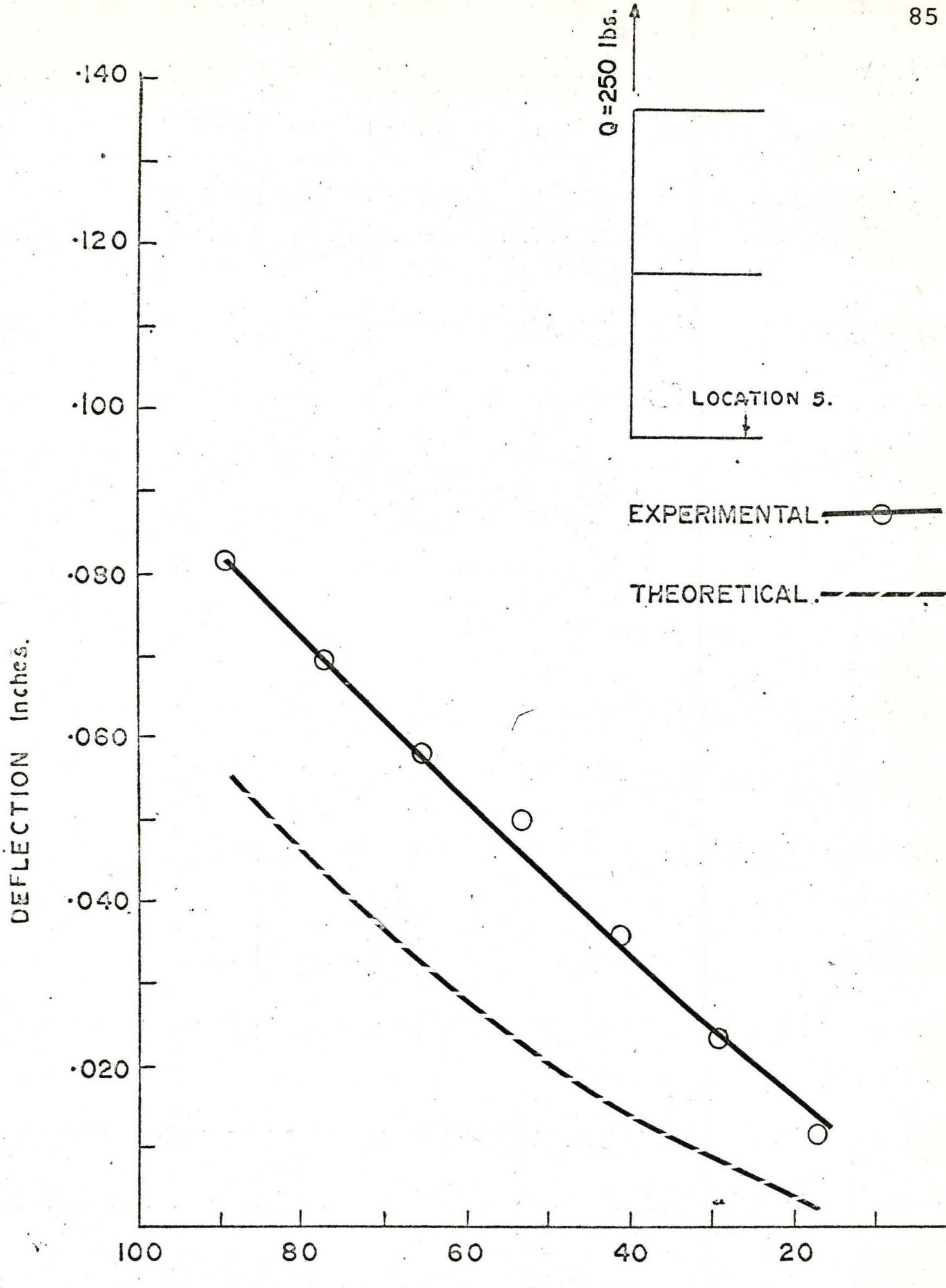

FIG.29 _ COMPARISON OF DEFLECTIONS.

ROSMAN S THEORY MODEL NO.1.

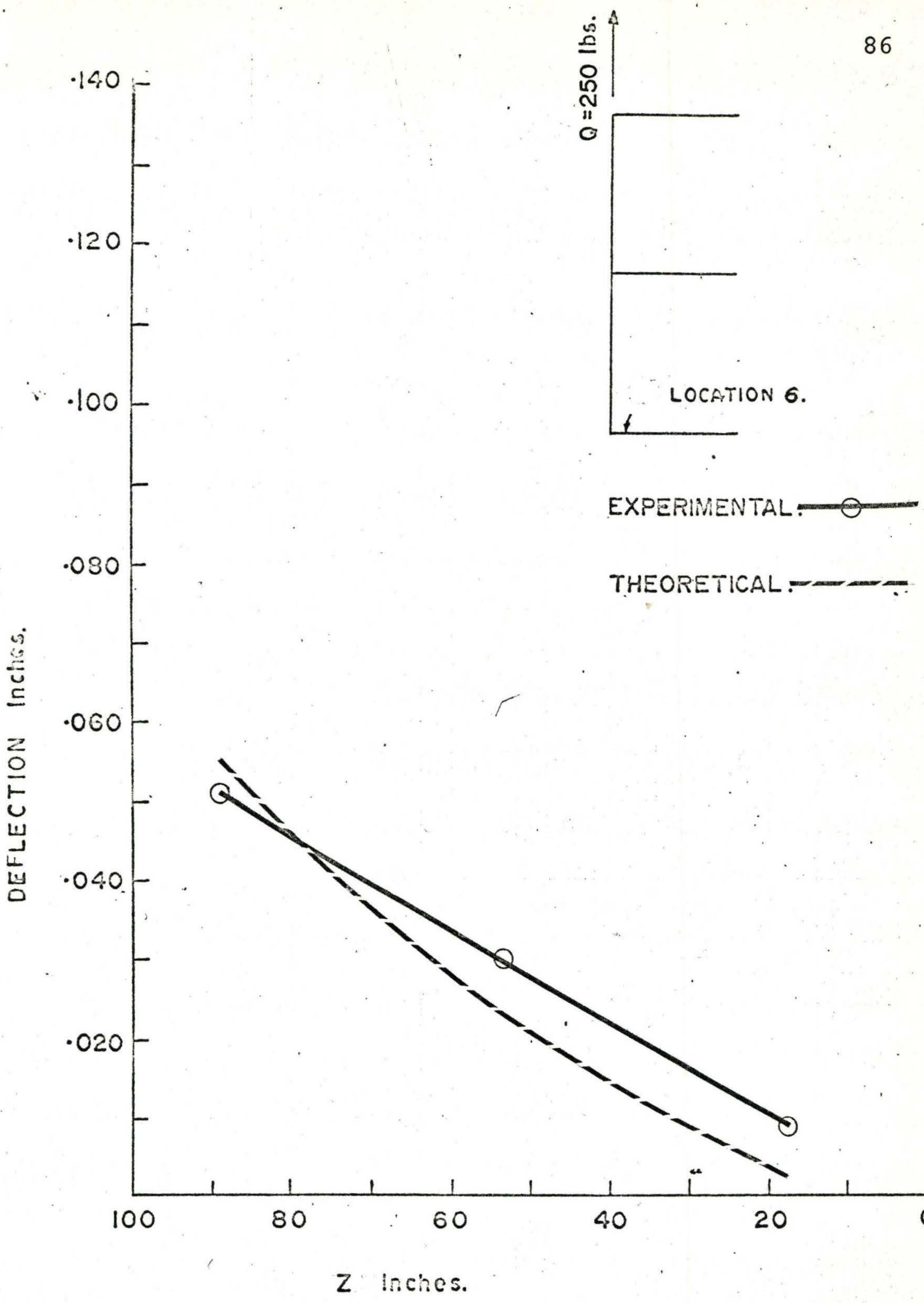

FIG.30 _ COMPARISON OF DEFLECTIONS.

ROSMAN S THEORY MODEL NO.I.

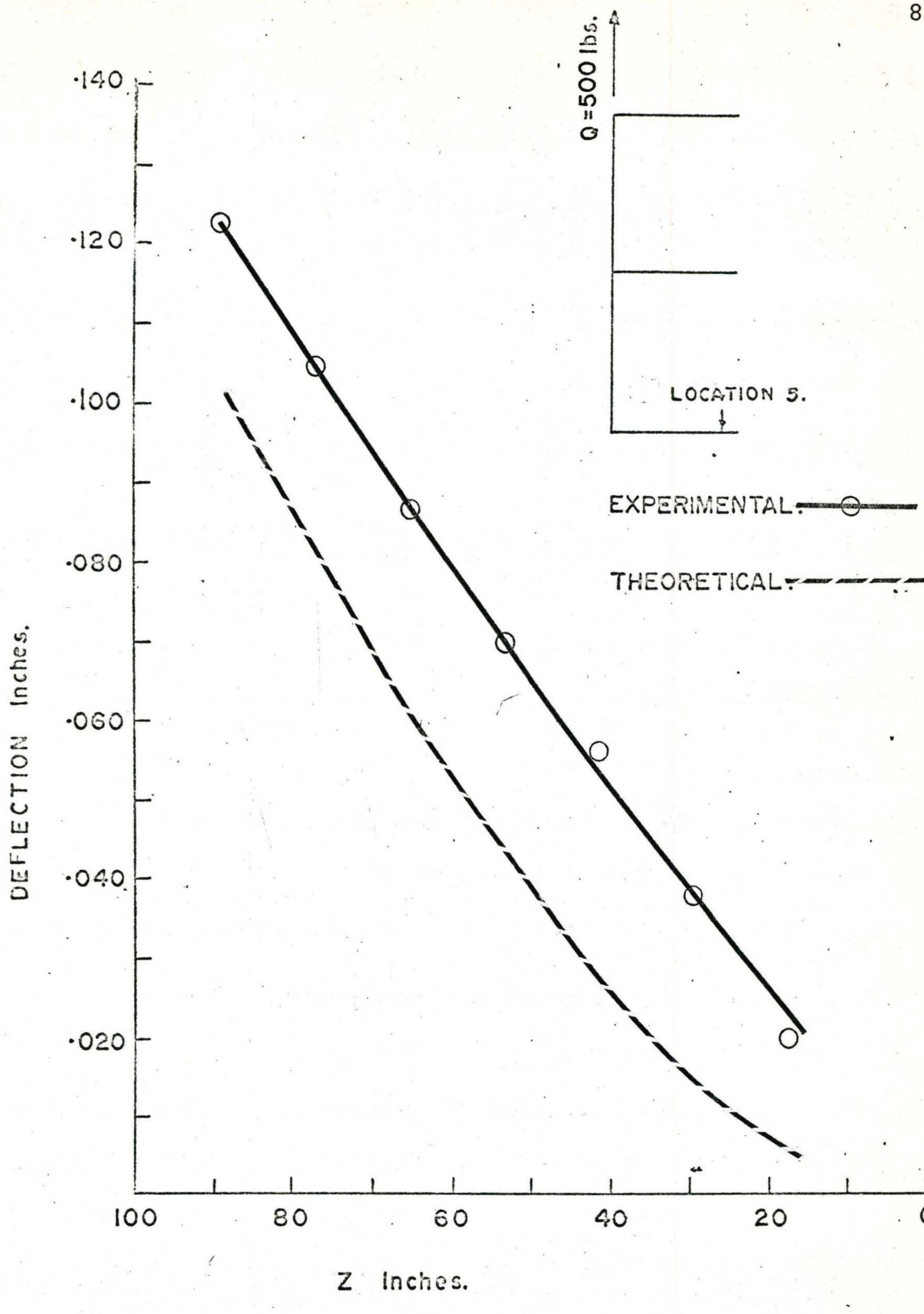

FIG.31 _ COMPARISON OF DEFLECTIONS.

ROSMAN S THEORY MODEL NO.2.

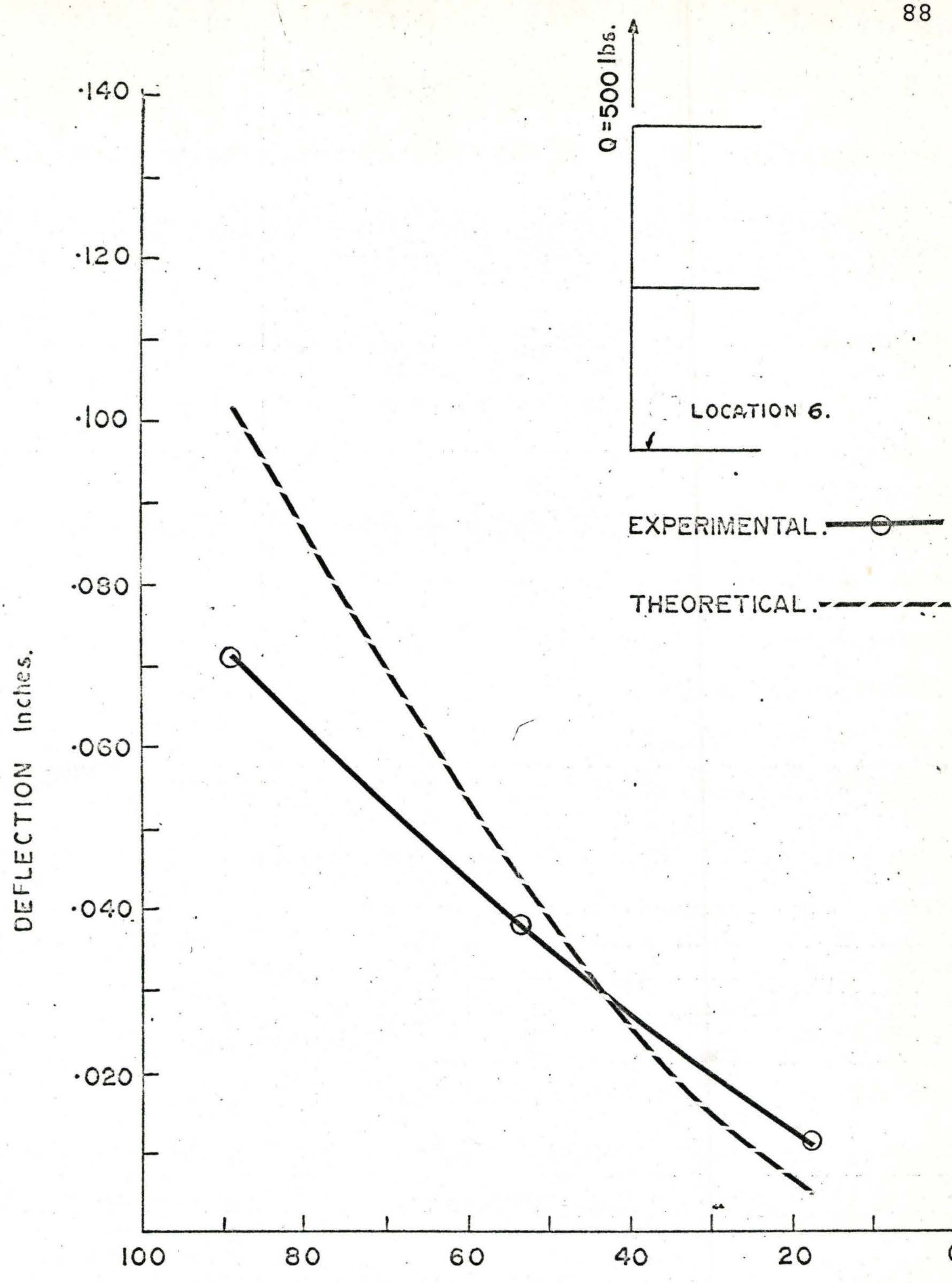

FIG.32 _ COMPARISON OF DEFLECTIONS.

ROSMAN S THEORY MODEL NO.2.

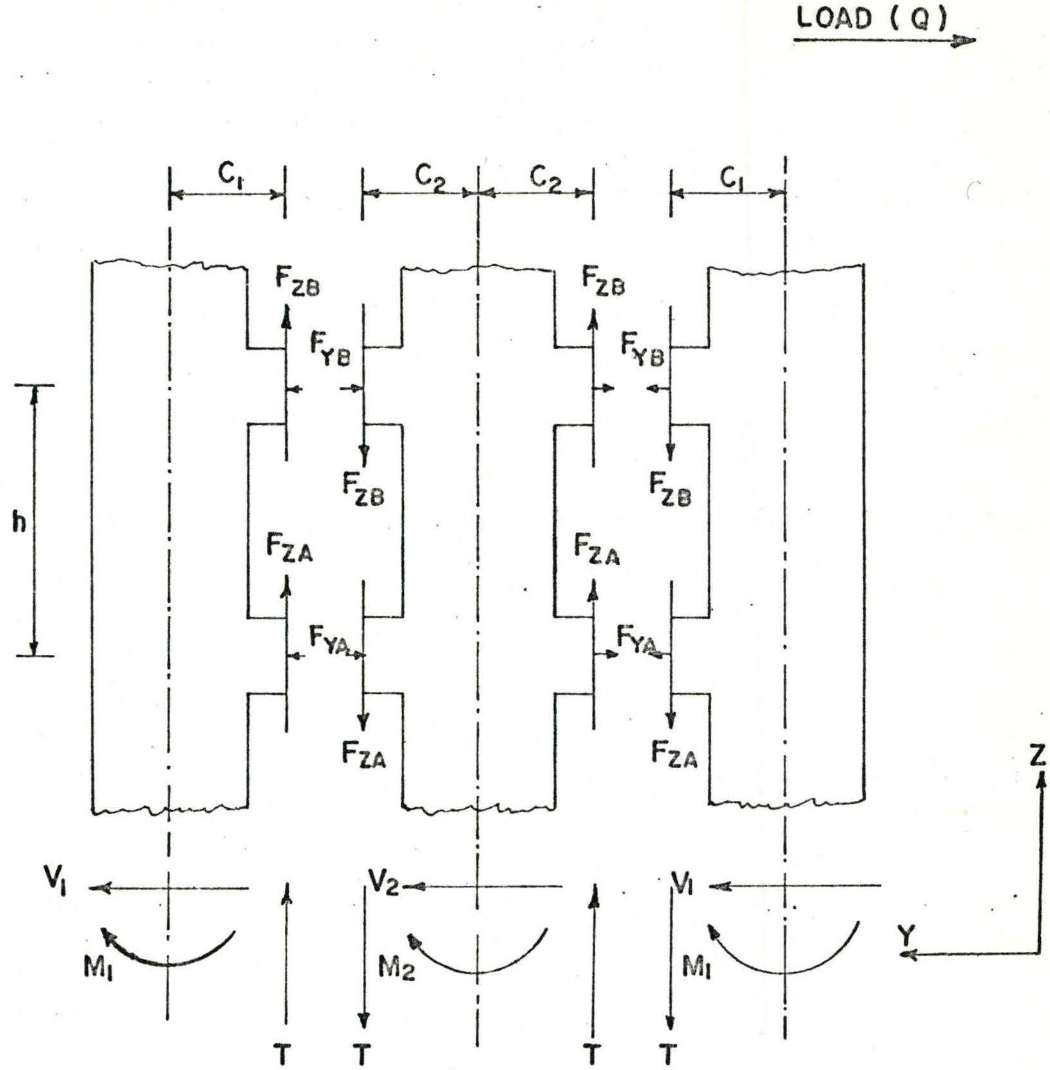

FIG.33_FREE BODY DIAGRAM SHOWING THE FORCES ACTING ON THE CONNECTING BEAMS TRANSFERRED TO THE PIERS.

APPENDIX A

TABLES FOR EXPERIMENTAL DATA

All dial gauge and strain location numbers refer to those given in Fig. 7 - 9.

TABLE A-1 DEFLECTIONS FOR 2ND CYCLE (MODEL I)

Dial Gage Location	Height 'Z' Inches	Deflections in 10^{-4}x inch for loads in lbs. Loading 100	150	200	Unloading 150	100	No Load
1	17	39	67	91	81	66	26
2	17	26	43	60	53	44	17
3	17	41	69	93	82	70	31
4	17	25	44	60	56	47	23
5	17	33	59	80	74	63	27
6	17	22	42	60	60	51	24
7	17	37	64	86	72	62	25
8	17	1	4	7	5	3	0
9	17	33	51	65	57	51	23
1	29	76	107	175	164	142	64
3	29	50	104	150	127	107	35
5	29	75	125	170	145	125	55
1	41	120	200	270	226	196	80
3	41	120	200	270	225	200	90
5	41	110	190	250	210	180	70
1	53	160	270	360	300	260	110
2	53	100	170	150	75	30	0
3	53	165	275	365	303	270	110
4	53	100	165	220	180	160	70
5	53	150	250	330	280	240	100
6	53	80	140	210	170	150	70
7	53	100	175	240	190	160	60
8	53	15	40	60	40	30	0
9	53	70	105	135	115	105	50
1	65	205	340	450	375	230	140
3	65	200	330	445	370	330	145
5	65	190	330	430	360	320	130
1	77	220	390	520	430	370	140
3	77	230	385	513	430	380	165
5	77	240	390	520	430	380	160
1	89	275	470	620	510	440	180
2	89	170	280	380	310	270	110
3	89	270	455	605	495	440	180
4	89	170	290	380	310	280	115
5	89	260	450	590	520	420	170
6	89	170	280	380	310	280	110
7	89	200	340	460	380	320	120
8	89	30	60	100	10	50	0
9	89	140	220	280	240	220	100

TABLE A-2 DEFLECTIONS FOR 3RD CYCLE (MODEL I)

Dial Gage Location	Height 'Z' Inches	Deflections in 10^{-4} x inch for loads in lbs. 100	250	400	500	570	700	850
1	17	37	123	224	277	329	411	492
2	17	22	85	161	200	239	303	366
3	17	41	128	238	296	352	444	531
4	17	26	87	162	204	245	312	377
5	17	34	114	208	259	309	388	466
6	17	25	90	165	199	229	289	349
7	17	33	121	125	281	347	474	567
8	17	1	14	32	45	57	115	156
9	17	33	88	151	183	204	229	257
1	29	79	254	437	553	651	816	982
3	29	78	248	460	575	682	866	1030
5	29	70	230	430	535	640	805	960
1	41	115	334	665	830	980	1235	1465
3	41	120	370	690	860	1010	1270	1510
5	41	120	360	660	840	970	1210	1250
1	53	160	490	890	1110	1310	1650	1960
2	53	100	310	570	710	830	1060	1350
3	53	170	500	905	1130	1340	1670	1990
4	53	100	310	550	690	820	1030	1235
5	53	140	450	830	1010	1210	1650	1940
6	53	100	300	540	670	800	1020	1220
7	53	100	320	590	760	950	1270	1570
8	53	20	110	210	280	380	520	640
9	53	70	200	360	430	460	490	520
1	65	190	600	1100	1370	1630	2050	2440
3	65	200	610	1120	1390	1550	2070	2450
5	65	190	580	1060	1330	1580	1980	2360
1	77	240	730	1310	1630	1930	2420	2980
3	77	230	710	1310	1630	1920	2420	2860
5	77	225	700	1280	1590	1920	2350	2790
1	89	270	830	1520	1690	2240	2800	3320
2	89	170	520	950	1180	1400	1760	2100
3	89	270	820	1500	1870	2210	2760	3290
4	89	170	510	960	1190	1400	1990	3120
5	89	270	820	1490	1850	2180	2710	3660
6	89	165	510	940	1170	1400	1770	2120
7	89	200	650	1180	1490	1810	2390	2910
8	89	30	180	330	430	590	880	1120
9	89	140	380	640	780	850	890	930

TABLE A-3 DEFLECTIONS FOR 1ST CYCLE (MODEL II)

Dial Gage Location	Height 'Z' Inches	Deflections in 10-4 x inch for loads in lbs. Loading 50	100	150	Unloading 100	50	No Load
1	17	6	19	38	37	29	13
2	17	2	11	24	24	17	3
3	17	6	18	37	37	32	17
4	17	0	4	15	17	17	14
5	17	8	23	42	42	29	18
6	17	2	8	18	19	20	16
7	17	17	34	63	44	24	8
8	17	0	0	1	0	2	3
9	17	14	29	48	40	27	12
10	17	5	23	45	32	13	4
11	17	3	5	7	5	4	4
12	17	14	28	49	38	24	10
1	29	3	6	13	12	9	5
3	29	2	6	10	11	10	5
5	29	3	7	13	12	9	5
1	41	5	12	21	19	13	6
3	41	4	11	19	18	14	7
5	41	4	10	19	18	12	6
1	53	40	90	160	140	120	50
2	53	20	50	90	90	80	40
3	53	20	30	50	40	40	20
4	53	80	230	440	300	220	130
5	53	40	90	160	150	110	60
6	53	5	25	60	70	60	40
7	53	50	110	180	140	80	30
8	53	0	10	20	10	0	0
9	53	30	60	100	90	60	20
10	53	60	120	190	140	80	30
11	53	0	20	40	40	30	20
12	53	40	70	120	100	60	30
1	65	50	120	210	190	130	60
3	65	40	110	190	180	140	70
5	65	40	100	190	180	120	60
1	77	60	140	250	240	150	70
3	77	60	140	240	200	160	80
5	77	50	130	240	230	150	80

TABLE A-3 (cont'd). DEFLECTIONS FOR 1st CYCLE (MODEL II)

Dial Gage Location	Height 'Z' Inches	Deflections in 10^{-4} x inch for loads in lbs					
		Loading			Unloading		
		50	100	150	100	50	No load
1	89	70	150	300	270	180	80
2	89	70	100	170	170	120	70
3	89	70	170	280	270	180	90
4	89	30	80	150	160	130	80
5	89	60	160	260	260	170	80
6	89	30	70	140	150	110	50
7	89	90	170	290	230	140	50
8	89	0	30	50	40	20	10
9	89	60	110	180	150	100	40
10	89	80	170	270	230	150	50
11	89	10	40	80	70	40	20
12	89	50	100	150	120	70	30

TABLE A - 4

DEFLECTIONS FOR 3RD CYCLE (MODEL II)

Dial Gauge Location Number	Height 'Z' Inches	Deflection in Inch × 10^{-4} For Loads in Lbs.								
		100	250	350	450	500	600	700	800	900
1	17	21	70	117	164	184	232	278	326	377
2	17	18	68	93	131	147	180	207	241	271
3	17	19	70	122	178	200	249	288	333	377
4	17	6	36	70	105	123	145	172	196	219
5	17	19	71	123	177	198	245	284	326	405
6	17	8	35	67	99	111	140	158	177	202
7	17	33	92	147	203	227	301	386	474	578
8	17	2	5	11	19	24	41	63	89	124
9	17	27	70	103	134	147	177	209	237	264
10	17	34	98	158	217	243	317	409	499	603
11	17	3	16	33	48	54	83	112	143	187
12	17	27	72	92	118	127	155	189	219	248
1	29	40	135	175	335	375	475	550	645	735
3	29	40	130	230	330	370	450	490	550	610
5	29	45	135	205	330	375	465	535	620	735
1	41	60	210	350	500	560	700	820	940	1070
3	41	50	190	320	470	530	630	690	780	840
5	41	70	220	360	500	560	680	790	900	1040
1	53	90	290	480	680	760	950	1110	1300	1480
2	53	60	160	270	390	440	550	650	770	880
3	53	100	220	440	660	750	890	1080	1200	1390
4	53	50	90	110	150	160	180	240	340	430
5	53	90	270	440	620	700	840	950	1080	1230
6	53	40	130	220	340	380	440	590	770	850
7	53	110	310	490	680	760	1000	1260	1510	1790
8	53	20	60	100	150	170	240	320	410	530
9	53	60	160	230	320	350	430	530	610	680
10	53	100	300	480	650	730	960	1240	1510	1830
11	53	10	50	100	160	170	290	380	500	560
12	53	70	180	250	340	350	440	550	640	740
1	65	110	360	600	850	940	1170	1380	1600	1820
3	65	110	340	570	810	900	1100	1240	1410	1570
5	65	110	340	560	780	870	1080	1260	1440	1640
1	77	150	440	730	990	1110	1380	1630	1900	2160
3	77	130	420	700	980	1090	1350	1550	1770	1980
5	77	130	410	670	940	1050	1310	1530	1770	2010

TABLE A - 4

DEFLECTIONS FOR 3RD CYCLE (MODEL II) (cont'd)

Dial Gauge Location Number	Height 'Z' Inches	Deflection in Inch × 10^{-4} For Loads in Lbs.								
		100	250	350	450	500	600	700	800	900
1	89	170	520	840	1150	1280	1590	1880	2190	2490
2	89	80	280	460	650	730	910	1070	1230	1380
3	89	160	490	800	1120	1250	1560	1830	2140	2420
4	89	60	150	440	640	720	890	1040	1210	1350
5	89	120	460	810	1090	1230	1540	1830	2090	2390
6	89	70	260	440	630	710	880	1010	1170	1310
7	89	160	460	760	1050	1170	1520	1870	2250	2660
8	89	30	100	190	270	310	430	570	740	920
9	89	110	280	400	510	550	650	750	820	890
10	89	160	480	780	1080	1210	1560	1940	2320	2770
11	89	40	140	270	370	430	570	730	930	1100
12	89	100	250	360	470	510	620	720	790	860

TABLE A - 5

STRAINS FOR 2ND CYCLE (MODEL I)

Strain Gauge Location	Height 'Z' Inches	Strains in μ-inch/inch for Loads in Lbs. loading 100	150	200	unloading 150	100	No Load
1	17	+ 5	+ 8	+11	+ 9	+11	+ 7
2	17	- 4	- 9	-10	- 7	- 5	+ 3
3	17	+ 2	+ 3	+ 5	+ 6	+ 6	+ 7
4	17	+ 1	+ 4	+ 7	+ 6	+ 7	+ 7
5	17	+ 1	+ 2	+ 2	+ 5	+ 7	+ 9
6	17	+10	+14	+18	+17	+15	+11
7	17	+ 9	+13	+16	+15	+15	+ 9
8	17	+ 3	+ 6	+ 7	+ 8	+11	+ 7
9	17	+ 1	+ 2	+ 1	+ 3	+ 3	+ 6
10	17	- 5	- 9	-10	- 7	- 5	+ 1
1	53	- 3	+ 4	+ 2	+ 4	+ 1	+ 7
2	53	- 1	- 3	- 4	+ 1	0	+ 3
3	53	+ 4	+ 4	+ 8	+ 6	+ 7	+ 6
4	53	+ 4	+ 5	+ 6	+ 6	+ 6	+ 6
5	53	0	+ 2	+ 3	+ 4	+ 5	+ 6
6	53	+ 6	+11	+12	+13	+11	+ 8
7	53	+ 5	+10	+11	+11	+10	+10
8	53	+ 2	+ 6	+ 4	+ 7	+ 7	+ 7
9	53	+ 2	+ 3	+ 4	+ 3	+ 4	+ 4
10	53	- 2	- 3	- 3	- 1	0	+ 2
1	89	0	+ 5	+ 2	+ 3	+ 2	+ 5
2	89	+ 4	+ 5	+ 5	+ 6	+ 6	+ 6
3	89	+ 5	+ 6	+ 8	+ 6	+ 8	+ 6
4	89	+ 4	+ 5	+ 6	+ 6	+ 8	+ 7
5	89	+ 1	+ 3	+ 5	+ 5	+ 6	+ 6
6	89	+ 1	+ 3	+ 4	+ 5	+ 4	+ 4
7	89	+ 5	+10	+11	+11	+10	+10
8	89	+ 4	+ 6	+ 5	+ 5	+ 5	+ 7
9	89	+ 3	+ 4	+ 4	+ 5	+ 6	+ 6
10	89	+ 2	+ 5	+ 5	+ 5	+ 6	+ 5

TABLE A - 6

STRAINS FOR 3RD CYCLE (MODEL I)

Strain Gauge Location	Height 'Z' Inches	Strains in μ-inch/inch for Loads in Lbs.						
		100	250	400	500	570	700	850
1	17	+ 1	+ 6	+10	+11	+ 9	+ 4	0
2	17	- 6	-18	-30	-37	-42	-49	-55
3	17	+25	+25	+26	+31	+32	+27	+26
4	17	+ 2	+ 2	+ 5	+ 7	+ 7	+ 9	+ 9
5	17	+ 1	0	+ 1	+ 2	+ 1	0	- 2
6	17	+ 8	+17	+29	+35	+40	+48	+54
7	17	+ 7	+15	+27	+32	+38	+44	+51
8	17	+ 3	+ 8	+11	+16	+17	+21	+21
9	17	- 2	- 6	- 4	- 9	-10	-13	+15
10	17	- 7	-21	-31	-38	-42	-48	-58
1	53	- 1	+ 3	+ 4	+ 4	+ 2	+ 2	- 4
2	53	- 4	- 8	-12	-15	-17	-19	-22
3	53	+ 1	+ 3	+ 5	+ 5	+ 5	+ 6	+ 7
4	53	0	0	+ 2	+ 2	+ 2	+ 3	+ 3
5	53	0	- 1	- 3	- 5	- 4	- 4	- 6
6	53	+ 4	+11	+ 4	+ 8	+ 9	+14	+19
7	53	+ 5	+11	+20	+21	+25	+30	+32
8	53	+ 1	+ 3	+ 5	+ 6	+ 7	+ 9	+ 9
9	53	- 1	- 3	- 3	- 5	- 6	- 6	- 7
10	53	- 2	- 9	-14	-17	-19	-23	-27
1	89	- 2	- 1	- 3	- 5	- 4	- 6	- 7
2	89	0	0	+ 3	+ 3	+ 3	+ 3	+ 3
3	89	+ 2	+ 3	+ 3	+ 3	+ 3	+ 2	+ 1
4	89	+ 1	+ 1	+ 3	+ 4	+ 5	+ 5	+ 5
5	89	-21	-21	-19	-21	-19	-21	-21
6	89	0	+ 2	+ 4	+ 2	+ 2	+ 4	+ 3
7	89	+ 4	+ 3	+ 7	+ 8	+ 9	+ 7	+13
8	89	+ 3	+ 2	+ 3	+ 3	0	+ 1	+ 3
9	89	- 1	- 2	- 1	- 1	- 1	- 1	- 2
10	89	0	- 2	- 1	+ 5	+ 2	- 2	- 2

*The model failed at a load of 950 lbs.

TABLE A - 7

STRAINS FOR 1ST CYCLE (MODEL II)

Strain Gauge Location	Height 'Z' Inches	Strains in μ-inch/inch for Loads in Lbs. Loading 50	100	150	Unloading 100	50	No Load
1	5	+ 5	+13	+20	+18	+13	+ 2
2	5	- 5	- 5	- 9	- 5	- 5	- 2
3	5	+14	-61	-16	-23	-27	- 6
4	5	+ 1	+ 4	+ 3	+ 4	+ 3	0
5	5	- 6	- 6	-13	-10	- 5	- 5
6	5	+ 3	+ 6	+10	+ 8	+ 6	- 2
7	5	+ 3	+ 7	+ 9	+ 8	+ 7	0
8	5	+ 1	+ 4	+ 3	+ 3	+ 3	0
9	5	- 2	- 5	- 4	- 4	- 5	- 1
10	5	- 4	- 4	- 9	- 5	- 2	- 2
7	11	+ 3	+ 5	+ 8	+ 9	+ 6	- 1
8	11	+ 4	+ 6	+ 5	+ 8	+ 4	+ 2
9	11	- 1	- 3	- 1	- 4	- 1	- 2
10	11	- 6	-10	-16	- 6	- 3	- 2
11	11	0	+ 1	+ 1	+ 2	+ 2	- 2
12	11	- 1	- 3	- 6	+ 1	+ 2	+ 1
1	53	- 5	-10	- 4	- 1	- 2	- 7
2	53	- 3	- 1	- 3	- 1	+ 2	0
3	53	- 3	- 1	- 1	0	+ 2	- 1
4	53	- 4	0	0	0	+ 1	- 2
5	53	- 2	+ 1	+ 1	+ 1	+ 3	0
6	53	+ 1	+13	+17	+14	+ 9	+ 8
7	53	+ 6	+ 8	+ 9	+12	+ 5	0
8	53	- 2	+ 2	+ 4	- 1	0	- 1
9	53	- 1	- 2	- 3	- 2	- 3	0
10	53	- 3	- 1	- 2	- 1	+ 2	- 1
1	89	0	- 2	- 4	- 1	- 3	- 4
2	89	- 2	- 1	+ 1	0	+ 3	- 1
3	89	- 2	+ 1	+ 2	+ 1	+ 3	- 1
4	89	- 2	+ 2	+ 1	+ 2	+ 4	- 1
5	89	- 6	- 2	- 2	- 1	- 1	0
6	89	- 1	+ 2	- 1	+ 1	+ 3	- 2
7	89	- 2	+ 1	+ 3	+ 6	+ 2	0
8	89	0	+ 3	+ 3	+ 3	+ 4	+ 2
9	89	- 2	- 2	- 2	- 2	- 4	0
10	89	- 2	- 2	0	0	- 2	- 2

TABLE A - 8

STRAINS FOR 3RD CYCLE (MODEL II)

Strain Gauge Location	Height 'Z' Inches	Strains in μ-inch/inch for Loads in Lbs.								
		100	250	350	450	500	600	700	800	900
1	5	+14	+38	+55	+71	+79	+92	+114	+129	+143
2	5	- 1	-13	-18	-26	-25	-43	- 51	- 60	- 70
3	5	-12	-11	-39	-33	-23	-35	- 17	- 25	- 26
4	5	+ 6	+10	+14	+18	+18	+15	+ 18	+ 16	+ 9
5	5	- 5	-17	-29	-41	-43	-65	- 83	-100	- 78
6	5	+ 8	+24	+30	+38	+45	+40	+ 44	+ 49	+ 65
7	5	+13	+24	+31	+40	+44	+39	+ 50	+ 53	+ 59
8	5	+ 7	+15	+20	+23	+26	+25	+ 29	+ 29	+ 21
9	5	- 6	-15	-21	-24	-27	-25	- 34	- 32	- 28
10	5	- 1	- 6	-14	-16	-17	-28	- 32	- 38	- 51
7	11	+ 4	+16	+24	+34	+40	+40	+ 49	+ 52	+ 55
8	11	+ 3	+11	+16	+21	+25	+30	+ 36	+ 32	+ 32
9	11	- 5	- 6	- 9	-15	-17	-15	- 23	- 23	- 21
10	11	- 7	-16	-21	-22	-27	-40	- 39	- 52	- 63
11	11	+ 4	+10	+14	+20	+23	+22	+ 30	+ 31	+ 28
12	11	0	+ 2	- 4	- 6	-10	- 1	- 6	- 3	- 1
1	53	+ 1	+ 7	+14	+13	+21	+ 4	+ 17	+ 14	+ 9
2	53	0	- 1	- 2	- 2	- 2	- 7	- 7	- 10	- 19
3	53	+ 2	+ 5	+ 5	+ 7	+10	0	- 8	- 17	- 32
4	53	+ 4	+ 9	+11	+13	+16	+13	+ 18	+ 17	+ 12
5	53	0	+ 3	0	+ 5	+ 7	+ 8	+ 9	+ 10	0
6	53	+ 8	+17	+24	+25	+35	+27	+ 34	+ 42	+ 36
7	53	+ 7	+17	+19	+27	+33	+32	+ 35	+ 37	+ 36
8	53	+ 4	+13	+16	+15	+22	+14	+ 22	+ 25	+ 19
9	53	+ 3	+ 9	+10	+14	+17	+14	+ 19	+ 18	+ 13
10	53	0	+ 1	+ 1	0	+ 2	- 5	- 5	- 8	- 17
1	89	+ 3	+ 3	+ 4	+ 8	+15	+ 8	+ 15	+ 11	+ 7
2	89	+ 3	+ 6	+ 8	+ 8	+13	+ 8	+ 11	+ 8	+ 2
3	89	+ 3	+ 7	+ 8	+12	+14	+10	+ 13	+ 12	+ 9
4	89	+ 5	+ 9	+13	+14	+17	+12	+ 17	+ 15	+ 11
5	89	+ 3	+ 9	+12	+15	+17	+15	+ 19	+ 19	+ 15
6	89	+ 6	+10	+12	+12	+18	+12	+ 17	+ 14	+ 8
7	89	+ 2	+ 8	+13	+13	+20	+15	+ 20	+ 18	+ 15
8	89	- 1	+ 4	+ 6	+20	+23	+16	+ 14	+ 9	+ 2
9	89	+ 5	+10	+11	+13	+18	+12	+ 17	+ 15	+ 11
10	89	+ 4	+ 8	+ 8	+10	+12	+ 6	+ 6	+ 6	0

* The model failed at a load of 940 lbs.

APPENDIX B

DEFINATION OF SECTORIAL AREAS AND EXPRESSIONS FOR CALCULATIONS OF SOME GEOMETRIC PROPERTIES OF THE MODEL SECTION

(a) Sectorial area, ω

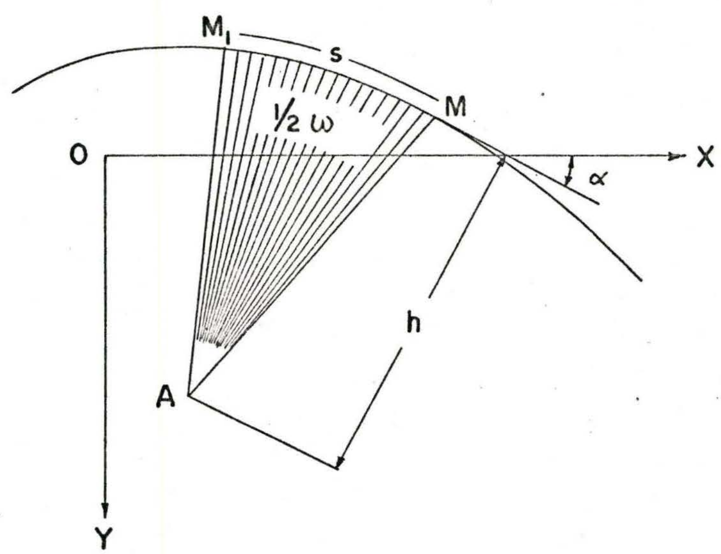

Fig. 34 - Sectorial Area

The sectorial area ω, for any point M on the profile line, is twice the area of the sector enclosed between the arc MM_1 of the profile line and two lines AM_1, AM, joining the ends of this segment with A. Point A is called the pole of the pole of the sectorial areas and point M_1 the sectorial origin. The line AM is called the mobile radius vector.

Alternately, sectorial area for point M

$$\omega = h.s$$

where h = length of perpendicular from the point A to the tangent of the profile line at M.

The sectorial areas are considered positive if the mobile radius vector AM moves clockwise when observed from the negative Z direction. For principal sectorial areas, the shear centre of the section serves as the pole of the sectorial areas.

(b) Coordinates of the shear centre

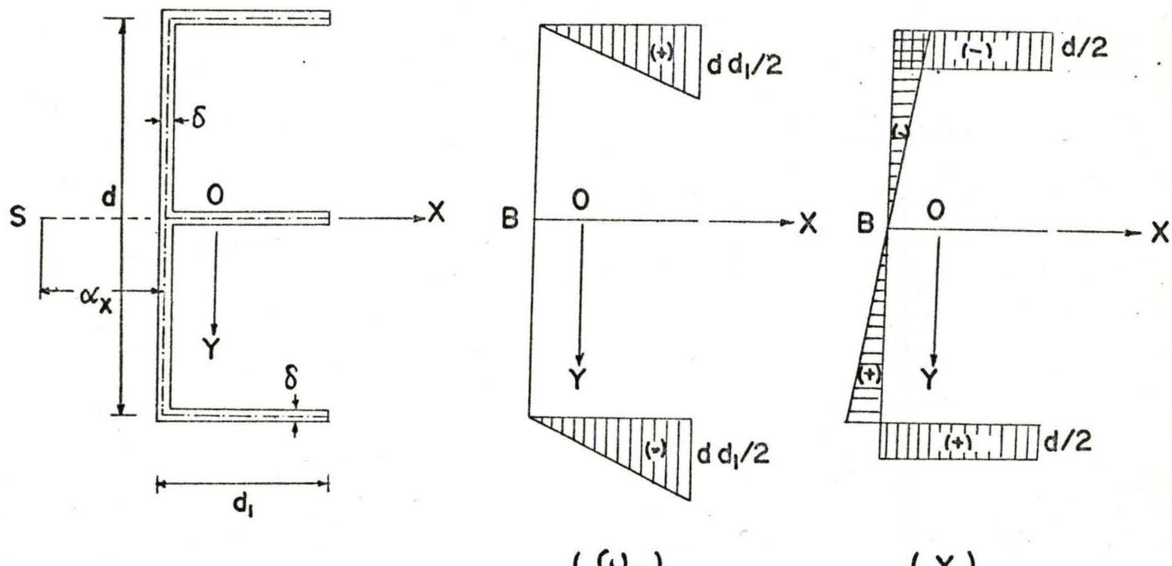

Fig. 35 - Determination of the Shear Centre of the Section

The shear centre 's' lies on the axis of symmetry ox. Point 'o' is the centroid of the section. The diagram of the sectorial area ω_b with point B as an auxiliary pole is shown in Fig. 35. The diagram of the ordinates y is also on the same figure. Hence,

$$I\omega_B y = \int_A y\, \omega_B\, dA = -\frac{\delta d^2 d_1^2}{4} \qquad \text{(i)}$$

Also,

$$I_x = \int_A y^2\, dA = \delta\frac{d^3}{12} + \frac{\delta\, d_1 d^2}{2} \qquad \text{(ii)}$$

where A is the area of the section. If α_x is the distance of the shear centre from the wall, then

$$\alpha_x = \frac{I_{\omega_B} y}{I_x} = -\frac{d_1^2\ \delta_1}{2d_1\delta_1 + \frac{d\delta}{3}} \qquad \text{(iii)}$$

(c) Principal Sectional Areas

The diagram of the principal sectional areas is skew-symmetrical with respect to the axis ox, as shown in Fig. 36. Point B at the point of intersection of the web and the axis ox, serves as the origin of the areas. The sectorial areas for the points on the web below the axis ox, will be positive, since these areas are swept in the clockwise direction by the radius vector. The absolute value of the sectorial for the flanges of the section decreases as it gets further away from the web. At the point c, removed from the web a distance equal to that of the shear centre s from the web, the sectorial area vanishes.

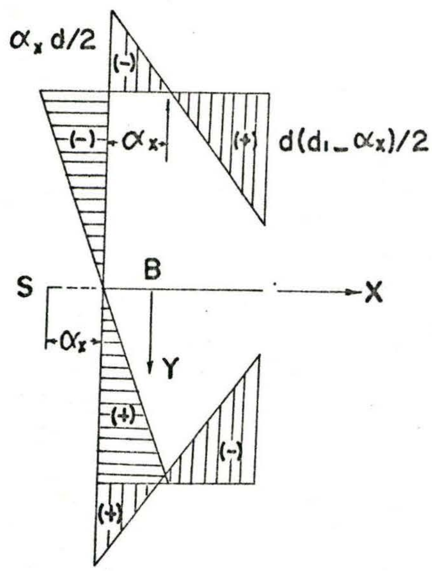

Fig. 36 - The Diagram of the Principal Sectorial Areas

(d) Principal Sectorial Areas, I_ω*

$$I_\omega = \int_A \omega^2 \, dA$$

Hence,

$$I_\omega = \alpha_x^2 \frac{d^2}{4} \left(\frac{d}{6} + d_1\right) + \frac{d^2 d_1^2}{12} (d_1 - 3\alpha_x) \qquad \text{(iv)}$$

---

* For derivation refer to reference [3].

(e) Calculations for I_d,

$$I_d = \frac{\alpha}{3} \ \Sigma \ d \ \delta^3$$

Taking $\alpha = 1$

$$I_d = \frac{1}{3} \left(\delta^3 \ d + 2 \ \delta_1^3 \ d_1 + \delta_2^3 \ d_1\right) \qquad \text{(v)}$$

APPENDIX C

1. DERIVATION OF PRIMARY EQUATIONS FOR ROSMAN'S THEORY:

(a) Formulation of the Problem

The basic idea in this approach consists in the replacements of the connecting beams by a continuous connection. This connection has a stiffness over the height of any floor, equivalent to that of a beam at that floor. The continuous connection can be imagined as consisting of laminas of height dx and stiffness $I_p dx/h$ extending one after the other along the whole height, as shown in Fig. 23 (a,b).

Assume the continuous connections be cut along their axes. Along the intersected lines act shear forces T' per unit length. The integral shear force T,

$$T = \int_{o}^{z} T' dz \tag{1}$$

is the statically redundant function. The integration is performed from the upper edge of the wall to the cross-section considered.

Not only deformations due to bending moments, but also the deformations due to normal forces in the piers and shear forces in the connecting beams are taken into account. The shear deformation in the connecting beams is taken into account by introducing the reduced moments of inertia of the connecting beams

$$I_p = \frac{I_{po}}{1+2.4(\frac{h_p}{b})^2} \qquad (2)$$

where I_{po} is the moment of inertia of a connecting beam of height h_p.

The behaviour of the function T between its boundary values is governed by a differential equation. The coefficients of this differential equation depend on the geometrical characteristics of the piers, the connecting beams and on the type of loading of the structure. They do not depend on the manner in which the pier is connected at its lower end with other structural elements.

In the following, the differential equation (8) of the integral shear force is derived with the walls containing two bands of openings.

The displacement δT of the laminas consists of the following components as shown in Fig. 23 (c).

(a) Shear deformations $\delta_1 = \frac{2(hT')(b/2)^3}{3EI_p}$

$$\text{i.e. } \delta_1 = \frac{hb^3}{12EI_p}T'$$

(b) Combined flexural and Axial deformations, δ_2

Assuming that the curvatures of all the piers are equal at a given section

$$\frac{M_1}{EI_1} = \frac{M_2}{EI_2} = \frac{(2M_1+M_2)}{E(2I_1+I_2)}$$

where moment in pier 1, $M_1 = c_1 \int_z^{\ell} T\, d\, z$

moment in pier 2, $M_2 = 2c_2 \int_z^{\ell} T\, d\, z$

Therefore, $2M_1 + M_2 = 2H \int_z^{\ell} T\, d\, z$.

For this case, there would not be any resultant longitudinal force on middle pier. Hence,

$$\delta_2 = \frac{M_1 c_1}{EI_1} + \frac{M_2 c_2}{EI_2} + \int_z^{\ell} \frac{T\, d\, z}{E\, A_1}$$

$$= \frac{(2M_1 + M_2)}{E(2I_1+I_2)} (c_1+c_2) + \int_z^{\ell} \frac{T\, d\, z}{E\, A_1}$$

$$= \frac{1}{E} \left(\frac{2H^2}{2I_1+I_2} + \frac{1}{A_1}\right) \int_z^{\ell} T\, d\, z$$

The total displacement of the end of a laminate

$$\delta_T = \delta_1 + \delta_2 + \delta_{HT}$$

where δ_{HT} = Displacement at the bottom of the wall.

Now the displacement due to force Q,

$$\delta_Q = \frac{M_1 c_1}{EI_1} dz + \frac{M_2 c_2}{EI_2} dz + \delta_{HQ}$$

where δ_{HQ} = Value of the displacement δ_Q at the bottom of the pier.

$$\delta_Q = \frac{2M_1+M_2}{E(2I_1+I_2)} (c_1+c_2)\, dz + \delta_{HQ}$$

In the case where the lower end beam is infinitely stiff, the displacements δ_{HT} and δ_{HQ} at the bottom of the wall vanish.

The compatibility condition requires,

$$\delta_T = \delta_Q \tag{3}$$

Substituting values of δ_T and δ_Q

$$\frac{h\ b^3}{12EI_p} T' + \frac{1}{E} \left(\frac{2H^2}{2I_1+I_2} + 1/A_1\right) \int_z^{\ell} T\ d\ z$$

$$= \int_z^{\ell} \frac{Q\ H\ z}{E(2I_1+I_2)}\ dz + \delta_{HQ} - \delta_{HT}$$

By introducing the abbreviations:

$$\alpha^2 = \left(\frac{2H^2}{2I_1+I_2} + 1/A_1\right) \frac{12\ I_p}{h\ b^3} \tag{4}$$

and

$$\gamma = \frac{QH}{2I_1+I_2} \frac{12\ I_p}{h\ b^3} \tag{5}$$

and simplifying, the resultant expression is

$$T' + \alpha^2 \int_z^{\ell} T\ dz = \gamma \int_z^{\ell} z\ dz + (\delta_{HQ}-\delta_{HT}) \frac{12\ I_p}{h\ b^3} \tag{6}$$

After differentiation and the use of the well known expressions:

$$\left.\begin{aligned} \frac{d}{dz}\left(\int_z^{\ell} T\ dz\right) &= -T \\ \frac{d}{dz}\left(\int_z z\ dz\right) &= -z \end{aligned}\right\} \tag{7}$$

The equation (6) becomes

$$\frac{d^2T}{dz^2} - \alpha^2 \, T = - \gamma \, . \, z. \tag{8}$$

Boundary Conditions:

At the top of the wall no restraint against a relative vertical translation of the piers is imposed. In that case the functions T should vanish

$$T_0 = 0 \tag{9}$$

At the base, the piers are fixed in the same foundation. Assuming that the supporting structure completely restrains the ends of the piers against a relative rotation and translation,

$$\left(\frac{dT}{dz}\right)_{\ell} = 0 \tag{10}$$

(b) Solution of the Problem

The solution of equation (8) is of the form

$$T = C \text{ Sinh } \alpha z + D \text{ Cosh } \alpha z + \frac{\gamma}{\alpha^2} \, z \tag{11}$$

Applying boundary conditions (9) and (10) the equation (11) becomes

$$T = C \text{ Sinh } \alpha z + \frac{\gamma}{\alpha^2} \, z \tag{12}$$

where

$$C = -\frac{\gamma}{\alpha^3 \text{ Cosh } (\alpha z)} \tag{13}$$

The bending moment at any arbitrary point 'z' of the wall,

$$M_x = 2TH - Q.z \tag{14}$$

Since all piers must have the same deflection at any section throughout the whole height 'ℓ', the total bending moment is divided among them proportionally to their moments of inertia. Therefore,

$$M_{x1} = \frac{I_1}{2I_1+I_2} M_x \tag{15}$$

$$M_{x2} = \frac{I_2}{2I_1+I_2} M_x \tag{16}$$

In the present study, refer to Figure 24.

Putting $$H_1 = c_2 + c_1 \cos \theta \tag{17}$$

where 'θ' is the angle of inclination of principal axis x_p with x-axes and,

$$\alpha^2 = \left(\frac{2H_1^2}{2I_1+I_2} + 1/A_1\right) \frac{12I_p}{h\ b^3} \tag{18}$$

Piers 1 and 3 will also have moment about their principal axis y_p.

$$M_{yp1} = M_{x1} \text{ Sin } \theta + T \cdot n_1 \tag{19}$$

$$M_{xp1} = M_{x1} \cdot \text{Cos } \theta \tag{20}$$

Stresses at any point of the middle pier having coordinates (x_2, y_2) with respect to principal axis will be

$$\sigma_2 = \frac{M_{x2}}{I_{x2}} y_2 - \frac{M_{y2}}{I_{y2}} x_2 \tag{21}$$

and for the side pier, stress at any point having coordinates (x_{p1}, y_{p1}) with respect to principal axes,

$$\sigma_1 = \frac{M_{xp1}}{I_{x1}} y_{p1} - \frac{M_{yp1}}{I_{y1}} x_{p1} + \frac{T}{A_1} \qquad (22)$$

2. EXPRESSIONS FOR BENDING MOMENTS AND DEFLECTIONS FOR SIDE PIERS:

As derived earlier, the expressions for bending moments about the principal axes of the side piers are, (Ref. See Fig. 23a) for $0 \leqslant z \leqslant \ell$

$$M_{xp1} = M_{x1} \, . \, \text{Cos } \theta \qquad (1)$$

$$M_{yp1} = M_{x1} \, . \, \text{Sin } \theta + T.n_1 \qquad (2)$$

Substituting for M_{x1} and T, the equation (1) and (2) yield

$$M_{xp1} = [2HC \text{ Sinh } \alpha z + 2H \frac{\gamma}{\alpha^2} z - Qz] \frac{I_1}{2I_1+I_2} \, . \, \text{Cos } \theta \qquad (3)$$

$$M_{yp1} = [2HC \text{ Sinh } \alpha z + \frac{2H\gamma}{\alpha^2} z - Q.z] \frac{I_1}{2I_1+I_2} \, . \, \text{Sin } \theta$$

$$+ n_1 C \text{ Sinh } \alpha z + \frac{n_1 \frac{\gamma}{2}}{\alpha^2} .z \qquad (4)$$

In case $\ell \leqslant z \leqslant \ell_m$, the expressions for bending moments become

$$M_{xp1} = [2HC \text{ Sinh } \alpha\ell + \frac{2H\gamma}{\alpha^2} \ell - Qz] \frac{I_1}{2I_1+I_2} \, . \, \text{Cos } \theta \qquad (5)$$

$$M_{yp1} = [2HC \text{ Sinh } \alpha\ell + \frac{2H\gamma}{\alpha^2} \ell - Q.z] \frac{I_1}{2I_1+I_2} \text{ sin } \theta$$

$$+ n_1 \text{ C Sinh } \alpha\ell + \frac{n_1\gamma}{\alpha^2} \ell \qquad (6)$$

Integrating the equations (5) and (6) twice and putting the boundary conditions

$$\frac{d\eta}{dz} = 0 \quad \text{at } x = \ell_m$$

$$\eta = 0 \quad \text{at } x = \ell_m$$

where η denotes the deflection along the principal axes.

The expressions for deflections obtained are,

$$E I_{y1}\eta_{x1} = \frac{I_1}{2I_1+I_2} \text{ Cos } \theta [2HC \text{ Sinh } \alpha\ell + \frac{2H\gamma}{\alpha^2} .\ell - Q\frac{z^3}{6}]$$

$$+ C_1 z + C_2 \qquad (7)$$

where,

$$C_1 = \frac{I_1}{2I_1+I_2} \text{ Cos } \theta [Q \frac{\ell m^2}{2} - \frac{2H\gamma}{\alpha^2} - 2HC \text{ Sinh } \alpha\ell]$$

and,

$$C_2 = \frac{I_1}{2I_1+I_2} \text{ Cos } \theta [Q \frac{\ell m^3}{6} - C_1 \frac{\ell m.(2I_1+I_2)}{I_1 \text{ Cos } \theta}$$

$$- \frac{2H\gamma}{\alpha^2} \ell - 2HC \text{ Sinh } \alpha\ell]$$

$$EI_{x1}\eta_{y1} = \eta_1 C \text{ Sinh } \alpha\ell + \frac{\eta_1\gamma}{\alpha^2} + \frac{I_1}{2I_1+I_2} \text{ Sin } \theta$$

$$[2HC \text{ Sinh } \alpha\ell + \frac{2H\gamma}{\alpha^2} .\ell. - \frac{Qz^3}{6}] C_3.z + C_4 \qquad (10)$$

where,

$$C_3 = \frac{I_1}{2I_1+I_2} \text{ Sin } \theta \,[Q.\ \frac{\ell m^2}{2} - 2HC \text{ Sinh } \alpha\ell + \frac{2H\gamma}{\alpha^2} . \ell\,]$$

$$- \eta_1 C \text{ Sinh } \alpha\ell - \frac{\eta\gamma}{\alpha^2}\ \ell \qquad (11)$$

and

$$C_4 = \frac{I_1}{2I_1+I_2} \text{ Sin } \theta \,[Q.\ \frac{\ell m^3}{6} - 2HC \text{ Sinh } \alpha\ell - \frac{2H\gamma}{\alpha^2}\ \ell]$$

$$- \ell m . C_1 - \eta_1 C \ \text{ Sinh } \alpha\ell - \frac{\eta_1\gamma}{\alpha^2}\ \ell \qquad (12)$$

BIBLIOGRAPHY

1. FRISCHMANN, W. W. and PRABHU, S.
"Planning Concepts Using Shear Walls"
Symposium on tall buildings, University of
Southampton, April, 1966, Pergamon Press London.

2. FRISCHMANN, W. W. and PRABHU, S.
"Shear Wall Structures - Design and Construction Problems"
Symposium on tall buildings, University of Southampton,
April, 1966, Pergamon Press London.

3. AFSAR, M.
"Lateral Loading of Shear Wall Models"
Thesis submitted to Civil Engineering Department in
partial fulfilment of the requirements for the degree of
Master of Engineering, McMaster University, August 1967.

4. COULL, A. and SMITH, S.B.
"Analysis of Shear Wall Structures",
A review of previous research,
Symposium on tall buildings, University of Southampton
April 1966, Pergamon Press London.

5. GREEN, N. B.
"Bracing Walls for Multistorey Buildings"
Journal American Concrete Institute 24, 1952.

6. FRISCHMANN, W.W., PRABHU, S. S. and TOPPLER, J. F.
"Multistorey Frames and Interconnected Shear Walls Subject to Lateral Loads"
Concrete and Construction Engineering 58, Nos. 6 and 7, 1963.

7. BECK, H.
"Contribution to the Analysis of Shear Walls"
Journal American Concrete Institute 33, 1962.

8. ERIKSSON, O. E.
"Analysis of Wind Bracing Walls in Multistorey Housing".
Ingenioren International Edition 5, 115, 1961.

9. ROSMAN, R.
"Approximate Analysis of Shear Walls Subject to Lateral Loads".
Journal American Concrete Institute, 35, 1964.

10. LIVESLEY, R. K.
"Matrix Methods of Structural Analysis"
Pergamon Press, 1964.

11. McHENRY, D.
"A Lattice Analogy for the Solution of Stress Problems".
Journal The Institution of Civil Engineers, December, 1943.

12. HRENNIKOFF, A.
"Solution of Problems of Elasticity by the Frame-Work Method"
Journal of Applied Mechanics, December, 1941.

13. McCORMICK, C. W.
"Plane Stress Analysis" .
Journal of the Structural Division, A.S.C.E. 89, 1963.

14. GRINTER, L. E.
"Statistical State of Stress Studied by Grid Analysis".
Numerical Methods of Analysis in Engineering,
McMillan, 1949.

15. McLEOD, I. A.
"Lateral Stiffness of Shear Walls with Openings".
Symposium on tall buildings, University of Southampton,
April 1966, Pergamon Press London.

16. VLASOV, V. Z.
"Thin-Walled Elastic Beams".
Israel programme for scientific translations, Jerusalem,
Israel, 1961.

17. BENJAMIN, J. R. and WILLIAMS, H. A.
"The Behaviour of One-storey Reinforced Concrete
Shear Walls".
Proceedings A.S.C.E.; August 1960.

18. BENJAMIN, J. R. and WILLIAMS, H. A.
"The Behaviour of One-storey Reinforced Concrete
Shear Walls Containing Openings".
Journal American Concrete Institute, November 1958.

19. BENJAMIN, J. R. and WILLIAMS, H. A.
"Reinforced Concrete Shear Wall Assemblies".
Proceedings A.S.C.E.; August 1960.

20. BENJAMIN, J. R.
"Statically Indeterminate Structures".
McGraw Hill, 1959.

21. FUTAMI, H. and FUJIMUTO, M.
"Experimental Study on Lateral Force Distribution by Photoelasticity".
Transactions Architectural Institute of Japan.

22. CHITTY, L. and WEN-YUH, W.
"Tall Building Structures under Wind Load".
Proc. 7th Int. Conf. for App. Mech., Vol. 1, 1948.

23. CHITTY, L.
"On the Cantilever Composed of a Number of Parallel Beams Interconnected by Cross Girders".
Philosophical Magazine London, October 1947.

24. BARNARD, P. R. and SCHWAIGHOFER, J.
"The Interaction of Shear Walls Connected Solely Through Slabs".
Symposium on tall buildings, University of Southampton, April 1966, Pergamon Press London.

25. STILLER, M.
"The Effect of Wall Openings on the Stresses and Edge Shear Forces in Diaphragm Systems"
Symposium on tall buildings,University of Southampton, April 1966, Pergamon Press London.

26. SCHWAIGHOFER, J.
"Door Openings in Shear Walls".
Journal American Concrete Institute, Nov., 1967.

27. MICHAEL, D.
"The Effect of Local Wall Deformations on the Elastic Interaction of Cross Walls Coupled by Beams".
Symposium on tall buildings , Univ. of Southampton April 1966, Pergamon Press London.